Institut Teknologi Sepuluh Nopember

TESIS TE-2099

PENINGKATAN PERFORMA JARING DISTRIBUSI RADIAL RADIAL TIGA FASA TIDAK SEIMBANG DAN TERDISTORSI HARMONISA MELALUI PENEMPATAN OPTIMUM KAPASITOR MENGGUNAKAN DSA

HAPPY APRILLIA
2212201012

DOSEN PEMBIMBING
PROF. IR. ONTOSENO PENANGSANG, M.SC., PH.D
PROF. DR. ADI SOEPRIJANTO, ST., MT.
JAI GOVIND SINGH, B.ENG., M.TECH., PH.D.

PROGRAM MAGISTER
BIDANG KEAHLIAN TEKNIK SISTEM TENAGA
PROGRAM STUDI TEKNIK ELEKTRO
FAKULTAS TEKNOLOGI INDUSTRI
INSTITUT TEKNOLOGI SEPULUH NOPEMBER
SURABAYA
2014

THESIS TE-2099

PERFORMANCE ENHANCEMENT OF AN UNBALANCED AND HARMONICALLY DISTORTED THREE PHASE RADIAL DISTRIBUTION NETWORK BY OPTIMAL PLACEMENT OF CAPACITOR USING DSA

HAPPY APRILLIA
2212201012

ADVISORS
PROF. IR. ONTOSENO PENANGSANG, M.SC., PH.D
PROF. DR. ADI SOEPRIJANTO, ST., MT.
JAI GOVIND SINGH, B.ENG., M.TECH., PH.D.

MASTER PROGRAM
POWER SYSTEM ENGINEERING
ELECTRICAL ENGINEERING DEPARTMENT
FACULTY OF INDUSTRIAL TECHNOLOGY
INSTITUT TEKNOLOGI SEPULUH NOPEMBER
SURABAYA
2014

TESIS TE-2099

PENINGKATAN PERFORMA JARING DISTRIBUSI RADIAL TIGA FASA TIDAK SEIMBANG DAN TERDISTORSI HARMONIK MELALUI PENEMPATAN OPTIMUM KAPASITOR MENGGUNAKAN DSA

HAPPY APRILLIA
2212201012

DOSEN PEMBIMBING
PROF. IR. ONTOSENO PENANGSANG, M.SC., PH.D
PROF. DR. ADI SOEPRIJANTO, ST., MT.
JAI GOVIND SINGH, B.ENG., M.TECH., PH.D.

PROGRAM MAGISTER
BIDANG KEAHLIAN TEKNIK SISTEM TENAGA
PROGRAM STUDI TEKNIK ELEKTRO
FAKULTAS TEKNOLOGI INDUSTRI
INSTITUT TEKNOLOGI SEPULUH NOPEMBER
SURABAYA
2014

TESIS TE-2099

PERFORMANCE ENHANCEMENT OF AN UNBALANCED AND HARMONICALLY DISTORTED THREE PHASE RADIAL DISTRIBUTION NETWORK BY OPTIMAL PLACEMENT OF CAPACITOR USING DSA

HAPPY APRILLIA
2212201012

DOSEN PEMBIMBING
PROF. IR. ONTOSENO PENANGSANG, M.SC., PH.D
PROF. DR. ADI SOEPRIJANTO, ST., MT.
JAI GOVIND SINGH, B.ENG., M.TECH., PH.D.

PROGRAM MAGISTER
BIDANG KEAHLIAN TEKNIK SISTEM TENAGA
PROGRAM STUDI TEKNIK ELEKTRO
FAKULTAS TEKNOLOGI INDUSTRI
INSTITUT TEKNOLOGI SEPULUH NOPEMBER
SURABAYA
2014

THESIS TE-2099

PERFORMANCE ENHANCEMENT OF AN UNBALANCED AND HARMONICALLY DISTORTED THREE PHASE RADIAL DISTRIBUTION NETWORK BY OPTIMAL PLACEMENT OF CAPACITOR USING DSA

HAPPY APRILLIA
2212201012

ADVISORS
PROF. IR. ONTOSENO PENANGSANG, M.SC., PH.D
PROF. DR. ADI SOEPRIJANTO, ST., MT.
JAI GOVIND SINGH, B.ENG., M.TECH., PH.D.

MASTER PROGRAM
POWER SYSTEM ENGINEERING
DEPARTMENT OF ELECTRICAL ENGINEERING
FACULTY OF INDUSTRIAL TECHNOLOGY
SEPULUH NOPEMBER INSTITUTE OF TECHNOLOGY
SURABAYA
2014

MASTER'S THESIS RECOMMENDATION FORM

A thesis submitted in partial fulfillment of the requirements for the degree of Master of Engineering
in
Sepuluh Nopember Institute of Technology

by :
HAPPY APRILLIA
NRP. 2212201012

Examination Date : 30 June 2014
Graduation Period : September 2014

Approved by:

1. **Prof. Ir.Ontoseno Penangsang, M.Sc., Ph.D.** (Advisor)
   NIP. 194907151974121001

2. **Prof. Dr. Ir. Adi Soeprijanto, MT** (Co-Advisor)
   NIP. 196404051990021001

Director of Graduate Program

Prof. Dr. Ir. Adi Soeprijanto, MT.
NIP. 196404051990021001

CERTIFICATE OF ORIGINALITY

I, the undersigned hereby declare that

Name	:	Happy Aprillia
Student ID	:	2212201012
Department	:	Electrical Engineering
Program	:	Master - Power System Engineering
Faculty	:	Faculty of Industrial Technology (FTI)

With thesis entitled,

Performance Enhancement of an Unbalanced and Harmonically Distorted Three Phase Radial Distribution Network by Optimal Placement of a Capacitor Using DSA

is my own original work carried out as a Master's student at the Sepuluh Nopember Institute of Technology (ITS) except to the extent that assistance from others in the thesis/research study/project's design and conception or in style, presentation and linguistic expression are duly acknowledged.

All sources used for the thesis/research study/project have been fully and properly cited. It contains no material which to a substantial extent has been accepted for the award of any other degree at ITS or any other educational institution, except where due acknowledgment is made in the thesis/research study/project.

Surabaya, 25 July 2014

Happy Aprillia
2212201012

PENINGKATAN PERFORMA JARING DISTRIBUSI RADIAL TIGA FASA TIDAK SEIMBANG DAN TERDISTORSI HARMONIK MELALUI PENEMPATAN OPTIMUM KAPASITOR MENGGUNAKAN DSA

Nama	**:**	**Happy Aprillia**
NRP	**:**	**2212201012**
Dosen Pembimbing	**:**	**Prof. Ir.Ontoseno Penangsang, M.Sc., Ph.D**
		Prof. Dr. Ir. Adi Soeprijanto, MT

ABSTRAK

Jaring Distribusi Radial adalah jaring yang paling banyak digunakan untuk distribusi listrik karena arsitektur yang sederhana dan biaya investasi yang rendah. Pesatnya pertambahan pelanggan mengakibatkan jaring distribusi menjadi tidak seimbang dan terdistorsi harmonisa. Hal-hal ini menyebabkan jaring distribusi mengalami rugi-rugi daya yang besar. Rugi-rugi daya dapat diatasi dengan pemasangan kompensator daya reaktif, namun, kompensator daya reaktif ini harus dipasang secara benar untuk menghindari peningkatan harmonisa melebihi standar IEEE 519-1992.

Oleh karena itu, pada makalah ini diusulkan *Direct Search Algorithm* (DSA) untuk menyelesaikan penempatan kapasitor pada jaring distribusi tidak seimbang dan terdistorsi harmonisa. *Loss Sensitivity Factor* (LSF) digunakan untuk menentukan calon lokasi dengan pengurangan kerugian daya maksimum. Algoritma yang diusulkan telah diuji pada sistem uji IEEE jaring distribusi radial 13 bus. Perbandingan kinerja DSA dilakukan melalui pencarian penurunan rugi-rugi daya maksimum untuk tiga kasus yaitu tanpa penempatan kapasitor, tanpa batasan THD dan dengan batasan THD. Hasil penelitian menunjukkan bahwa strategi yang diusulkan pada kasus ketiga memberikan penghematan lebih besar dari kasus-kasus lain.

Kata kunci: penempatan kapasitor, *harmonic power flow*, *distribution power flow*, *direct search algorithm*

PERFORMANCE ENHANCEMENT OF AN UNBALANCED AND HARMONICALLY DISTORTED THREE PHASE RADIAL DISTRIBUTION NETWORK BY OPTIMAL PLACEMENT OF A CAPACITOR USING DSA

Nama	**:**	**Happy Aprillia**
NRP	**:**	**2212201012**
Dosen Pembimbing	**:**	**Prof. Ir.Ontoseno Penangsang, M.Sc., Ph.D**
		Prof. Dr. Ir. Adi Soeprijanto, MT

ABSTRACT

Radial Distribution System is the most widely used system for power distribution because it has simple architechture and low investment costs. In contrast, due to the addition of the customers some challenges are rised about power system losses, unbalance issues and spread of harmonics which are both single phase and three phase customers. The power system losses can be overcome with the proper installation of reactive power compensator. This reactive power compensator must be installed approriately to avoid the system harmonic level exceeding the IEEE 519-1992 standard. Capacitor will be installed for compensating reactive power to maintain the voltage profile of the system.

To overcome this problem, an effective algorithm is needed to identify the optimal location and capacity of capacitor in this system. This study will use harmonic power flow for distribution system. The load flow calculated voltage profile and harmonic distortion level on each bus voltage. Direct Search Algorithm works with loss sensitivity factor to find the most appropriate location and capacity of reactive power compensator without increasing harmonic distortion on the system. By considering THD, the best and location and capacity of reactive power compensator will be yielded while maintaining the voltage profile and minimize the power system losses.

Keywords: Capacitor, Radial Distribution Power Flow, Harmonic Power Flow Algorithm, Direct Search Algorithm, Loss Sensitivity Factor

ACKNOWLEDGEMENTS

Alhamdulillahirobbilalamin.

Foremost, my sincere thanks also goes to Prof. Ontoseno Penangsang and Prof. Adi Soeprijanto as my thesis advisor in Sepuluh Nopember Institute of Technology (ITS) who give me supports and knowledge of my Master research. Dr. Matt Syai'in, Dr. Rony Seto Wibowo, Doctoral Student Mrs. Fitri Suhartati and Dimas Fajar Putra Uman, my classmate Ms., Indri Suryawati, for leading me working on diverse exciting projects and for enlightening me the first glance of research in Power System Simulation Laboratory in ITS.

I would like to express my sincere gratitude to my advisor in AIT, Dr. Jai Govind Singh, for the continuous support of my Master study and research, for his patience, motivation, enthusiasm, and immense knowledge. I would like to thank to the honourable committees: Dr. Weerakorn Ongsakul and Dr.Shobakar Dhakal, for their encouragement, insightful comments, and advices.

I thank my fellow and labmates in both AIT and ITS for the stimulating discussions, for the sleepless nights we were working together before deadlines, and for all the fun we have had in the this years.

I thank to AIT, ITS and DIKTI especially to members of Graduate Program of ITS and Ms. Citra Amitiurna to give me this opportunity to study abroad and give me support on my financial needs in Thailand. Thanks for AIT that give me financial supports for my thesis.

Last but not the least, I would like to thank my family: my parents Endah Dwi Purwanti and Suratno and also my sister Lia for giving spirit to me at the first place and supporting me spiritually throughout my life.

Surabaya, July 2014

DAFTAR ISI

TABLE OF CONTENTS

LIST OF APPENDIX

LIST OF FIGURES

LIST OF ABBREVIATIONS

BCBV	Branch Current to Bus Voltage
BIBC	Bus Injection to Branch Current
DLF	Distribution Load Flow
DSA	Direct Search Algorithm
FBM	Full Body Matrix
HA	Harmonic Analysis matrix
HLF	Harmonic Load Flow
HPF	Harmonic Power Flow
LSF	Load Sensitivity Factor
PSO	Particle Swarm Optimization
RDPF	Radial Distribution Power Flow
THD	Total Harmonic Distortion

LIST OF SYMBOLS

K_p	Active power loss annual cost per unit (US$/kW/year)
K_{ci}	Reactive power loss annual cost per unit at i-bus (US$/kVAr/year)
Q_{ci}	Injected reactive power at i-bus (kVAr)
n_{Cap}	total unit of reactive power installment
P_{losses}	total power loss (kW)
n_{branch}	number of branch;
h_0	first harmonic orde;
h_{max}	maximum harmonic order;
P_j	active power loss at bus-j (kW)
Q_j	reactive power loss at bus-j (kVAr)
R_k	line resistance at branch- ij (kVAr)
V_j	voltage at bus j
V_{base}	voltage base which is 4.16 kV
$position_{particle}$	initial random size of capacitor
$lb_{particle}$	lower bound of the size of capacitor
$ub_{particle}$	upper bound of the size of capacitor
$position_{location}$	initial position to be the place of capacitor
$lb_{location}$	lower bound of position to be the place of capacitor
$ub_{location}$	upper bound of position to be the place of capacitor

LIST OF TABLES

CHAPTER 1
INTRODUCTION

1.1 Background

Distribution system is a vital component in the power system. Radial Distribution System (RDS) is the most widely used system for power distribution because it has a simple form and also low investment costs. Regardless of the advantages of RDS system, distribution system is highly vulnerable to the spread of harmonics. Increased use of power electronic components led to the addition of harmonics by customers on the system. Harmonic penetration can cause a decrease in the efficiency of power system components, equipment overheating, pressure on the insulation equipment, and communication interference. The worst effects of harmonics can be resulted when the existing harmonics exceeds the IEEE 519-1992 standard. It can cause permanent damage to the electrical equipment.

In the implementation of RDS, it raises some challanges about line loss and unbalance issues due to the addition of the number of customers both single phase and three phase customers. The line loss can be overcome with the installation of reactive power compensator, but the installment of reactive power compensator must be in approriate and correct manner which if it is not properly installed it may result in resonance and great harmonics impacts in the system. Due to that problems, an effective algorithm is needed in optimization of investigating the location and capacity of reactive power compensator in three-phase unbalanced harmonic distorted distribution system. System condition can be observed through the Total Harmonic Distortion (THD) at each bus of RDS.

For analyzing the effect of harmonic distortion on the three-phase unbalanced distribution system, Radial Distribution Power Flow Algorithm (RDPF) will be combined with Harmonic Power Flow Algorithm (HPF). RDPF will provide a profile of the voltage at each bus and HPF will provides harmonic distortion voltage profile at each bus for each order harmonics caused by the installation of the load harmonic source. The voltage profile is used to determine the Total Harmonic Distortion (THD) of each bus. THD is used as the basis for determining the location and capacity of reactive power compensator. After that, Direct Search Algorithm (DSA) is used to find the global optimal solution according to the objective function and limit the bus voltage .

1.2 Statement of the Problems

- How to analyze three-phase unbalanced condition in distribution system?
- How does the calculation to analyze of three-phase power flow in unbalanced condition?
- What methods will be used to formulate the problem of three phase unbalanced distribution system?
- How to modify single phase radial distribution power flow method to study three phase radial distribution power flow?
- What will be the control parameter to be include in placement and sizing calculation algorithm?
- How to use DSA in harmonic power flow analysis for 3-phase unbalanced system?
- What can be the best location and size of reactive power compensator?
- How will DSA be verified its performance?

1.3 Objectives of the Research

1.3.1 Overall objective

- To obtain appropriate harmonics distortion effects and voltage profile in distribution power system

1.3.2 Specific objectives

- Robust and fast three-phase power flow analysis application for unbalanced radial system.
- Presents the analysis of the combination of three-phase power flow and power flow for investigate unbalanced radial system with harmonics distorted condition.
- Knowing the optimal location and capacity of reactive power compensator with Direct Search Algorithm (DSA) in unbalanced radial harmonics distorted three phase system.

1.4 Scope and Limitation

- Harmonic source has been obtained from preliminary data (not through a reduction of the initial models)
- The combination of RDPF and HPF will only work as a passive power flow that can’t handle an active operation like Distributed Generation effects in power system.
- Verification of the proposed method through the comparison of results between DSA and PSO

CHAPTER 2
LITERATURE REVIEW

2.1 Review

Power system distribution is the most important component in the delivery of electricity to fulfill customers demand. Without a reliable distribution system, electricity can be optimally recieved by customers. With the same condition as analysis in transmission power flow, power flow analysis on the distribution system needs preliminary data in the form of three-phase bus voltage, real and reactive power of all loads and also load models. Types of load model are constant power, constant impedance, constant current or a combination of several models of the load (Kersting, W.H., 2002). In some conditions, the complex power supplied to the input feeder has also been known.

Characteristics of distribution system cause some difficulties to analyze the problem with power flow by traditional techniques such iterative techniques Newton-Raphson and fast decoupled (Teng, J. H., 2000). When the technique is applied to the distribution system, the technique can not achieve convergence in the finding for power flow solutions. Therefore, this system requires power flow method that can accommodate its special characteristics of the distribution system. In contrast to the transmission system, distribution system have special characteristics (Kersting, W.H., 2002) are as follows:

a. Radial structure
b. Untransposed Line
c. Has many nodes
d. Unbalanced load which is consist of single phase and three phase
e. Have high R/X ratio.

In the ideal power system, electrical energy is transferred in a constant single frequency and at a constant voltage level. But, the development of society including the industry, residential customer, enterprises and also utility increase the amount of electrical loads and added new complexity in distribution system. The high awareness of energy efficiency and global warming in people nowdays indirectly increases the usage of nonlinear loads, such as uninterruptible power supply, Variable Speed Drive (VSD), LED lamp and another power electronics devices, that will cause changes in the power quality. Wave defects is caused by the interaction between the system sinusoidal waveform with another waveform with integer multiplied of fundamental frequencies which better known as harmonics component according to (IEEE standard 519-1992) definition. Harmonic distortion will result in losses in the system, including the occurrence of resonance with the inductance of the system. One possible reason of this occurence is the installation of reactive power compensator. This resonance will increase the voltage harmonics which are quite large on the capacitor's bus and can damage the capacitor itself and other system components. Therefore, in order to gain efficiency and quality of electric power systems, the harmonic effect should be taken into account of power system analysis.

Harmonic power flow has been a long concern in power system analysis. The harmonic power flow studies have been conducted in 1990 by using Fast Decoupled method (Elamin, I.M., 1990). The research already models the load and transformer that varied with the changing of frequency. The load composition of this research is already available accurately which are consist of HVDC transformer and non linear load. Fast decoupled method is applied to the loop scheme system (transmission system), not the radial system. Therefore, this method needs jacobean matrix and has high R/X ratio because impedance in transmission system is very small. Undertaking the transmission's line characteristic will less time efficient to find the solution.

Recent years, power flow analysis on the three-phase radial system has been developed. Method of Forward Backward does not require the jacobean matrix and can accommodate the high R/X ratio (Teng, J.H., 2000; Ulinuha, *et al*, 2007). This study has added consideration of the reactive power compensator placement and effects of harmonics occurence after capacitor placement. The power flow is constrained by the error between updated voltage. With FB method, the current and voltage equation is derived from the equation and not simplified as a relation matrices. Because of that, FB method requires a long time to calculate this replacement of forward/backward process.

To overcome those problems, research on the calculation using network topology approach is developed. Network-topology radial distribution approach requires only Bus-Injection Branch-Current (BIBC) matrix and Branch-Current to Bus-Voltage (BCBV) matrix. BIBC matrix used to determine changes in bus injection current and branch currents while BCBV is used to determine changes in bus voltages and branch currents (Eajal, *et al*, 2010). The BIBC and BCBV matrices facilitated the calculation and provide branch current and bus current without much time consuming. This research provides the robust harmonic power flow method eventhough the real load composition is not clearly explained. However, this study does not consider the probability of reactive power compensator installation strategy.

From reference (Teng, J.H., 2003) , network topology radial distibution load flow approach is an upgraded method from Forward Backward loadflow technique. The sophisticated performance of this algorithm are its simple algorithm to directly solve the load flow. This type of loadlflow will identify the topology characteristics of the network which only needs conventional bus-branch oriented utility's data. This method will be faster that Forward Backward since it does not require LU decomposition and Backward Forward Jacobean matrix substitution that will be require more time for computation.

Application of Particle Swarm Optimization (PSO) has been done to determine the location and capacity of reactive power compensators (Eajal and El-Hawary, 2010). The research included a consideration of harmonic distortion in the calculation algorithm. This research also succeeded in reducing the levels of harmonic distortion through placing reactive power compensator in system. Because of the using of PSO as the optimization tool, this research can use a random initial location and size to identify the best result. This research was done without any sensitivity factor.

The performance of PSO in capacitor allocation have been conducted by (Singh and Rao, 2012). The strategy to allocate the capacitor is based on the dynamic sensitivity factor for the first location identification. The sensitivity analysis point out the place that is potential with the high loss. Then the rest performance will be continued by PSO to give the random initial size for the following location. This research has significant performance because it can determine both fixed capacitor or switch capacitor.

Artificial Bee Colony-Based approach has been also conducted to maximize the net saving in capacitor placement. (El-Fergany, *et al,* 2014) uses load sensitivity factor and combination with system stability enhancement. The focus of this research is to obtain maximum net saving with concerning the voltage stability of the system. In this research, the load sensitivity analysis does not give best result to identify prospective bus. The performance of the load sensitivity result is uncertain, therefore the voltage instability index is included in the analysis.

Another research of optimization technique to determine the location and capacity of reactive power compensator has been done by using Direct Search Algorithm (DSA) (Raju, *et al*, 2012). DSA is proven to minimize line losses better than PSO. This research proved that DSA algorithm has faster performance and high robustness on large scale systems than PSO, but there is no consideration of harmonic distortion in that research.

2.2 Capacitive Compensator Purpose

Power losses and voltage drops are main problems in distribution feeders which are typically radial and too long. The voltage in the end of long distance feeders will be very poor and exceed the voltage regulations. With the load operation, voltage profile will also decrease under the acceptable operating limits. Because of this, by the represent relationship in power, P=V.I. cos φ, if the voltage decreases, the current will be higher compare to the normal voltage condition and this condition will point to increase the power loss in system due to power relationship $P= I^2R$, which P, V, I, and R are defined as active power (Watt), current (Ampere), voltage (Volt), and resistance (ohm) respectively. Studies have indicate that losses in distribution is aproximately 13 % of generated active power. Because of this condition, electricity demand will increase and require upgrading the distribution infrastructure which need more cost.

To solve this problems, shunt capacitors are commonly used in distribution system. Capacitor compensator placement will improve the voltage profile, release system capacity and also maximize the net saving of distribution system (Aman, M.M *et al*, 2014). But, to take the optimal benefits of this capacitor placement, installation have to be proper and correct. But, the adding of capacitor in system without harmonic consideration can lead the increasing of harmonic distortion levels due to resonance between capacitors and the various inductive elements in the system (Blooming, and Carnovale, D.J, 2008). The spread of harmonics in distribution system must be taken into account. Harmonic is produced by the use of power electronics device and will cause equipment overheating due to the excessive losses and potential malfunctioning of electric equipment.

When voltage profile in distribution system become poor by the voltage drops, this voltage profile needed to be maintained by placing shunt capacitor as reactive power compensator. This voltage drop affects in increasing the energy losses in distribution power system. Energy losses in lines and transformers are of two kinds: resistive and reactive. The former are caused by resistive component of the load and can not be avoided. The latter, coming from reactive component of the load, can be avoided. To have proper understanding about capacitor installation effect in power system, the following Figure 2.1 is shown as follows:

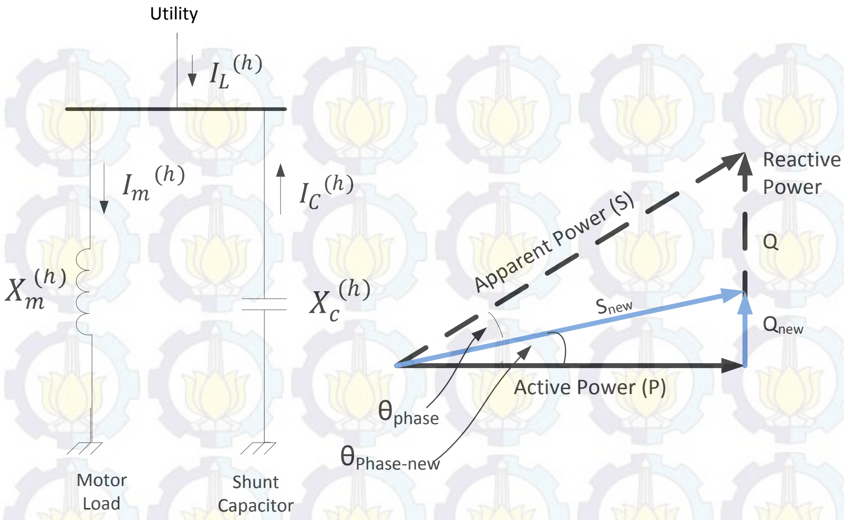

Figure 2.1 Capacitor installation in power system

Without capacitor installed, the current flowing in line, $I_L^{(h)}$ is equal with current flowing in load $I_m^{(h)}$. The current component is also composed from real and imaginary part. However, what contributes in the active power losses is the magnitude of the current which is the power losses comes from line resistance multiplied by square of line current magnitude. But with the installation of capacitor, this shunt capacitor supplied reactive power which produces purely imaginary current or reactive current ($I_C^{(h)}$). This reactive current reduced the imaginary part of the line current which result in the reduction of line current magnitude. This new line current passed through line impedance and thus, the amount of voltage drop is reduce while the power factor of system is improved. This line current reduction also reduced the line power losses. Depicted in Figure 2.1, the power triangle relation shows that the apparent power used in system will decrease when the reactive power decrease. Because of capacitor placement, the total reactive power demand of the system is reduced as much as the amount of installed capacitor which resulted in higher power factor than before installation. Higher power factor provide more apparent power (S) to be utilized to supply more loads. The efficiency of the system will increase.

Therefore, harmonic is very undesirable and have to be maintained well by several standards which have been develop to limit harmonic injections into the power system. IEEE standard 519-1992 limits the harmonic injection by the customers and also those by the electrical utilities itself.

2.3 Objective Function Review and Direct Search Algorithm

Direct Search Algorithm is a heuristic method which is done according to the basic technical guideline which are developed based on experience in practical guidelines (Aman, M.M *et al*, 2014). This algorithm can work fast and effective with the reduced searching space based on practical strategy. This method can be conducted by using sensitivity node, cost consideration, or voltage sensitivity index to obtain the objective. The common approach to this algorithm is by using loss sensitivity analysis to identify the inital placement of the capacitor.

Direct search algorithm is used to yield optimal locations with suitable sizes of capacitors resulting in minimum active power loss and maximum net saving without harmonic consideration (Raju, *et al*, 2012). This algorithm also considers three levels of load which are light, nominal and peak. This condition will place different size capacitors which would be suitable for different load levels at the optimal location for minimizing the total cost function.

$$S = K_e \sum_{j=1}^{L} T_j P_j + \sum_{i=1}^{n_{Cap}} K_c Q_{ci} \quad (US\$) \qquad \text{Equation 2.1}$$

Where,

K_e = the energy cost per each kWh

K_c = purchase cost of capacitor per kVAr

Q_{ci} = size of capacitor placed at i-th bus

n_{Cap} = number of candidate locations

P_j = active power loss during jth load level

T_j = duration for which a j th load level operates

L = type of load level that operates

This objective function Equation 2.1 will accomodate the minimum total cost function of the sistem. To improve the performance of the objective function, (Eajal and El-Hawary, 2010) takes harmonics into account and the objective function become equation 2.2 as follow:

$$F = K_p P_{loss} + \sum_{i=1}^{n_{Cap}} K_{ci} Q_{ci} \quad (US\$) \qquad \text{Equation 2.2}$$

Where,

K_p = Active power loss annual cost per unit (US$/kW/year);

K_{ci} = Reactive power loss annual cost per unit at i-bus (US$/kVAr/year);

Q_{ci} = Injected reactive power at i-bus (kVAr);

n_{Cap} = total unit of reactive power installment;

P_{loss} = total power loss (kW).

Total power loss can be calculated from equation 2.3:

$$P_{loss} = \sum_{i=1}^{n_{branch}} {P_{loss}}^{(1)} + \sum_{i=1}^{n_{branch}} \sum_{h=h_0}^{hmax} {P_{loss}}^{(h)} \quad (kW) \qquad \text{Equation 2.3}$$

Where,

n_{branch} = number of branch;

When compared with power losses at the fundamental fequency, the total value of power losses in harmonic distortion is relatively small. Although, on the portion of harmonics, these losses can be increased according to the increase of harmonic current injection by the sources of harmonics and harmonic pollution in equipment and systems extensively spread.

2.4 Conclusion

Based on the review on previous subsection, therefore, the proposed research will be conducted to obtain optimal reactive power compensator placement and size that located in three phase unbalanced distribution system. The disribution system will be distorted by harmonics that produced by nonlinear load and shunt capacitor. Because of the fact that harmonics always penetrates in the system, it is necessary to include the harmonics consideration in the analysis by using direct search algorithm. With the robustness of direct search algorithm explored in (Raju, *et al*, 2012), the allocation strategy will be derived using direct search algorithm with the help of load sensitivity factor for initial guess. It is applied to achieve more net saving, maintain the voltage profile and keep the THD level within the limit. It will also be compared with the PSO performance to determine the quality of direct search algorithm in optimization of capacitor allocation.

CHAPTER 3
METHODOLOGY

This chapter describes the methodology of the study on the optimal placement and capacity of capacitors in three phase radial distribution system by direct search algorithm. This chapter describe the system modelling, Radial Distribution Power Flow (RDPF), Harmonic Power Flow (HPF), and Direct Search Algorithm.

3.1 System Modelling

Distribution network is a vital connection due to its location which is nearby the customers. Distribution network consists of residential, commercial, and industrial loads. The type of network is not only single phase but also three phase system. This combination will lead to unbalanced condition in distribution system. This unbalance condition can be observed from the phase of transmission lines which are also not always equally loaded and overhead lines in distribution systems are untransposed type unlike those in transmission system. Because of all these factors, distribution system must be modeled differently from transmission system. In harmonics analysis of transmission system, the system component can be modeled by their single-phase positive sequence equivalent models. However, distribution system are totally different from their counterparts in the sense they are inherently unbalanced because multiple single-phase harmonics source (nonlinear loads) and single phase shunt capacitors are distributed throughout distribution system.

The accuracy of system elements and power flow solution are required to manage harmonics analysis, the following characteristics that need to be satisfied are as follows:

- Skin effects representation must be applied on overhead lines and underground cables representation in harmonics-based analysis.
- Representation of nodal impedance matrices or admitance matrices to cover wide range of harmonic frequency.
- Analysis should be capable to identify the spread of multiple harmonics source throughout radial distribution system and analysis must determine system impedance matrices at any load bus to trace resonance condition
- The harmonics current flowing along the feeders in RDS should be obtained at any harmonic frequency
- The other system components should be modeled in detail such as transformer, load, and capacitors).

To be specific, more explanation will be describe as follows:

3.1.1 Overhead Lines and Under Ground Cables

Overhead lines and underground cables are represented as PI model especially for the balance system condition. At this operating conditions, overhead lines and underground cables should be represented by their single-phase positive sequence models (Arrillaga, *et al,* 2003). A series of PI model represents long lines for a more accurate model. Transmission system is linked by series impedance to the rest of system for the PI model representation. Then, two shunt capacitances is applied to take the shape of the symbol PI. To model the three phase short lines, the PI model can also be be implemented in unbalanced distribution systems which can be seen in Figure 3.1. In this analysis, simplified PI model is used by considering only the sequence impedance of the line and neglecting the shunct capacitances.

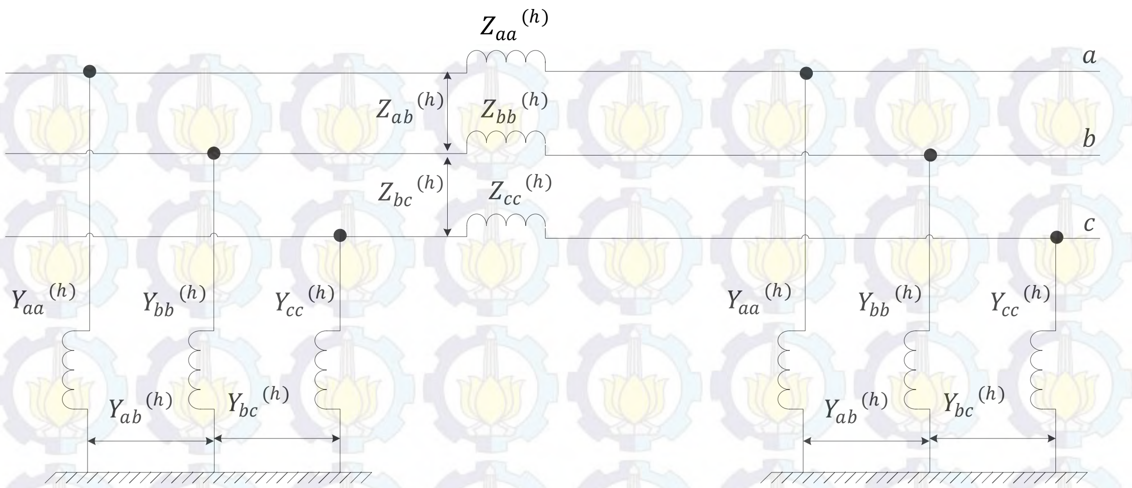

Figure 3.1 PI model of short three phase line

3.1.2 Shunt Capacitors

When the system is high polluted by harmonic, right model of shunt capacitors should be a necessary concern. Shunt capacitor can increase the harmonic distortion levels. Reactive power rating and voltage rating are well specified to define shunt capacitors characteristic. Single-phase shunt capacitors are presented by single phase shunt capacitances while three phase capacitors are described by three phase shunt capacitances. Frequency will be change each capacitor reactance which is defined as follows:

$$X_{Cap}^{(h)} = \frac{{V_k}^2}{hQ_{Cap}} \qquad \text{Equation 3.1}$$

Where,

V_k = the nominal voltage

h = the harmonic order

Q_{Cap} = the capacitor reactive power injection

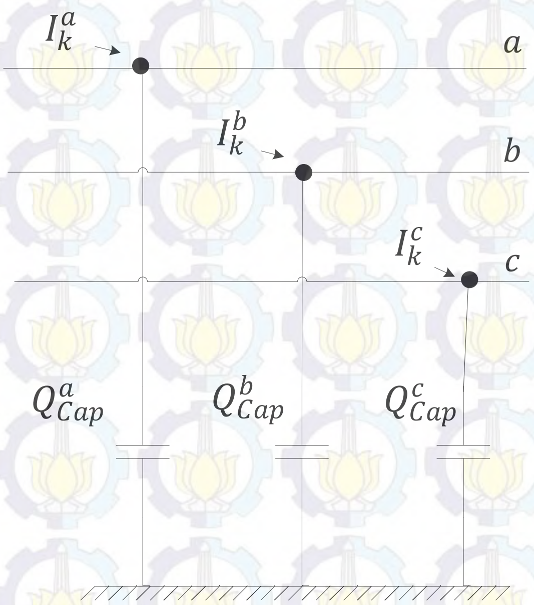

Figure 3.2. Three-phase shunt capacitor model

3.1.3 Three-Phase Transformer

Power transformer can be represented from two impedances which are inductance and resistance. They are the leakage impedance and the magnetizing impedance (IEEE standard 519-1992). Under normal circumstance, operating transformer can be modeled without concerning leakage impedance. Nevertheless, transformer model should always incude the transformer magnetizing part which is represented by a harmonic current source for the saturated operating condition. For harmonic studies, transformer is modelled as reactance in series with resistance and paralelled by shunt resistance as illustrated in Figure 3.3 to replace the leakage impedance (Arrillaga, *et al*, 2003).

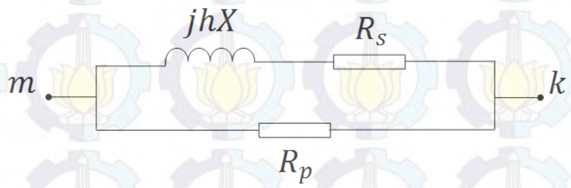

Figure 1.3 Transformer model for harmonic analysis

3.1.4 Linear and Nonlinear Loads

In term of harmonics, load can be described as linear load because this load reacts as passive loads. Reacting as passive loads in the term of harmoncis means eventhough harmonics is high penetrated to the system, linear load will always withdraw the sinusoidal load current without any changing in frequency changing and distortion in the current and voltage output. (Pesonen, M. A., 1981) introduced loads in term of harmonic analysis as shown in Figure 3.4. There are four type of linear load which is A, B, C and D model.

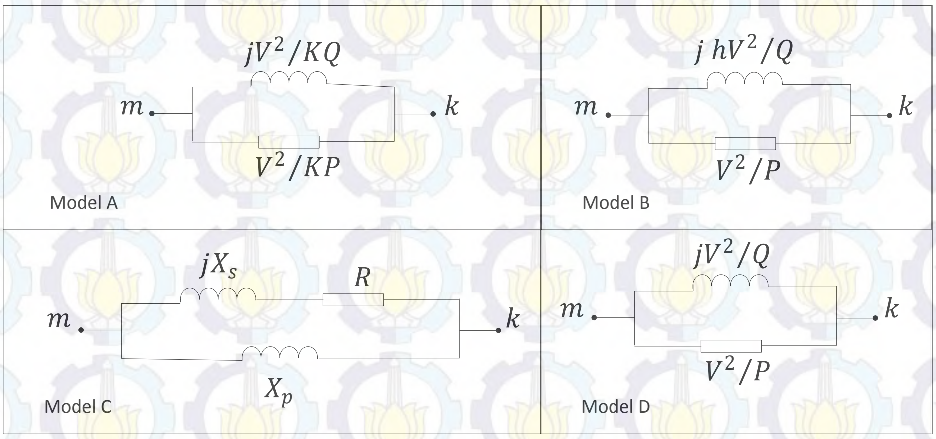

Figure 3.2 Load Models for harmonics analysis

Model A is arranged with single impedance. The impedance is derived from the relation of complex power of the load and the nominal voltage. Model B is set by the resistances that remains relatively has not any changing for all frequencies, while the reactance is considered to change over the range of frequencies. Represented by of a resistance (R) in series with a reactance (X), model C has the resistance and reactance which are both connected in parallel with another reactance (X_p). For a clear understanding, (P) and (Q) stand for the real load and reactive power respectively. The C-model can be described as follows:

$R = \frac{V^2}{P}$ Equation 3.2

$X_s = 0.073hR,$ Equation 3.3

$X_p = \frac{hR}{6.7\,tan\varphi - 0.74} \quad with\ \varphi = \frac{Q}{P}$ Equation 3.4

Model D is basically the load impedance measured at the fundamental frequency and the value of loads impedance remains the same for all frequency.

Nonlinear loads are loads that inject harmonics into distribution system and will cause waveform distortion in voltage or currents which is not sinusoidal anymore. Nonlinear load are commonly modeled as harmonic current sources that injected to distribution system. The harmonic current magnitude of this load is achieved from the relation between the typical harmonic spectrum and the rated current of the load at the fundamental frequency as folow:

$I^{(h)} = I_{rated} \frac{I_{h-spectrum}}{I_{1-spectrum}}$ Equation 3.5

Where,
h-spectrum = typical harmonic-producing load spectrum of the harmonic-producing loads.

Harmonic-producing loads model are represented as constant PQ in the fundamental frequency. After obtaining the rated nonlinear current at the fundamental frequency, the phase angle of the harmonic current can be derived from as follows:

$\theta_h = \theta_{h-spectrum} + h(\theta_1 - \theta_{1-spectrum})$ Equation 3.6

Where,
θ_1 = the phase angle of rated current at the fundamental frecuency.

Eventhough there are citation that described in reference, the information about the actual load composition is still lack. To find the accurate result, it may be important to conduct field measurements for determining the portion of harmonic-producing loads in system. For harmonic analysis, a general load can be represented in Figure 3.5 as follows:

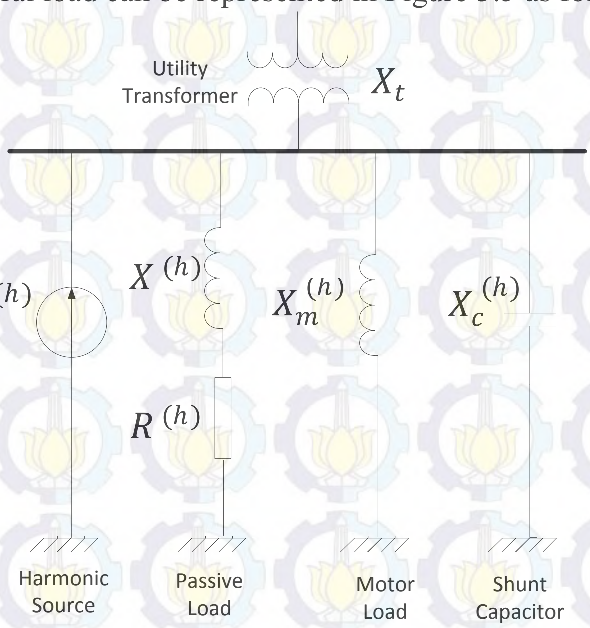

Figure 3.3 General load representation for harmonic analysis

3.2 Data Preparation

IEEE-13-Node-Test-System is used to be applied by this work. The system has 10 MVA Base and line-to-line base voltage is the same as the feeder nominal rating which is 4.16 kV. The test system consist of overhead line and underground line. As shown in Figure 3.6, the line configuration of this test system is unbalance which there are several parts are 3-phase, 2-phase, and 1-phase. The test system supplies both spot load and distributed load which have total amount of power are 1158 kW 606 kVAr, 973 kW 627 kVAr, and 1135 kW 753 kVAr for each phase-A, phase-B and phase-C which is mentioned in Table 3.1 and Table 3.2. The loads are classified as constant power, constant impedance and constant current. More detail information can be seen according to (Distribution System Analysis Subcommittee, 2004).

Loads that produce harmonic are namely flourscent lighting, adjustable speed drive (ASD) and non specific sources such as PCs, TVs and etc are considered. For the spectrum of harmonic and harmonic components that include in the test system, the details of harmonic-producing-load are available in (Task Force in Harmonics Modelling and Simulation, 1996).

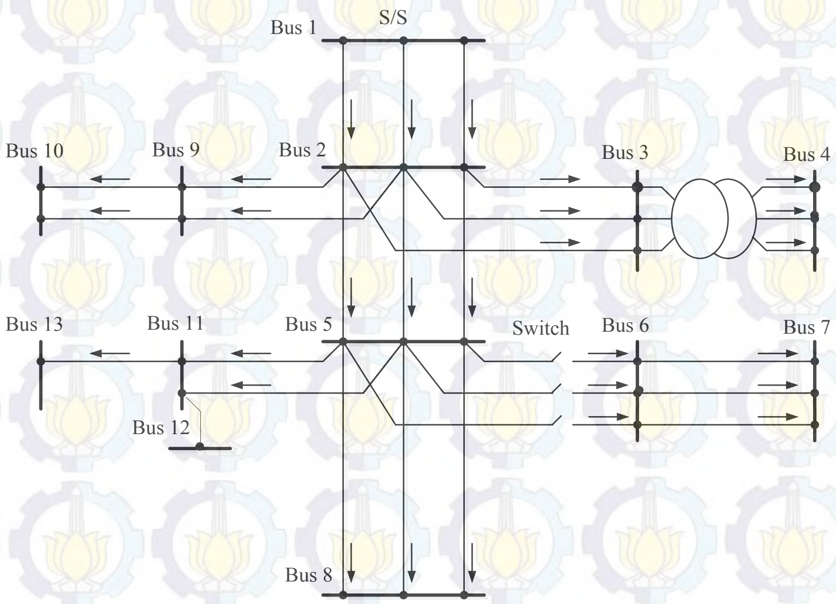

Figure 3.6 13-bus-unbalance-system configuration

Table 3.1 Spot Load Data of 13-bus-Unbalance-System

Node	Load	Phase-A		Phase-B		Phase-C	
	Model	kW	kVAr	kW	kVAr	kW	kVAr
4	Y-PQ	160	110	120	90	120	90
9	Y-PQ	0	0	170	125	0	0
10	D-Z	0	0	230	132	0	0
12	Y-Z	128	86	0	0	0	0
5	D-PQ	385	220	385	220	385	220
7	Y-PQ	485	190	68	60	290	212
6	D-I	0	0	0	0	170	151
13	Y-I	0	0	0	0	170	80
	TOTAL	1158	606	973	627	1135	753

Table 3.2 Distributed Load Data of 13-bus-Unbalance-System

Node A	Node B	Load	Phase-A		Phase-B		Phase-C	
		Model	kW	kVAr	kW	kVAr	kW	kVAr
2	5	Y-PQ	17	10	66	38	117	68

The test system condition as shown in Figure 3.7 is the condition when loads are considered with its harmonics penetration. Bus-3 conected to bus-4 via 3-phase transformer and there is no load in bus-3. Bus-5 to bus-6 are coneccted by switch. Each loads consist of different percentage that shown the parts of involved load such as motor, passive load, flourscent lamp or non specific loads. Node-5 and node-7 are loaded by 3-phase balance load, while node-4 and node-4 and node-12 are loaded only in phase-A. Besides that, node-9 is loaded in phase-B and the rest of the node is loaded in phase-C only. All the details of the load can be seen in Table 3.3 as follows:

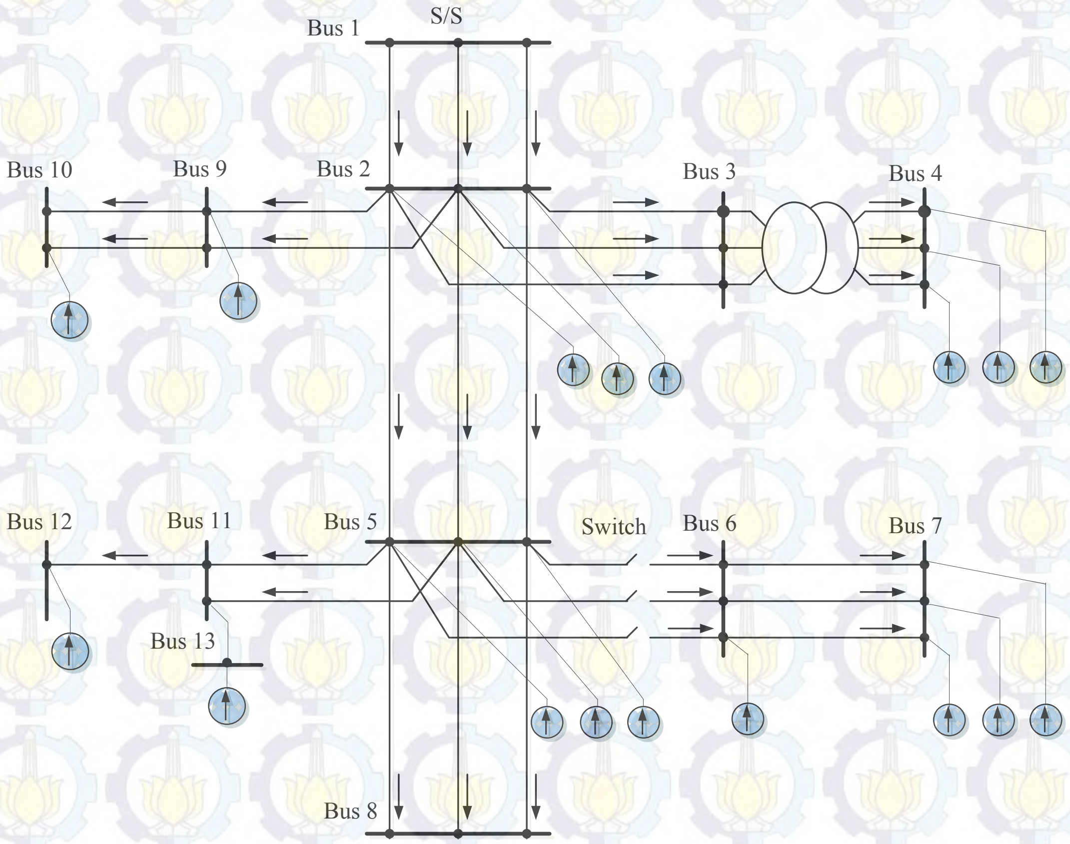

Figure 3.7 13-bus-unbalance-system with harmonic-producing-load

From Table 3.3, the load distribution are mostly centered in phase-C, phase-A and phase-B as the last which the total power of each phase are 1040.25 kW 400.8 kVAr, 1244.14 kW 522.98 kVAr and 622.44 kW 255.5 kVAr respectively. The most influenced harmonic-producing loads are motors in phase-A (12.9% of total load percentage) while phase-C are mostly influenced by passive loads, flourescent lamp and others (16.7%, 7.92% and 5.07% of total load percentage respectively). The system is mostly affected by motors and passive loads which are acted like harmonics loads with 31.25% and 38.33% of total load percentage respectively.

Table 3.1 Load Data

Node	Phase-A		Phase-B		Phase-C	
	kW	kVAr	kW	kVAr	kW	kVAr
4	42.63 Motor Passive	15 60% 40%				
5	383.7 Motors Flou. Passive	140.95 60% 30% 10%	383.7	140.95 60% 30% 10%	383.7	140.95 60% 30% 10%
6					170.53 Motors Flou. Passive Others	51.38 15% 15% 50% 20%
7	468.02 Motors Flou. Passive Others	189.07 15% 15% 50% 20%	468.02	189.07 15% 15% 50% 20%	468.02	189.07 15% 15% 50% 20%
9			170.53 Motors Flou. Passive Other	54 20% 20% 40% 20%		
10					230 Motors Flour. Passive Others	73 20% 20% 40% 20%
12	127.8 Motors Passive Flou. ASD	55.79 20% 60% 10% 10%				
13					170 Motors Flou. Passive Others	45 15% 15% 50% 20%
Total	1,040.25	400.8	622.44	255.5	1,244.14	522.98

For another test system, this harmonic load composition can not be applied. But the percentage of harmonic penetration of non specific load can be taken for the calculation of total harmonic distortion in the system, as mention in (Task Force in Harmonics Modelling and Simulation, 1996).

3.3 Radial Distribution Power Flow and Harmonic Power Flow Method

Power flow analysis performed by network topology approach of RDPF. Network topology approach can determine the model of network by using K-matrix. K-matrix is one part of the graph theory which is also called branch-path incidence matrix (Syai`in, *et al,* 2012; Teng, J. H., 2000). K-matrix is a square matrix with size of (n_{branch} x n_{bus} - 1). n_{branch} is the number of branch while n_{bus} is the number of bus. Line elements of the K-matrix states branch of the system and column elements state the reference bus. K-Matrix is a matrix that describes the route (path) from the bus to the reference bus (bus 1). So that, column of K-matrix starts from bus 2. Value of the K-matrix elements expressed as +1 if the branch is in the path of the bus to the reference in the same direction and vice versa, if the K-matrix elements will be -1 if the branch is in the path of the bus heading in the opposite direction reference (Teng, J. H., 2000). To clarify RDPF algorithm, flowchart of RDPF can be seen from Figure 3.6 as follow:

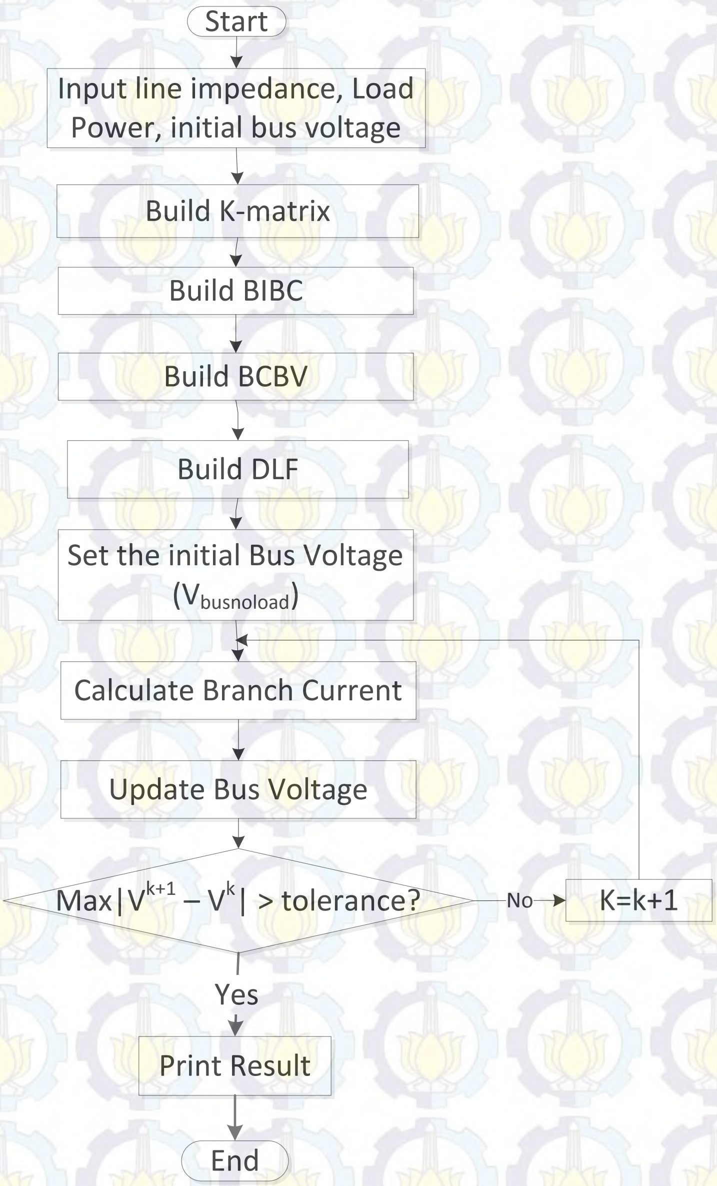

Figure 3.8 Radial Distribution Power Flow (RDPF) flowchart

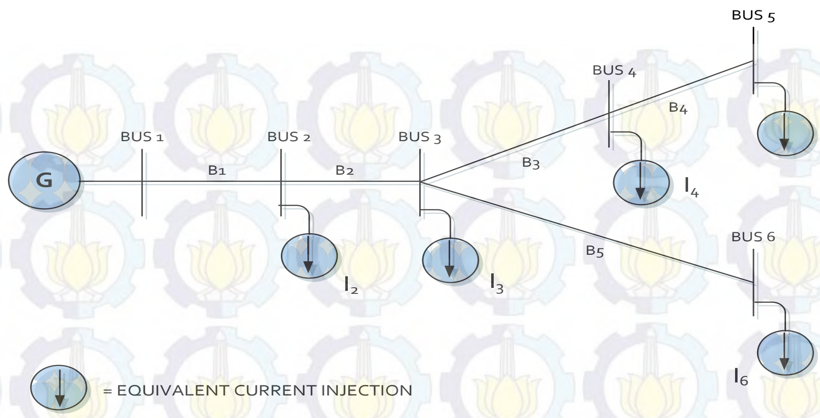

Figure 3.9 Three-phase Radial Distribution Network

$$\begin{array}{ccccc} & & & & & (Bus) & 2 & 3 & 4 & 5 & 6 \end{array}$$

$$K - matrix = \begin{bmatrix} -1 & -1 & -1 & -1 & -1 \\ 0 & -1 & -1 & -1 & -1 \\ 0 & 0 & -1 & -1 & 0 \\ 0 & 0 & 0 & -1 & 0 \\ 0 & 0 & 0 & 0 & -1 \end{bmatrix} \begin{matrix} B1 \\ B2 \\ B3 \\ B4 \\ B5 \end{matrix} \; (Branch)$$

Equation 3.7

Once the K-matrix is formed, the next step is to build a matrix BIBC, BCBV, Full Body Matrix (FBM) and Distribution Load Flow (DLF). FBM is a matrix with the same size as K-matrix but its element consist of impedance of each line.

$$\begin{array}{cccccc} (Bus) & 2 & 3 & 4 & 5 & 6 \end{array}$$

$$BIBC = K - matrix = \begin{bmatrix} 1 & 1 & 1 & 1 & 1 \\ 0 & 1 & 1 & 1 & 1 \\ 0 & 0 & 1 & 1 & 0 \\ 0 & 0 & 0 & 1 & 0 \\ 0 & 0 & 0 & 0 & 1 \end{bmatrix} \begin{matrix} B1 \\ B2 \\ B3 \\ B4 \\ B5 \end{matrix} \; (Branch)$$

Equation 3.8

BCBV and DLF can be calculated with equation 3.8 and 3.9 respectively. Meanwhile, DLF is a matrix which describes distribution system that formed by equation 3.10:

$$BCBV = BIBC' \; x \; FBM$$ Equation 3.9

$$DLF = BIBC \; x \; BCBV$$ Equation 3.10

Then the injection currents and voltages at each bus can be calculated by the equation 3.11 until 3.13.

$$I_{bus(n_{bus})}^{(k)} = \left(\frac{P_{(n_{bus})}^{sh} + jQ_{(n_{bus})}^{sh}}{V_{Bus(n_{bus})}^{(k)}} \right)^{*}$$ Equation 3.11

$$V_{Bus}^{(k)} = DLFx \; I_{bus}^{k}$$ Equation 3.12

$$V_{Bus}^{(k+1)} = V_{bus_{noload}} - V_{Bus}^{(k)}$$ Equation 3.13

Where,

$P_{(i)}^{sh}$ = system real power

$Q_{(i)}^{sh}$ = system reactive power

$V_{Bus}^{(k)}$ = delta bus voltage on k-iteration

I_{bus}^{k} = updated bus current on k-iteration

V_{bus_noload} = initial voltage

k = number of iteration

n_{bus} = number of bus

V_{bus_noload} is the initial voltage on each bus which is equal to the reference voltage, or in other words, V_{bus_noload} is any bus voltage at no-load conditions. Iteration process will stop if $\Delta V_{bus}^{(k+1)}$ is smaller than the tolerance $\Delta V_{bus}^{(k+1)}$ is the voltage difference between $V_{bus}^{(k)}$ and $V_{bus}^{(k+1)}$. The results obtained from power flow process that has been described above are bus voltage magnitudes and angles, branch currents and complex power losses.

To calculate the line losses, it is necessary to have line current data. Therefore, from the relation of BIBC and bus injection current, line current can be calculated by the relation between BIBC and bus injection current which are as follows:

$$I_{line} = BIBC * I_{bus}$$ Equation 3.14

After distribution power flow process is complete, the results will be used by to analyze the influence of harmonics. From Figure 3.8, it can be seen that the distribution network has several sources of harmonics. In general, harmonic source will inject harmonic currents (Ih) which can be divided into two types of source, namely :

1. Harmonic currents from nonlinear loads (Ss) or power electronic equipment.
2. Harmonic currents from Shunt Device (Sh) is the capacitor bank.

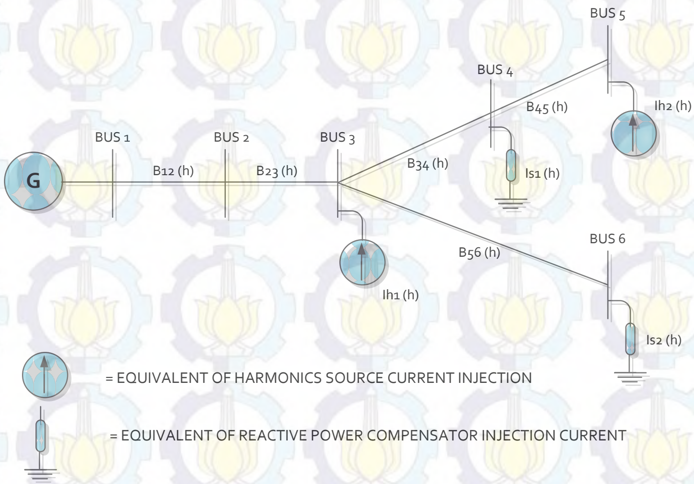

Figure 3.10 Three-phase Radial Distribution Network with harmonic source

Harmonic power flow will form HA-matrix to detect the presence of harmonic sources, differentiating the nonlinear load type and reactive power compensator type. After HA-matrix is known, the harmonic injection currents affecting each bus can be determined through the relationship between the bus voltage, HA-matrix and harmonics order injected by the harmonic source. Harmonic injection current changes will affect the harmonic distortion voltage at each bus. With the iteration process, harmonic distortion votage will reach a steady value after after complete desired error limits. Harmonic distortion voltage will be used to determine the THD on each bus. Simple flowchart of harmonic power flow analysis can be seen in figure 3.9.

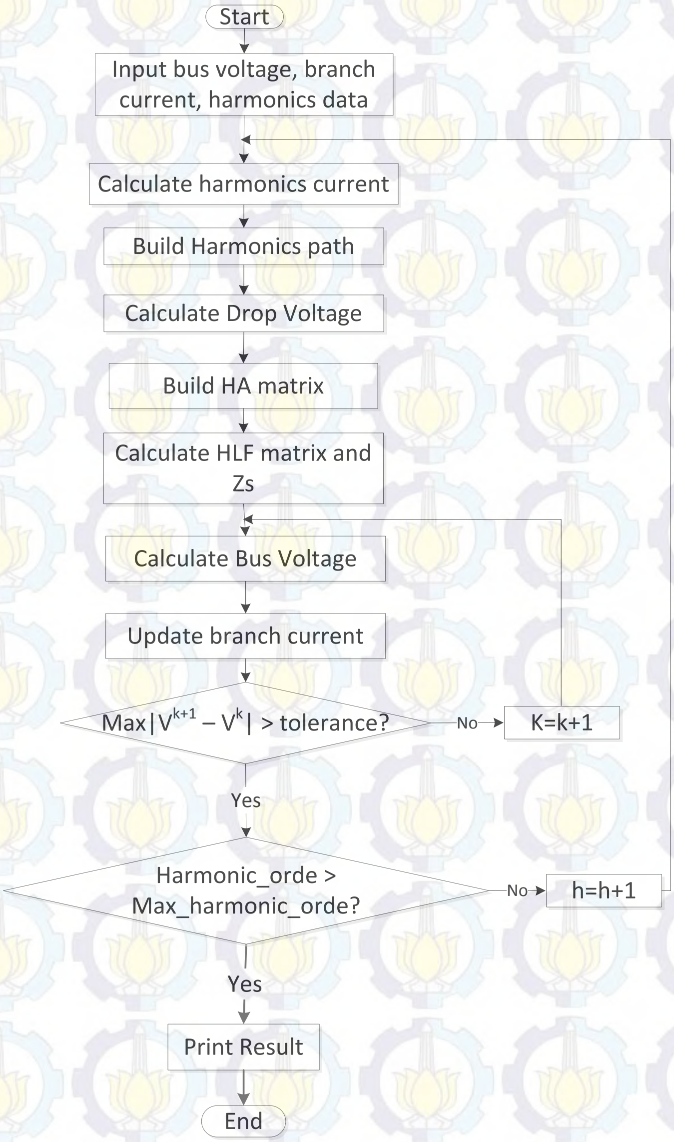

Figure 3.11 Harmonic Power Flow (HPF) flowchart

Therefore, the relationship between the current system with harmonic currents due to harmonic load and shunt capacitors are as follows :

$$\left[\boldsymbol{I}_{n_{bus}}{}^{(\boldsymbol{k})}\right] = \begin{bmatrix} \boldsymbol{Ih}_{n_{bus}}{}^{(\boldsymbol{h})} \\ \vdots \\ \boldsymbol{Is}_{n_{bus}}{}^{(\boldsymbol{h})} \end{bmatrix}$$ Equation 3.15

Where,

$I_{n_{bus}}{}^{(k)}$: system harmonics current

$Ih_{n_{bus}}{}^{(h)}$: harmonics current from nonlinear load

$Is_{n_{bus}}{}^{(h)}$: harmonics current from shunt capacitor

The relationship of the harmonic sources presence can be known through HA-matrix. HA matrix is a matrix that describes the relationship between the bus and the location of harmonic sources. The following equation is an equation for HA-matrix.

$$HA=\left[\begin{pmatrix} 1 & \cdots & H_{n\_H} \\ \vdots & \ddots & \vdots \\ n_{branch} & \cdots & \end{pmatrix} : \begin{pmatrix} 1 & \cdots & S_{n\_S} \\ \vdots & \ddots & \vdots \\ n_{branch} & \cdots & \end{pmatrix}\right] \quad \text{Equation 3.16}$$

Where,
H_{n_H} = Nonlinear load impedance
S_{n_S} = shunt device impedance
n_{branch} = number of branch

Note that there are two sources of harmonics for each source type of harmonic , then the composition of the HA-matrix is as follows :

$$HA = \begin{bmatrix} Z12^{(h)} & Z12^{(h)} & Z12^{(h)} & Z12^{(h)} \\ Z12^{(h)} + Z23^{(h)} & Z12^{(h)} + Z23^{(h)} & Z12^{(h)} + Z23^{(h)} & Z12^{(h)} + Z23^{(h)} \\ Z12^{(h)} + Z23^{(h)} & Z12^{(h)} + Z23^{(h)} + Z34^{(h)} & Z12^{(h)} + Z23^{(h)} + Z34^{(h)} & Z12^{(h)} + Z23^{(h)} \\ Z12^{(h)} + Z23^{(h)} & Z12^{(h)} + Z23^{(h)} + Z34^{(h)} + Z45^{(h)} & Z12^{(h)} + Z23^{(h)} + Z34^{(h)} & Z12^{(h)} + Z23^{(h)} \\ Z12^{(h)} + Z23^{(h)} & Z12^{(h)} + Z23^{(h)} & Z12^{(h)} + Z23^{(h)} & Z12^{(h)} + Z23^{(h)} + Z36^{(h)} \end{bmatrix}$$

$\boldsymbol{H1}$ $\boldsymbol{H2}$ $\boldsymbol{S1}$ $\boldsymbol{S2}$ ....

. Equation 3.17

Harmonic voltage distortion at each bus can be calculated through the relationship between HA-matrix and harmonics injected current. Calculation of harmonic distortion voltage can be calculated through the following equation :

$[Vn_{bus}{}^{(h)}]= [HA] \times [In_{bus}{}^{(h)}]$ Equation 3.18

Where,
$Vn_{bus}{}^{(h)}$: harmonic distortion voltage of h-order at n_{bus}
$In_{bus}{}^{(h)}$: harmonic current of h-order at n_{bus}

By repeating iterations until the error $In_{bus}{}^{(h)}$ to reach the desired tolerance, this proccess will obtain harmonic distortion voltage at each bus in the folowing order. After that, the harmonic distortion at each bus can be determined by the following equation :

$$THD_{n_{bus}}(\%)=\frac{\sqrt{\sum_{h=h_0}^{h_{max}}\left|V_{n_{bus}}^{(h)}\right|^2}}{\left|V_{n_{bus}}^{(1)}\right|^2} \quad \text{Equation 3.19}$$

Where,
$THDn_{bus}$: total harmonic distortion at n_{bus} (%)
$V_{n_{bus}}^{(1)}$: n_{bus} bus voltage magnitude of fundamental frequency

$V_{n_{bus}}^{(h)}$: n_{bus} bus voltage magnitude of harmonics frequency
h_0 : minimum orde of harmonic
h_{max} : maximum order of harmonic

From the previous explanation, distribution power flow yields both magnitude and degree of bus voltage. With this information, power loss in system can be calculated. It need characteristics data of distribution system such as line impedance, initial voltage, number and capacity of loads that installed, geometric mean radius (GMR), and also length of network. After the process, harmonic power flow needs specific data of system loads include linear and non linear load with the harmonics current percentage at every orde of harmonic, transformer and also bus voltage. Harmonic power flow yields the bus voltage in fundamental and harmonic frequencies at each bus. With this information, power loss and THD as the impacts of harmonic penetration in system can be calculated. It is also can sense the increase of system current because of the harmonics.

3.4 Power Losses Calculation

From the previous voltage and current profile, power losses can be calculated. Power losses can be derived from the mismatch between generation power and load power. Before that, power profile on generation and load must be calculated. The following equations will be considered to calculate fundamental power losses.

$$S_{gen} = \sum_{n=2}^{nbus} V_n I_n^* = \sum_{n=2}^{nbus} S_{load} + S_{losses} \qquad \text{Equation 3.20}$$

$$S_{losses} = \{\sum_{n=2}^{nbus} S_{gen} - S_{load}\} = I_{branch}{}^2 . Z_{branch} \qquad \text{Equation 3.21}$$

Where,
S_{gen} = generation apparent power
S_{load} = load apparent power
S_{losses} = losses apparent power
V_n = voltage at bus-*n*
I_n = injected current at bus-*n*
I_{branch} = branch current
Z_{branch} = branch impedance, R+jX

In case of considering harmonic, power loss must be calculated at all harmonic frequencies. The harmonic power losses can be derived from the relationship between node-to-node voltage and admitance of that branch due to each harmonic order as mentioned in equation (3.22) as follows:

$$P_{losses} = \sum_{j=1}^{nbus} \sum_{m=1}^{nbus} V_j{}^{(1)} V_m{}^{(1)} Y_{jm}{}^{(1)} \cos(\theta_j{}^{(1)} - \theta_m{}^{(1)} - \delta_{jm}{}^{(1)}) \qquad \text{Equation 3.22}$$

$$Ploss_{harmonic} = \sum_{n=1}^{nharmonic} Ploss^{(h)} \qquad \text{Equation 3.23}$$

$$Ploss_{harmonic} = \sum_{h=1}^{nharmonic} [\sum_{j=1}^{nbus} \sum_{m=1}^{nbus} V_j{}^{(h)} . V_m{}^{(h)} . Y_{jm}{}^{(h)} \cos(\theta_j{}^{(h)} - \theta_m{}^{(h)} - \delta_{jm}{}^{(h)})]$$

Where,

$Ploss_{harmonic}$ = aggregated active power losses including all fundamental frequency and harmonic frequencies
$Ploss^{(1)}$ = active power losses at fundamental frequency
${V_j}^{(1)}$ = voltage magnitude at node *j* at fundamental frequency
${V_m}^{(1)}$ = voltage magnitude at node *m* at fundamental frequency
${Y_{jm}}^{(1)}$ = admitance between node j-m at fundamental frequency
${\theta_j}^{(1)}$ = voltage angle at node *j* at fundamental frequency
${\theta_m}^{1)}$ = voltage angle at node *m* at fundamental frequency
${\delta_{jm}}^{(1)}$ = admitance angle at node j-m at fundamental frequency
$Ploss^{(h)}$ = active power losses at *h* harmonic frequency
${V_j}^{(h)}$ = voltage magnitude at node *j* at *h* harmonic frequency
${V_m}^{(h)}$ = voltage magnitude at node *m* at *h* harmonic frequency
${Y_{jm}}^{(h)}$ = admitance between node j-m at *h* harmonic frequency
${\theta_j}^{(h)}$ = voltage angle at node *j* at *h* harmonic frequency
${\theta_m}^{(h)}$ = voltage angle at node *m* at *h* harmonic frequency
${\delta_{jm}}^{(h)}$ = admitance angle at node j-m at *h* harmonic frequency

3.5 Direct Search Algorithm Performance

Without using any artificial intelligent, allocation of shunt reactive compensator can be done by simple algorithm namely direct search. Direct search method will specify the suitable size and location based on the power losses and voltage profile of each phase. In case of capacitor placing, the nonlinear integer with discrete variables constraints will be a problem in optimization. The load sensitivity factor will be used to minimize the searching space of this optimization. Direct search algorithm is used to yield minimum objective function whose meaning is that by placing proper size and location of shunt capacitors, a minimum active power loss and maximum net saving with harmonic consideration will be obtained. The objective function will be presented in the form of total cost of power losses that can be compensated due to the installation of some number of capacitor in the system. The following subsections will explain each part to build direct search algorithm for optimal capacitor placement and size.

3.4.1 Objective Function

Objective function is derived to find minimum cost from relation of power losses and reactive power compensated by capacitor placement. Direct search algorithm will lead to find the minimum losses with the suitable number of capacitor according to the reactive power demand. To obtain objective that can accomodate net saving while considering harmonic into account by using direct search algorithm, the objective function as mentioned in (Eajal and El-Hawary, 2010) will be used in equation 3.23 as follows:

$$objective\ function = F = K_p\, P_{losses} + \sum_{i=1}^{\mathrm{n_{Cap}}} K_{ci} Q_{ci} \quad (US\$) \qquad \text{Equation 3.24}$$

Where,
$\mathrm{K_p}$ = Active power loss annual cost per unit (US$/kW/year);

K_{ci} = Reactive power loss annual cost per unit at i-bus (US$/kVAr/year);
Q_{ci} = Injected reactive power at i-bus (kVAr);
n_{Cap} = total unit of reactive power installment;
P_{losses} = total power loss (kW).

To take harmonic into account, power losses that used will be the total losses will be the aggregated power that takes fundamental frequency and all order of harmonic penetration into power losses calculation. Total power loss can be calculated from equation 3.24 which is as follows:

$$P_{losses} = \sum_{i=1}^{n_{branch}} P_{loss}^{(1)} + \sum_{i=1}^{n_{branch}} \sum_{h=h_0}^{hmax} P_{loss}^{(h)} \quad (kW)$$ Equation 3.25

Where,
n_{branch} = number of branch;
h_0 = first harmonic orde;
h_{max} = maximum harmonic order;

The cost of losses is assumed as USD 168 kW/year in reference (Eajal and El-Hawary, 2010). This cost is coming from the relation between energy cost, total utilization time for losses per year and capacity factor of the power plant. It is assumed that the power plant is gas fired power plants (Jordanger, *et al*, 2001) which is a natural gas power plant with either conventional nor advance combustion turbine which whose capacity factor is around 32%. The power plant is assumed to be utilized at 24 hour every day in a year. The following equation will show the relation of each parameter to obtain price of losses:

$$Kp = energy\ cost\ x\ utilization\ time\ (annual)\ x\ capacity\ factor$$ Equation 3.26

$$Kp = (\ 0.06\ US\$/kWh)x\ (8760\ h)x\ (0.32) = 168.2\ US\$/kWh\ per\ year$$

Where,
Average Energy cost = 0.06 US$/kWh (Fergany and Abdelaziz, 2014)
Capacity Factor of Natural gas power plant type Conventional Combustion Turbine = 30-35%*

(*Source: Levelized Cost and Levelized Avoided Cost of New Generation Resources in the Annual Energy Outlook 2014, www.eia.gov, Date of Release: April 17, 2014. Date of Access: July 07, 2014)

3.4.2 Equality and Inequality Constraints

To approach the minimum objective function, the voltage and THD level of the system must be kept within the proper limit. Therefore, the system needs to be constrained by equality and inequality constraints. Equality constraint is all about dealing with the nonlinearity of the power flow calculation is used. Inequality constraints consists of bus voltage, THD levels and reactive power compensator to be installed. Restrictions that given to achieve the most efficient optimization is as follows :

1. Bus Voltage, $V_{min} \leq |V_i| \leq V_{max}$

2. THD level, $THD_{bus}(\%) \leq THD_{max}$
3. Reactive compensator (shunt capacitor size), $n_{tcap} \cdot Q_{cap} \leq Q_{demand}$

3.4.3 Load Sensitivity Factor

Load sensitivity factor (LSF) is predictor factor that estimated the lowest losses reduction while the reactive capacitor is installed to the system. Bus condition that has high losses and lower voltage will be more identified as a prospective candidate of solution. The more addition of reactive power injected by capacitor will result in the more power losses abatement. The following equation (3.25) and (3.26) will present the load sensitivity factor in fundamental frequency and aggreagated frequency including harmonic frequency:

$$LSF - fund = \frac{\partial P_j{}^{(1)}}{\partial Q_j{}^{(1)}} = \frac{2 \times Q_j{}^{(1)} \times R_{ij}{}^{(1)}}{V_j{}^{(1)}} \quad \text{Equation 3.27}$$

$$LSF - aggre = \frac{\partial P_j{}^{(h)}}{\partial Q_j{}^{(h)}} = \frac{2 \times Q_j{}^{(h)} \times R_{ij}{}^{(h)}}{V_j{}^{(h)}} \quad \text{Equation 3.28}$$

Where,

P_j = active power loss at bus-j (kW)
Q_j = reactive power loss at bus-j (kVAr)
R_k = line resistance at branch- ij (kVAr)

While the prospective bus is already arranged by the constraints mentioned in subsection (3.4.2), load sensitivity factor will be arranged the order of the prospective bus by arranging the LSF value into descending order. Direct search algorithm will consider LSF to decide the order of recieving-end line for locating the capacitor. This factor will help to reduce the searching space of direct search algorithm in locating best size of compensator. Recieving-end buses that has higher LSF and lower voltage profile have more chance to be placed as the prospective location for obtaining the objective function.

3.4.4 Direct Search Algorithm Applied on Test System

Based on the power flow analysis, direct search algorithm is applied to find the most approriate location and capacity of reactive power compensator. The following rationals are the assumptions to do direct search algorithm which are as follows:

1. The maximum system losses is determined from the result of power flow analysis. This uncompensated loss is considered to be maximum loss in the system.
2. Capacitor placement is determined with the minimum system condition where there is no reactive power compensator on all buses ($Q_{compensator} = 0$). This assumption will be taken to approach the minimum reactive power loss ($Q_{loss\_bus} \approx 0$). This step will be done to aim the optimal size of capacitor size and location
3. All locations and capacity compensator of each bus will be evaluated on a limited range between the maximum and minimum voltage constraint. The prospective minimum loss is limited to have THD within the minimum and maximum THD constraint
4. When it is required to compensate the largest amount of reactive power, algorithm will do some searching by multiplying of the smallest capacity of reactive power compensator availeable to reach the required value. This step will be continue till the number of capacitor size already tried to the following objective.

5. From step 3, to evaluate and search the total active power losses with the level of THD under maximum THD limit

Based on the above objective functions and supported data, direct search algorithm can be done through the following steps :

1. The maximum loss of system is determined from the total reactive power demand of test system. This uncompensated loss is considered to be maximum loss in the system.
2. Loss is determined as the worst system condition where there is no reactive power compensator on all buses ($Q_{cap} = 0$)
3. Find prospective buses which is within the constraint $V_{min} \leq |V_i| \leq V_{max}$
4. Calculate loss sensitivity factor and sort the prospective bus in descending order.
5. Normalize the voltage with the following equation (3.27) and select the prospective buses whose voltage is lower than minimum voltage limit.

$$norm(j) = \frac{V_j}{V_{base}} \qquad \text{Equation 3.29}$$

6. Because there are some options of capacitor size, run the power flow for each capacitor size for all the number of possible prospective buses from step , keep each result on matrix that represent number of prospective buses. The following table will represent the number of capacitor size and price for each kVAr

Table 3.4 Capacitor Size and Price

Q_c (kVAr)	150	300	450	600	750	900	1050	1200	1350	1500
K_c ($/kVAr)	0.500	0.350	0.253	0.220	0.276	0.183	0.228	0.170	0.207	0.201

7. Calculate the objective function (3.23), save the solution.
8. Find the lowest cost from the previous calculation. Update the minimum objective function refference.
9. Repeat point 1-8 with the next capacitor size. Find the position of capacitor that resulting lowest objective function among different capacitor size. Save the position as the result.

Direct search algorithm analyzes and chooses optimal capacitor placement in particular bus and yield the best performance that will limit the harmonics penetration in system within the range of allowable limit of THD. The capacitor placement considers the reactive power demand as maximum reactive power compensation limit to avoid overcompensated system by the placement of capacitor. Computational procedure of strategy DSA algorithm shown in figure 3.10 as follows.

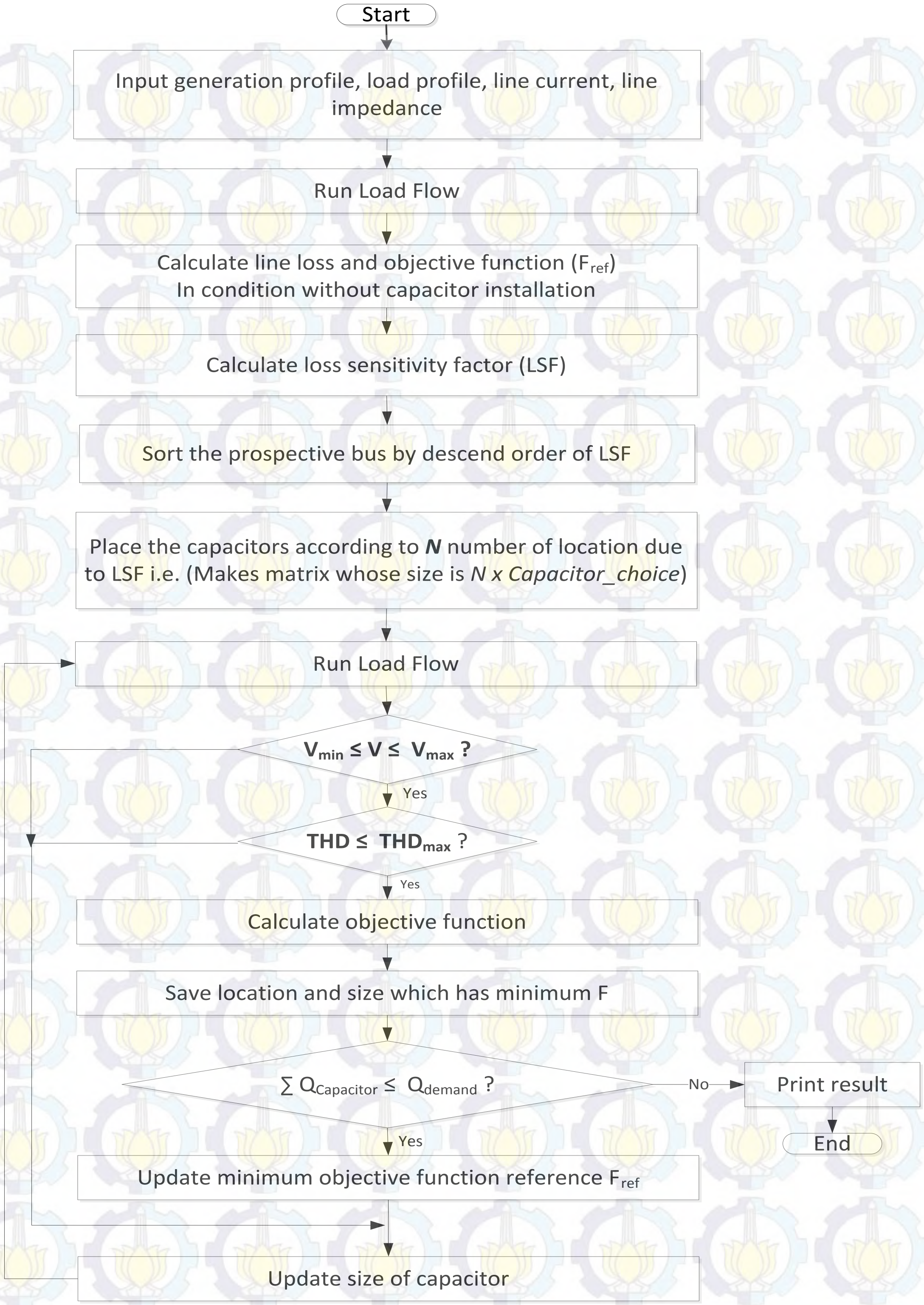

Figure 3.4 Direct Search Algorithm Flowchart

The steps which are performed in Figure 3.12 are as follows :

1. As the initial data, the direct search algorithm requires initialization of data such as bus voltage, line impedance, and the load power for each harmonic order and fundamental frequency. The initial data used for harmoonic power flow. Harmonic power flow will generate bus voltages and currents at fundamental frequency.

2. Those data will be used by power flow to analyze THD level in every bus in the system in any order harmonics. Power flow will identify THD level and harmonic voltage of the system.
3. Calculate the power generation, power demand and power losses from the voltage and current profile that obtained before. Then, calculate the objective function before capacitor installation and save that objective function as reference for the next capacitor sizing process.
4. With the result of load flow, calculate the loss sensitivity factor (LSF) and sorts the bus based in descending order. The bus that has highest LSF will be prioritized first because LSF is defined to identify which bus suffered reactive power the most.
5. Determine how many location to be placed with capacitor, the number of this locations is taken from the sorted prospective bus by LSF.
6. All capacitor choices is placed in the prospective bus. After that, the load flow is called to calculate the losses after capacitor placement.
7. Check the results. If the voltage profile after capacitor placement exceeds the voltage constraint, change the capacitor size. The same process is done for the THD constraint.
8. Then, the objective function is computed. Find the minimum objective function and save the index of location and capacitor size that yield the minimum objective function.
9. Check the reactive power injected by shunt capacitor. If the total reactive power of shunt capacitor is below the reactive power demand, another shunt capacitor can be added. But, if the total reactive power of shunt capacitor is exceeds the reactive power demand, the process is stopped and the previous total installed shunt capacitor is saved as the final size of each location.
10. When the total reactive power of shunt capacitor is below the reactive power demand, update the reference of minimum objective function and update the size of capacitors. Then, repeat the following step 6-9

CHAPTER 4
RESULTS AND DISCUSSION

This chapter describes result of simulations that done according to the methodology of the study on the optimal placement and capacity of capacitors in three phase radial distribution system by direct search algorithm. The simulation approaches will be classified as two parts which are harmonic power flow simulation and direct search algorithm.

4.1 Harmonic Power Flow

Load data specification is mentioned in Table 3.1, 3.2 and 3.3 while the line configuration and harmonic load composistion in system is depicted in Figure 3.6 and 3.7 repectively. After the data preparation is done, those datas are used as the initial value of power flow. In details, those data are line connection, line configuration, line impedances, load data, harmonic data and initial voltage profile. The steps of the harmonic power flow can be calculated as follows:

4.1.1. Building BIBC Using K-Matrix

Line configuration in Figure 3.6 will be extracted to K-matrix whose size is number of branch square. Because the total number of bus is 13, then the the number of branch will be 13-1=12 and because it is 3-phase system, the size of K-matrix is 36 x 36. The following K-matrix can be seen in detail at Figure 4.1 which is -1 because the current flows from substation to each loads.

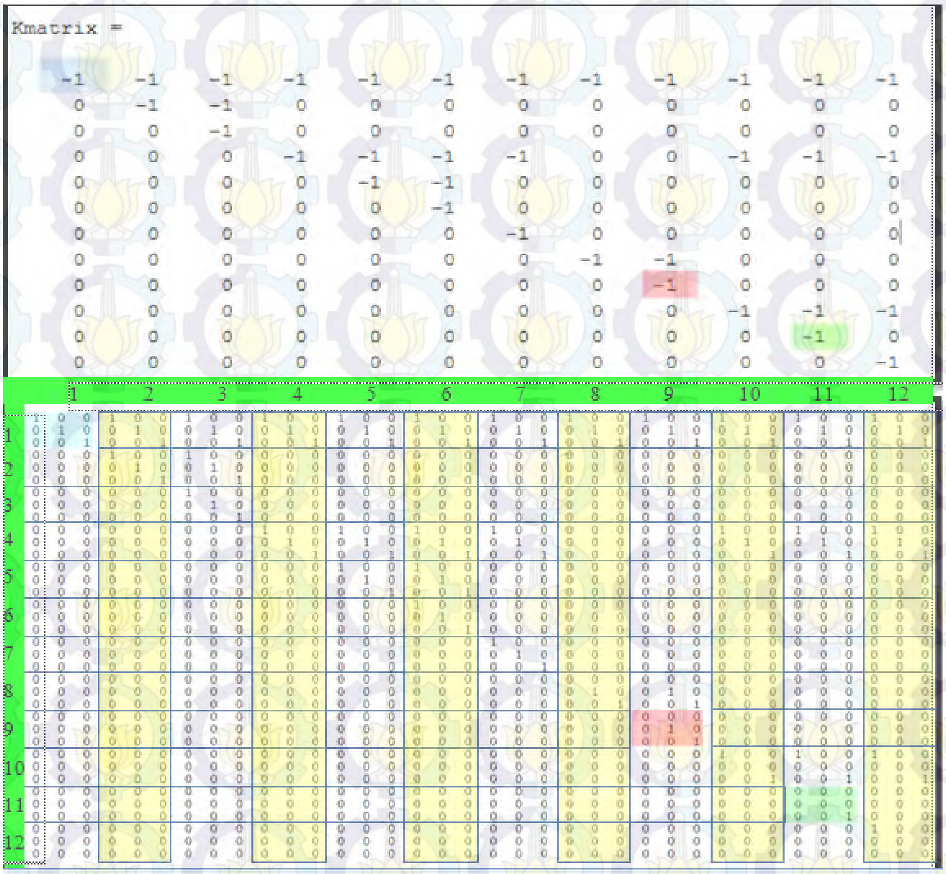

Figure 4.1 (upper) 1-phase-K-matrix of 13-bus-test-system (lower) 3-phase-BIBC-matrix

Blue box in Figure 4.1 represents one sample of 3-phase configuration, while red box and green box represent 2-phase and 1-phase configuration respectively. 3-phase configuration has full diagonal element, which is 1st, 2nd, and 3rd of diagonal element represent phase-A, phase-B and phase-C respectively. If only two phase, for example is B-C configuration, the matrix element will be only filled in 2nd and 3rd diagonal element. To simplify the understanding, the upper parts of Figure 4.3 represents single-phase-K-matrix (12x12 size) which is amplified to become (36x36). After that BIBC can be simply found by multiplying K-matrix with -1. So that, the bottom part of Figure 3.6 for representing three-phase line configuration is shown and all the elements of this matrix is zero or 1.

4.1.2. Building BCBV matrix using BIBC and FBM matrix

Once the K-matrix and BIBC are formed, the next step is to build BCBV matrix. BCBV can be composed by multiplying the transpose of BIBC matrix with Full Body Matrix (FBM). FBM is matrix whose elements are consisted of both mutual impedances and line impedances. Diagonal element of FBM matrix will be the line impedance while the off diagonal represents the mutual impedance between two two phase. The matrix element of diagonal element will be also done with 1st, 2nd and 3rd of diagonal element represent the phase-A, phase-B and phase-C. FBM size is the same as BIBC size which is 36x36. All the rows of each column will be consist of impedances due to the line configuration. Each column is kept going due to the total number of branch. FBM matrix, can be seen in appendix on figure A.1 to A.4, has zero elements in column-7 until column-9 and column-19 until column-21. Column-7 until column-9 represents transformer at branch-3 and the other represents switch at branch-7. This condition happens because that branch is switch or transformer which assumed as having no impedances.

Then, BCBV can be calculated by multiplying the transpose of BIBC matrix with Full Body Matrix (FBM). The result of that will be similar to transposed BIBC whose element is impedances due to the configuration. In appendix, Figure A.5 until Figure A.8 shows the BCBV matrices which has size 36x36. This BCBV matrix represents the correlation between branch current to bus voltage which can be seen from the relation between impedance of the branch and path of the current flows.

The third column of BCBV matrix has zero elements in all rows of this column because in FBM matrix column-3 also has zero elements. That column become zero because column-3 represent branch-3 and there is a transformer in that branch, which connects node-3 and node-4. Same condition can be seen in the column-7 of BCBV matrix. This column also has zero elements because column-7 represents connection between node-5 and node-6 which is functionate as switch.

The other elements in column 8, 9, 10, 11, and 12 are combined with zero elements and impedance element. This is happened because of the line configuration of the system. The configuration consists of 1-phase and 2-phase which are phase-A-B, phase-A-C or phase-B-C.

4.1.3. Building DLF matrix

DLF is stand for Distribution Load Flow which is calculated by multiplying BIBC matrix with BCBV matrix. Every elements of DLF's matrix is consisted of line impedance or mutual impedance due to the configuration. Off diagonal is consisted of mutual impedance while diagonal is consisted of line impedance. Figure A.9 until Figure A.12 in appendix shows the DLF matrix which has size 36x36. DLF matrix represents the correlation between branch current which can be expressed from BIBC matrix and bus voltage which can be expressed from BCBV matrix. This matrix will be constant in every iteration because impedance of the system will be expressed as constant impedance. DLF matrix is used to find the mismatch of the voltage. The DLF is multiplied by current to extract initial voltage mismatch.

4.1.4. Finding the Updated Current and Voltage

Current for calculation can be derived from conjugated division of apparent power and bus voltage as mentioned in equation (3.11). At first iteration, apparent power is derived from the load data which is known at the beginning of data preparation. The bus voltage is derived from the initial bus voltage which is 4.16 kV for every node in which the degree of the voltage is 0^0, -120^0, and 120^0 due to the phase-A, phase-B and phase-C.

Then, DLF-matrix is multiplied by the current to obtain voltage mismatch at each bus. This voltage mismatch is the loss between initial voltage in main substation to the end node. The process from finding the current to voltage mismatch is calculated in the loop iteration until the error requirement fulfill the limit ($error<=10^{-5}$). With using 13-bus-test-system as the test system, iteration goes until 19-iteration to obtain error requirement. As mentioned in Table 4.4 and Table 4.5 which are showing the current profile on bus and branch respectively, bus current profile of varies between 2,118 Ampere to 134,950 Ampere while branch current varies between 22,07 Ampere to 300,11 Ampere. The following Table 4.1 is as follows:

Table 4.1 Bus Current

Bus	**Bus Injected Current**					
	Phase-A		**Phase-B**		**Phase-C**	
	mag. (Ampere)	*Angle(°)*	*mag. (Ampere)*	*angle(°)*	*mag. (Ampere)*	*angle(°)*
2	2.118	-37.773	18.623	-150.608	17.5708	83.7671
3	0	0	0	0	0	0
4	60.724	-34.786	37.351	-158.008	39.4492	80.3387
5	67.069	-34.174	108.354	-150.63	87.2358	86.7856
6	0	0	0	0	35.4193	74.2947
7	134.950	-26.523	22.068	-162.635	98.6448	80.1196
8	0	0	0	0	0	0
9	0	0	52.988	-156.779	0	0
10	0	0	0	0	65.1724	97.9622
11	0	0	0	0	0	0
12	35.918	-28.557	0	0	0	0
13	0	0	0	0	49.7773	99.8551

For Table 4.1**,** the first column represents the order of bus without slack bus. the second and third column represent the current for phase-A, fourth and fifth column represent phase-B and phase-C is represented by sixth and seventh column. the trend of the current profile are bus-2 has relatively light value in comparison with bus-7 this is because, bus-2 is supplying small load. Bus-7 phase-A is loaded by heavy load and because of this condition, this bus withdrawn more current than the other bus in phase-A. For the whole comparison, bus-2 in all phases, are loaded by light load because the current in this phase is relatively less than current that withdrawn at the other bus. The zero value which can be seen at bus-3, bus-8, bus-6 phase-A, for example, happened because those location are not loaded by any load.

For Table 4.2**,** the first and second column represents the order of line or branch. The third and fourth column represent the line current for phase-A, fifth and sixth column represent phase-B and phase-C is represented by seventh and eighth column. The trend of the line current will be flowing from the slack bus to the end of the bus which is represented by each row. More current will be there in beginning branch and less remaining current will be in the ending branch. For example, for phase-A, branch-1-2 is located at the beginning of the system. From branch-1-2, the current is flowing to three other branch which is branch-2-3, branch-2-5 and branch-2-9 respectively. These branches will also connect to the another branch for example: branch-2-3 will connected to branch-3-4. With this system's topology, according to the Kirchoff's Current Law, the current flowing in branch-1-2 will be more than current flowing in branch-3-4. The current in branch-2-3 phase-A has the same value with current in branch-3-4. This phenomenon happens because the load is located on bus-4 and there is no load in bus-3. The current will flow through branch-2-3. Similar explaination for the the other phase. Beside that, the value of current is decreased by the line impedance that located in every branch, except for branch that has transformer or switch, it is assumed that this branch does not has line impedance.

Table 4.2 Line Current

Branch Number		**Line Current**					
		Phase-A		**Phase-B**		**Phase-C**	
		mag. (Ampere)	*Angle (°)*	*mag. (Ampere)*	*Angle (°)*	*mag. (Ampere)*	*Angle (°)*
1	2	300.11	-30.22	238.76	-154.25	388.97	86.70
2	3	60.72	-34.79	37.35	-158.01	39.45	80.34
3	4	60.72	-34.79	37.35	-158.01	39.45	80.34
2	5	237.54	-28.99	130.02	-152.65	268.40	85.11
5	6	134.95	-26.52	22.07	-162.63	133.93	78.58
6	7	134.95	-26.52	22.07	-162.63	98.64	80.12
5	8	0	0	0	0	0	0
2	9	0	0	52.99	-156.78	65.17	97.96
9	10	0	0	0	0	65.17	97.96
5	11	35.92	-28.56	0	0	49.78	99.86
11	12	35.92	-28.56	0	0	0	0
11	13	0	0	0	0	49.78	99.86

Table 4.3 are showing the bus voltage profile which are the result after load flow running. First column of the table represent the order of bus, while the second and third column represent the voltage of phase-A. The fourth and fifth column represent the voltage of phase-B as well as the rest of the column for phase-C. The following Table 4.3 is as follows:

Table 4.3 Voltage Profile

Bus Number	Phase-A		Phase-B		Phase-C	
	Mag. (pu)	*angle* (◦)	*Mag.* (pu)	*angle* (◦)	*Mag.* (pu)	*angle* (◦)
1	1	0	1	-120	1	120
2	0.976	-2.235	0.983	-120.676	0.937	117.457
3	0.962	-2.631	0.977	-120.87	0.927	117.515
4	0.944	-3.163	0.965	-121.138	0.914	117.209
5	0.957	-4.535	0.984	-120.885	0.889	115.892
6	0.957	-4.535	0.984	-120.885	0.889	115.892
7	0.928	-5.13	0.988	-121.211	0.875	116.288
8	0.957	-4.535	0.984	-120.885	0.889	115.892
9	0	0	0.957	-120.452	0.916	116.446
10	0	0	0.955	-119.993	0.89	115.571
11	0.947	-4.963	0	0	0.869	115.441
12	0.935	-4.928	0	0	0	0
13	0	0	0	0	0.849	114.682

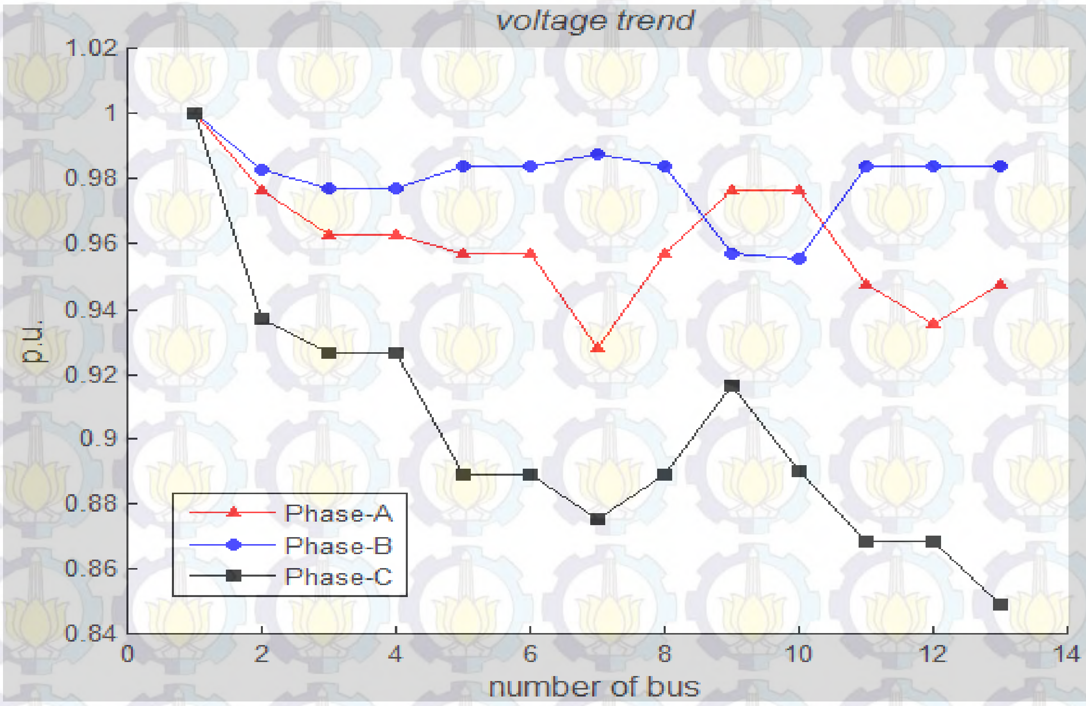

Figure 4.2 Voltage profile of 13-bus test system

Table 4.3 has similar trend with the line current in Table 4.2, the voltage in the sending-end bus of the system will have better voltage than the voltage in the recieving-end bus. Due to the topology of the system, which is for example, first bus path is bus-1-2-3-4. Bus-1 will have better quality of voltage while the voltage is decreased more and more by the voltage drop caused by line impedance between bus-1 and bus-4 (as the sending and recieving end bus). The little difference of voltage trend can be seen in second path which is bus 1-2-5-6-7. For phase-A of this path, the recieving-end bus will have less voltage than sending-end bus but bus-5 and bus-6 has the same voltage value. This phenomenon happened because branch-5-6 is a switch that is assumed to have no impedance that caused voltage drop. For phase-B, the voltage trend is not decreasing, but it is increasing. This phenomenon happened because the line impedance of the branch in this path is fifty percent less than impedance in phase-A while the load distribution in this path is unbalanced. the phenomenon phase-C at path in bus 1-2-5-6-7 is similar with phase-A. From the following table, the voltage drop happened in every branch and decrease the voltage profile in the recieving end of the system. while the heavier load is installed in the bus will withdraw more current and leads to make more voltage drop in the system. That phenomen of voltage drop is illustrated in Figure 4.2 which voltage near the slack bus is better than voltage at recieving-end bus.

4.1.5. Finding Total Harmonic Distortion

Total harmonic distortion level in voltage base can be derived from the relationship between harmonic injected current and impedances of system due to harmonic order. Harmonic current can be derived from impedance of harmonic load. This impedance will amplified due to the harmonic order. In harmonic power flow, load impedance that varies due to harmonic order will be saved in HA-matrix. HA matrix show the relation between number of bus and harmonic sources location. Figure A.13 and Figure A.14 in Appendix shows the HA-matrix that has sized at 36x18. HA-matrix represents that there is 6 harmonics loads that penetrate to the system and because this is a three-phase representation so that the size is multiplied by 3 and become 18.

Each element of HA-matrix will be added from each impedances that lied between first node to the end node. So each element due to the node position is the sum from impedances between that node to the first node. This impedance again will varies according to harmonic order. So that, in one running of the program, HA-matrix will be sized as nbus x nload x nharmonic. Those nbus, nload and nharmonic represent number of bus, number of harmonic load, and number of harmonic order respectively.

Once HA-matrix has build, harmonic voltage distortion at each bus can be calculated through the relationship between HA-matrix and harmonics injected current. Harmonic current is derived from HA-matrix multiplied by injected current. The injected current will be derived from percentage of harmonic penetration from each harmonic loads. This current is divided into two type of harmonic current, which are shunt capacitor and harmonic-produced-load current. Table 4.7 show about the harmonic current that injected to the system. From the units, it can be seen that the value of harmonic current is small (in micro Ampere). Although this current is relatively small, when this current is crossing the impedance, this will create some number of harmonic voltage that can be counted as voltage drop that resulted in power losses. The result can be seen in Figure 4.4.

Table 4.4 Harmonic Injected Current

Iteration = 1			
Branch	Mag. (uA)	Branch	Mag. (uA)
1-2 A	0.0441	5-8 A	0.0441
1-2 B	0.0424	5-8 B	0.0416
1-2 C	0.0286	5-8 C	0.0315
2-3 A	0.0441	2-9 A	0.0441
2-3 B	0.0424	2-9 B	0.1022
2-3 C	0.0286	2-9 C	0.0196

3-4 A	0.0441	9-10 A	0.0441
3-4 B	0.0424	9-10 B	0.1044
3-4 C	0.0286	9-10 C	0.0249
2-5 A	0.0441	5-11 A	0.0918
2-5 B	0.0416	5-11 B	0.0416
2-5 C	0.0315	5-11 C	0.0335
5-6 A	0.0441	11-12 A	0.0918
5-6 B	0.0416	11-12 B	0.0416
5-6 C	0.0315	11-12 C	0.0335
6-7 A	0.0441	11-13 A	0.0918
6-7 B	0.0416	11-13 B	0.0416
6-7 C	0.0315	11-13 C	0.0335

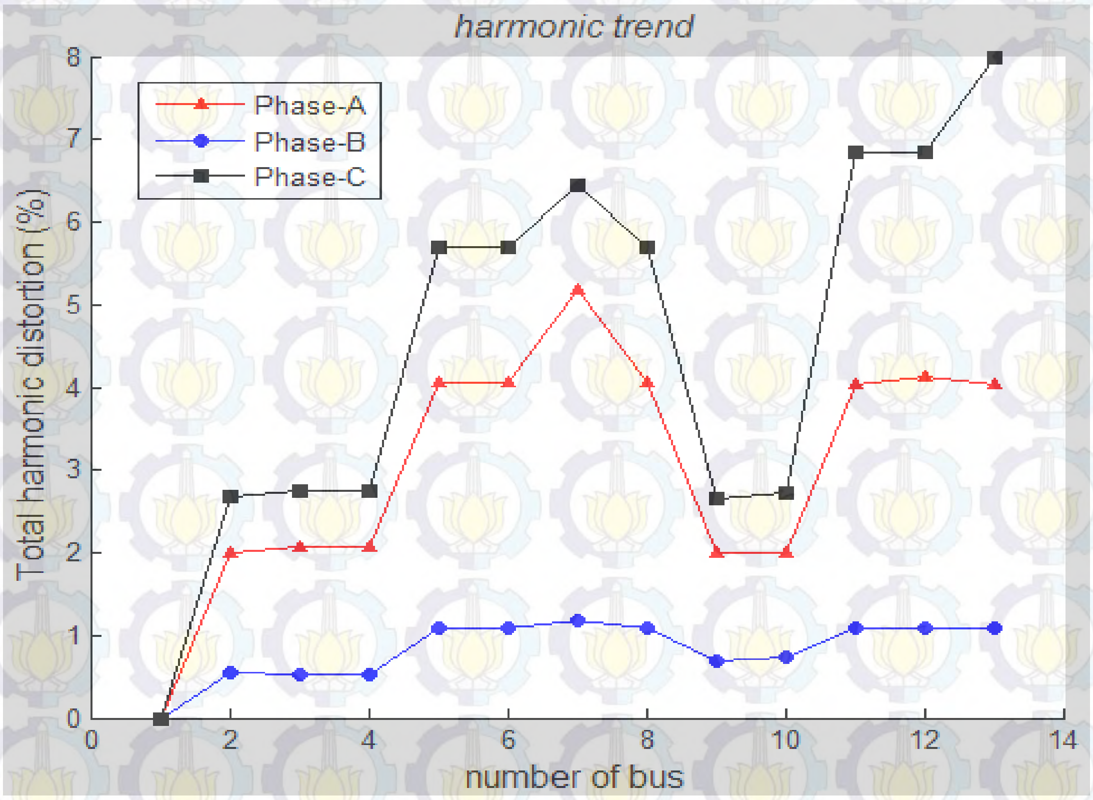

Figure 4.3 Total Harmonic Distortion

From Figure 4.3, the trend of harmonics are mostly penetrated between 0.4% to 8%. The lowest THD voltage level is occur in bus-4 for phase-B while the highest harmonic penetration happens in bus-13 for phase-C. With information that have been derived before such as voltage profile, current profile, and harmonic trend, power loss in system can be calculated.

4.2 Power Generation and Power Demand

With the previous load profile in subsection 1, loadflow uses that power demand profile, line impedance and initial voltage to calculate the power generation which is needed by the test system. The update power generation is derived from the relation between apparent power, current and voltage of loadflow result which is clearly explain in equation (3.19) and (3.20) as follows:

$$S_{gen} = \sum_{n=2}^{nbus} V_n I_n^{\,*} = \sum_{n=2}^{nbus} S_{load} + S_{losses} \qquad \text{Equation 3.19}$$

$$S_{losses} = \{\sum_{n=2}^{nbus} S_{gen} - S_{load}\} = I_{branch}^{\,2} . Z_{branch} \qquad \text{Equation 3.20}$$

From Table 4.5, GENERATION represents the power generated by the system to supply that much amount of load. Generation data is calculated and separated into each active power (kW), reactive power (kVAr) and apparent power (kVA). LOAD represents the total amount of power consumed by load. The LOAD data representation is same with data representation of GENERATION. LOSSES represents the losses of the system which can be derived from the line current and line impedance. The cost when the system suffers 180.423 kW active power losses is 30,253.944 USD/year which the losses price is 168 USD/kW/year taken from reference (Eajal and El-Hawary, 2010). The objective function of direct search algorithm will take this amount of cost as the reference to find the minimum net saving. Load reactive power demand will be the maximum limit of capacitor size that can be installed to the system. From the following equation, power generation, power demand and power losses can be seen in the following table,

Table 4.5 Generation, Load and Losses Power Result

GENERATION				
kW	1,049.486	764.351	1,477.587	3,291.423
kVAr	556.796	580.675	625.396	1,762.867
kVA	1,188.042	959.904	1,604.488	3,752.434
PF	0.883	0.796	0.921	
LOAD				
kW	1,055.000	809.000	1,247.000	3,111.000
kVAr	508.000	533.000	702.000	1,743.000
kVA	1,170.935	968.798	1,431.018	3,570.751
PF	0.901	0.835	0.871	
LOSSES				
kW	-5.514	-44.649	230.587	180.423
kVAr	48.796	47.675	-76.604	19.867
kVA	49.107	65.318	242.978	357.403
TOTAL LOSSES (US$)= 30,311.064				
*** with losses price=168 USD/kW/year				

4.3 Direct Search Algorithm for Capacitor Placement

To approach proper capacitor placement, fundamental system power losses need to be calculated. Knowing the system power losses is important for fixing the maximum limit of installed capacitor. This reactive power losses will limit the maximum reactive power injection to the system. Real power losses will varied due to the amount of reactive power injection. Then, the most critical bus which has most power losses and severes to have high THD level will be determine as the first initial place to be installed by capacitor. For more detail explaination, the approach for applying direct search algorithm will be divided into some sections as follows.

4.3.1. Power Losses

From the previous voltage and current profile, power losses can be calculated. Power losses can be derived from the mismatch between generation power and load power. Before that, power profile on generation and load must be calculated. The following equations (3.20) until (3.22) will be considered to calculate fundamental power losses and harmonic power losses.

$$P_{losses} = \sum_{j=1}^{nbus} \sum_{m=1}^{nbus} V_j^{(1)} V_m^{(1)} Y_{jm}^{(1)} \cos(\theta_j^{(1)} - \theta_m^{(1)} - \delta_{jm}^{(1)}) \quad \text{Equation 3.21}$$

$$Ploss_{harmonic} = \sum_{n=1}^{nharmonic} Ploss^{(h)} \quad \text{Equation 3.22}$$

$$Ploss_{harmonic} = \sum_{h=1}^{nharmonic} [\sum_{j=1}^{nbus} \sum_{m=1}^{nbus} Vj^{(h)}.Vm^{(h)}.Yjm^{(h)} \cos(\theta j^{(h)} - \theta m^{(h)} - \delta jm^{(h)})]$$

The power losses is calculated from equation (3.21) where line current is flowing from the sending-end node to the load location. The more distance of spreading of load, system will suffered higher power losses because its resistance along the line. It will cause the recieving-end nodes has lower voltage than the slack bus. The branch that located at the sending-end node will have higher losses due to the higher current at that position and vice versa. The following tables will show the result of losses calculation from fundamental frequency losses, harmonic power losses, and aggregated power losses which include total harmonic andfundamental frequency power losses.

Table 4.6 Losses at Fundamental Frequency

Branch (i-j)		Phase-A		Phase-B		Phase-C	
		P (kW)	Q (kVAr)	P (kW)	Q (kVAr)	P (kW)	Q (kVAr)
1	2	95.141	18.087	-34.779	52.236	-69.301	-149.586
2	3	5.051	-1.080	-0.411	1.927	-1.716	-1.396
3	4	5.051	-1.080	-0.411	1.927	-1.716	-1.396
2	5	59.059	13.886	-11.158	14.893	-36.902	-69.281
5	6	0	0	0	0	0	0
6	7	15.234	-6.730	0.204	0.381	-8.778	-1.461
5	8	0	0	0	0	0	0
2	9	0	0	-0.169	5.311	-3.826	-7.085
9	10	0	0	0	0	-3.826	-7.085
5	11	2.397	-0.484	0	0	-1.975	-4.253
11	12	1.496	-1.096	0	0	0	0
11	13	0	0	0	0	-1.974	-4.254

From the Table 4.6, 4.7, and 4.8 has the same style of table which are the first and second column represents the order of line or branch. The third and fourth column represent the line current for phase-A, fifth and sixth column represent phase-B and phase-C is represented by seventh and eighth column. It can be seen that the power losses in branch 5-6 is zero. This is because branch 5-6 is a switch and it is assumed that it will not affect on power losses. Besides that, branch 5-8 is also zero because on the recieving end of this branch (bus-8) there is no load. Bus without load will not absorb power which in another word bus will not draw current. Therefore, branch 5-8 does not have power losses. The other zero element in another branch is because those branch does not include in the test system (Figure 3.6). From the

Table 4.6**,** the losses somehow contain of negative and positive sign. The meaning between this sign is, most of the loads are withdrawing the current for positive sign while for negative sign, most of the loads are injecting current. The load that withdrawn current from utilities has the characteristic of passive load while the load that injected current to the utilities has the characteristic of active loadwhich is mainly in the form of power converted. This kind of load will produced more harmonic than passive load.

Table 4.7 Total Harmonic Power Loss

Branch (i-j)		Phase-A		Phase-B		Phase-C	
		P (kW)	*Q (kVAr)*	*P (kW)*	*Q (kVAr)*	*P (kW)*	*Q (kVAr)*
1	2	51.3164	26.596	-28.6164	24.4751	-14.9262	-97.5634
2	3	2.6397	0.7759	-0.6789	0.8085	-0.4694	-1.0938
3	4	2.6397	0.7759	-0.6789	0.8085	-0.4694	-1.0938
2	5	31.4006	18.0297	-8.8761	6.7754	-9.6763	-45.9874
5	6	0	0	0	0	0	0
6	7	4.7036	2.2651	-0.0485	0.1172	-1.4367	-2.3911
5	8	0	0	0	0	0	0
2	9	0	0	-1.5468	1.8313	0.6177	-3.5996
9	10	0	0	0	0	0.6177	-3.5996
5	11	0.991	0.4984	0	0	0.4921	-2.0574
11	12	0.4155	0.1243	0	0	0	0
11	13	0	0	0	0	0.4924	-2.058

Table 4.7 represents the total harmonic power losses in each bus for every harmonic orde. The harmonic active power losses is nearly half in comparison with fundamental active power losses. The amount of power losses is derived from the sum of all harmonic frequencies exceptthe fundamental frequency. From this result, at the harmonic frequency, harmonic load also withdrawn current which resulting in more losses. It is necessary to concern about harmonic on the system because harmonics can increase the current and when it flowing through branch impedance, the power losses of the system will be higher than normal condition.

Table 4.8 Aggregated Power Losses

Branch (i-j)		Phase-A		Phase-B		Phase-C	
		P (kW)	*Q (kVAr)*	*P (kW)*	*Q (kVAr)*	*P (kW)*	*Q (kVAr)*
1	2	146.4576	44.6828	-63.3952	76.7105	-84.2273	-247.15
2	3	7.6907	-0.3043	-1.0894	2.7356	-2.1851	-2.4896
3	4	7.6907	-0.3043	-1.0894	2.7356	-2.1851	-2.4896
2	5	90.4596	31.9156	-20.034	21.6688	-46.5786	-115.269
5	6	0	0	0	0	0	0
6	7	19.9375	-4.4649	0.1552	0.4979	-10.2147	-3.8522
5	8	0	0	0	0	0	0
2	9	0	0	-1.7157	7.1425	-3.208	-10.6845
9	10	0	0	0	0	-3.208	-10.6845
5	11	3.3883	0.0148	0	0	-1.4831	-6.3106
11	12	1.911	-0.9712	0	0	0	0
11	13	0	0	0	0	-1.4821	-6.3119

Table 4.8 represents the aggregated power losses which is the total of fundamental frequency power losses and harmonic power losses. It can be seen that with considering the total harmonic power losses, the actual power losses will be one and a half times of the fundamental power losses. Without proper design and harmonic consideration, distribution system will get higher stress from this additional power losses and will meet the thermal limit of the network.

The following Figure will describe the total harmonic power losses from different order of harmonic frequencies. In Figure 4.4, the power losses in third, fifth, seventh, and ninth are significantly larger while power losses in rest order of harmonic are very small. The more harmonic penetration will create more losses and without good planning, the system will be stressed.

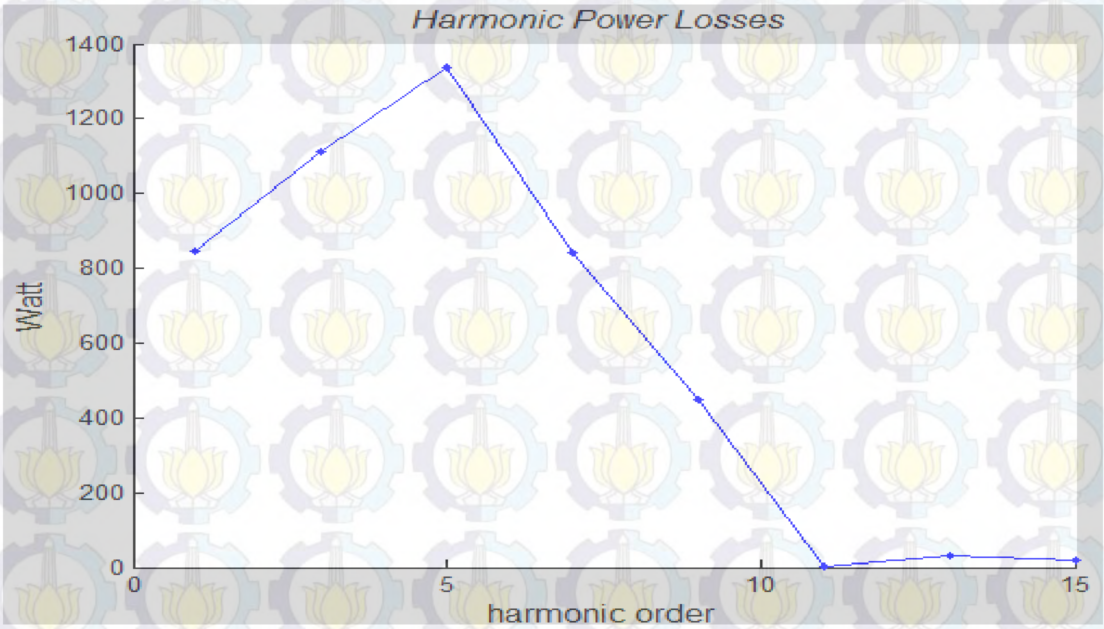

Figure 4.4 Total Harmonic Power Losses by Aggregated Power Loss

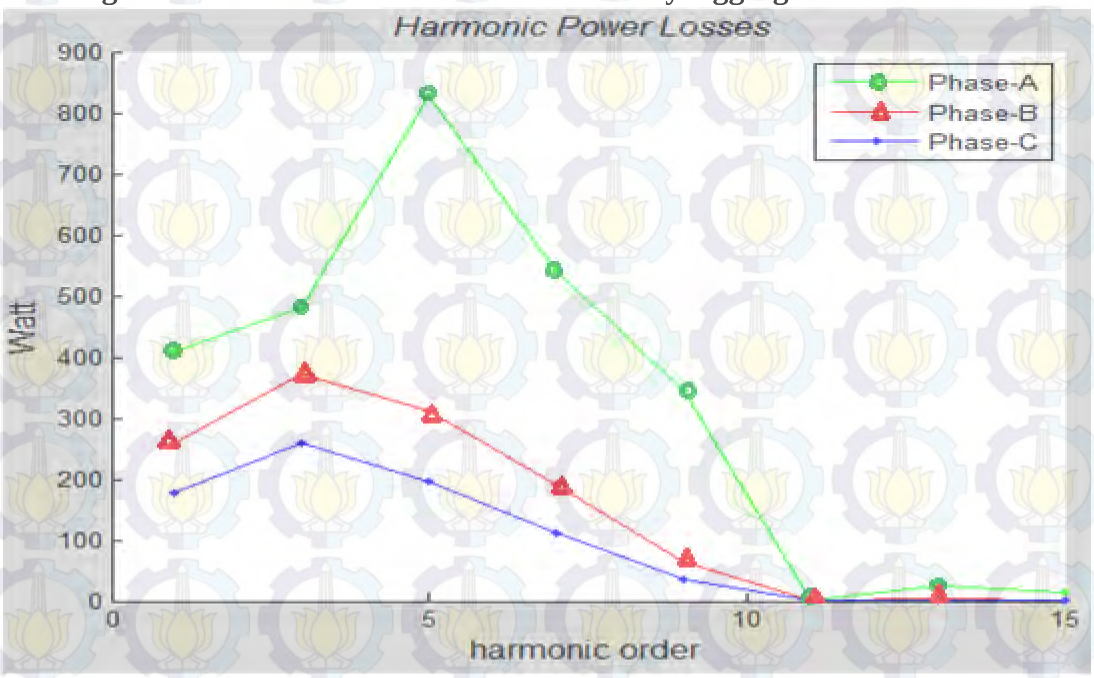

Figure 4.5 Harmonic Power Losses

From Figure 4.5, the power losses in third, fifth, seventh, and ninth are significantly larger while power losses in rest order of harmonic are very small. The more harmonic penetration in phase-A seems more severe than the other phases because it can reach two times from the power losses in fundamental frequency. From this result, for the next calcultation, direct search algorithm will use the aggregated power relation so that the system can be analyzed in to achieved more secure condition.

4.4.2. Prediction of Reactive Power Compensator Location Based on Load Sensitivity Factor

Load sensitivity factor is used to predict the location in which prospective bus will be placed by shunt capacitor. Load sensitivity factor is calculated with the relation between square of current, resistance and bus voltage for knowing the sensitivity between power losses and reactive power compensation. As the order will be descending, line that has higher LSF will be more attractive to be installed by capacitor than the lower LSF. With the use of power losses calculation as mentioned in Equation 3.25 and Equation 3.26, the result of load sensitivity factor are as follows:

Table 4.9 Comparison of LSF Between Fundamental and Aggregated Power

Branch		phase	LSF - fundamental	Branch		phase	LSF - aggregated
5	11	1	1.98	11	12	1	4.32
2	5	1	1.97	9	10	2	4.13
5	6	1	1.97	6	7	1	3.69
5	8	1	1.97	6	7	2	3.55
3	4	1	1.95	1	2	1	2.53
2	3	1	1.94	2	5	1	2.51
1	2	1	1.94	5	6	1	2.51
6	7	1	1.87	5	8	1	2.51
9	10	2	1.81	2	3	1	2.50
11	12	1	1.72	5	11	1	2.50
6	7	2	1.69	3	4	1	2.47
2	9	2	1.46	1	2	2	1.83
1	2	2	1.45	2	5	2	1.82
2	3	2	1.44	5	6	2	1.82
2	5	2	1.44	5	8	2	1.82
5	6	2	1.44	2	3	2	1.79
5	8	2	1.44	2	9	2	1.79
3	4	2	1.43	3	4	2	1.75
5	11	3	0.71	5	11	3	0.81
2	5	3	0.68	2	5	3	0.79
5	6	3	0.68	5	6	3	0.79
5	8	3	0.68	5	8	3	0.79
2	9	3	0.65	2	9	3	0.77
3	4	3	0.59	3	4	3	0.72
1	2	3	0.58	1	2	3	0.71
2	3	3	0.57	2	3	3	0.70
6	7	3	0.24	6	7	3	0.45
11	13	3	0.19	11	13	3	0.40
9	10	3	0.14	9	10	3	0.29

The first and second column of Table 4.9 represents the branch of the test system. The third column represents the phase of the branch. While in the phase column, 1,2, and 3 is the index of phase-A, phase-B and phase-C respectively. The fourth column represents the load sensitivity factor calculation of fundamental frequency. The similar order is done in the table of LSF –aggregated side.

From Table 4.8, the load sensitivity factor result is significantly different in both cases. Based on fundamental power losses, line (5-11) phase-A, (2-5) phase-A and (5-6) phase-C, will be prioritized over the rest of lines such as line (11-13) phase-C and (9-10) phase-C. Differently, the LSF result based on aggregated power losses will spot (11-12) phase-A, (9-10) phase-B and (6-7) phase-A which has higher priority than line (9-10) phase-C. This location prediction will be used as the sequence in which the reactive power compensator will be placed in the system. Reactive power compensator will be placed at the recieving end of the line (i.e) for the line (6-7C) the shunt capacitor will be placed at bus-7 phase-C.

4.3.3. Capacitor Installation Approach

From the previous step, the preliminary data for capacitor installation is complete. The next step for applying direct search algorithm can be described into the direction which are as follows. Two strategies has been done to see the performance of direct search algorithm which are applying single and mutiple fixed shunt capacitor without random initialization of shunt capacitor size and applying single and multiple fixed shunt capacitor with random allocation and random size prediction based on load sensitivity factor. More detail explanation will be described at the following which are as follows:

1. Direct search algorithm with load sensitivity factor

- Single Size Capacitor Installation

For single capacitor installation, each location will be tried one by one to be installed by one each capacitor size according to Table 3.4. Each result of the installation will be saved. The first trial result will be saved as the reference. When the second trial has better net savings, the reference will be updated to be the second trial result. The searching space will become the relation of total capacitor size number and total location which are 10 x 29.

- Maximum Size of Capacitor Installation

At this strategy, each location will be tried by each capacitor size. For example, the branch 11-12 phase-A which has highest LSF, bus-12 will be placed by 150 kVAr capacitor, and multiplied by integer number such as 1,2,3,.., n until n x Qcap less than the maximum reactive power demand. The highest net savings will be saved as the reference of bus-12. The same way will be done in bus-12 for the next capacitor size which is 300 kVAr and multiplied by integer number. The result will be saved and collect to be compared. The maximum net savings result will be saved as the best capacitor size in bus-12. Then the same way will be applied for the next location. The searching space of this method will be different for each size of capacitor which are as follows: 29 x 10 x n.

2. Direct search algorithm with LSF-based Random prediction

The strategy in this option is done by deciding the initial size and location with the random prediction. With deciding number of location of capacitor installation, the size of capacitor will be varied and constrained that the total prospective capacitor size will not exceed the reactive power demand. Then, the result in the first iteration will be saved as the reference. This algorithm will be run in 100 iteration for finding the best result.

The following subsections will explain the detail steps of each of these strategies which are as follows:

4.3.3.1. Single Size Capacitor Installation

The first strategy in this following subsection is considered as the placement without LSF. The capacitors is placed on all available bus one by one. After that, the minimum objective function is found to know the best location and of each size of capacitors. The following steps which explains the flowchart of DSA are as follows:

1. The maximum loss of system is determined from the total reactive power demand of test system. This uncompensated loss is considered to be maximum loss in the system. The refference that will be taken are as follows:
   i. Total cost of active power losses = 30,311.064 USD/year
   ii. Active power losses = 180.423 kW
   iii. Maximum reactive power limit for capacitor placement = 1,743.0 kVAr
   iv. Maximum THD level = 5 %
2. Because there are several options of capacitor size, run the power flow for each capacitor size for all the number of possible prospective buses from step, keep each result on matrix that represent number of prospective buses. Calculate the objective function Equation 3.23. The result will have 29 rows and 6 columns. 29 rows are from test system branch size. 6 columns represents the capacitor size, installation location, active power losses, cost of active power losses in US Dollar unit and voltage level. According to the option of capacitor bank in Table 1, the following result will be the possible solution of capacitor placement. For information, first column represents the size of capacitor and second column represents the bus and index of phase, which is 1,2 and 3 is the index of phase-A, phase-B, and phase-C respectively. The third, fourth and fifth column show the active power losses, net saving as objective function and set of maximum and minimum voltage respectively. The following result is the result after placed by capacitor. The detailed result is attached at Appendix B Table B.1.

Result of Single Size Capacitor Installation

Capacitor_Size	Location	Active_PLoss_kW	Losses_Price_USD	Vmax - Vmin
150	12 - 1	46.881	7876.052	0.986 - 0.838
150	10 - 2	47.721	8017.163	0.998 - 0.849
150	7 - 1	44.530	7481.080	0.988 - 0.842
150	7 - 2	49.795	8365.577	1.010 - 0.848
150	2 - 1	49.725	8353.740	0.987 - 0.846
150	5 - 1	47.473	7975.529	0.986 - 0.842
150	6 - 1	49.316	8285.095	0.986 - 0.842
150	8 - 1	49.091	8247.324	0.986 - 0.842

150	3 - 1	49.270	8277.353	0.987 - 0.845
150	11 - 1	48.567	8159.260	0.986 - 0.838
150	4 - 1	46.654	7837.792	0.987 - 0.845
150	2 - 2	49.672	8344.942	0.998 - 0.849
150	5 - 2	50.909	8552.683	1.007 - 0.848
150	6 - 2	48.994	8230.943	1.007 - 0.848
150	8 - 2	48.550	8156.387	1.011 - 0.848
150	3 - 2	48.888	8213.135	0.998 - 0.849
150	9 - 2	51.115	8587.255	0.998 - 0.849
150	4 - 2	50.381	8464.078	0.998 - 0.849
150	11 - 3	50.407	8468.458	0.981 - 0.885
150	5 - 3	45.399	7626.952	0.981 - 0.872
150	6 - 3	48.317	8117.228	0.981 - 0.872
150	8 - 3	50.571	8495.871	0.981 - 0.872
150	9 - 3	50.313	8452.636	0.985 - 0.860
150	4 - 3	46.915	7881.638	0.985 - 0.861
150	2 - 3	49.679	8346.099	0.985 - 0.860
150	3 - 3	50.405	8468.112	0.985 - 0.861
150	7 - 3	42.944	7214.646	0.980 - 0.872
150	13 - 3	43.098	7240.457	0.981 - 0.897
150	10 - 3	42.677	7169.800	0.985 - 0.860
300	12 - 1	40.736	6843.569	1.008 - 0.826
...				
1500	10 - 3	97.344	16353.713	1.155 - 0.858

3. Find the lowest cost from the previous calculation. Update the minimum objective function reference. Check the THD of the system, while the minimum objective function is not within the limit, then find the other solution. The following result is the lowest cost from the selection in the previous step. The result is as follows:

```
min_obj_all_find =
  4.6901e+003  -→ 4,690 USD/year

Best Size        = 900
Best Location  = 8 (1)
Max Voltage   = 1.106
Min Voltage    = 0.808
Max THD        = 8.9157
Min THD         = 0.5668
RealPowerLoss= 26.937
```

The following figure will describe the total harmonic power losses from different order of harmonic frequencies after placement of 900 kVAr single capacitor in bus-8 phase-A. Figure 4.6 represents the best solution from the 29x10 iteration. The last iteration point out the result from the reference to 4690 USD/year

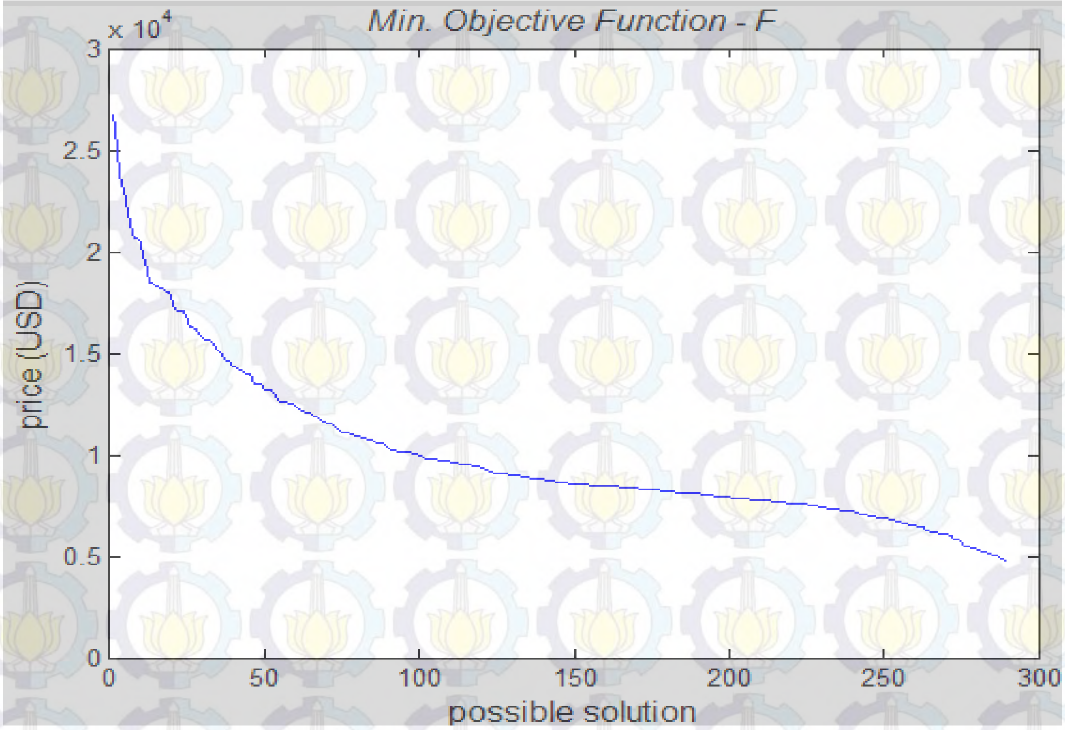

Figure 4.6 Minimum Objective Function by Placing 900 kVAr at bus-8A

Figure 4.7 represents the voltage profile of bus-8 phase-A after 900 kVAr placed. From the figure, the voltage profile at bus-13 phase-C is the lowest voltage and bus-8 phase-A has the highest voltage. The voltage condition is not within the standard. Only phase-A has the voltage quality that fullfilled the voltage level constraint.

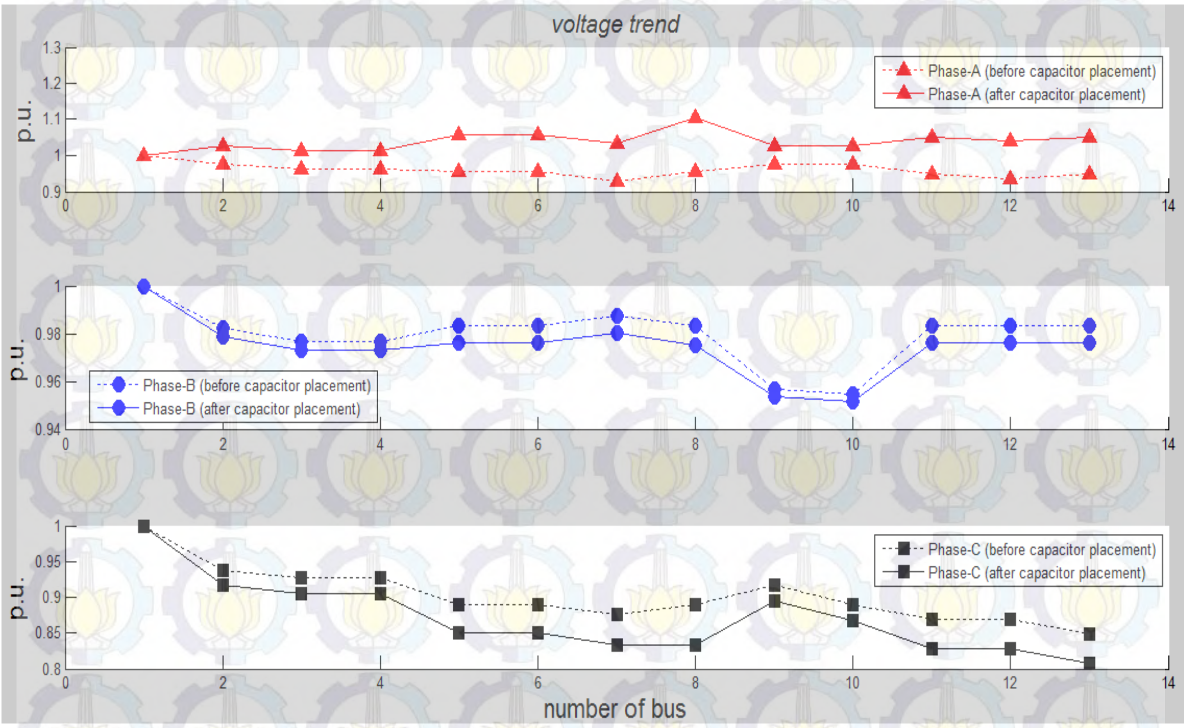

Figure 4.7 Voltage Profile by Placing 900 kVAr at bus-8A

Figure 4.8 depicted that the recent harmonic profile of the system are significantly within the limit with phase-C as exception. THD level of phase-C can not comply with the constraint, meanwhile the other phases harmonic level is within the limit which is not exceeding 5%.

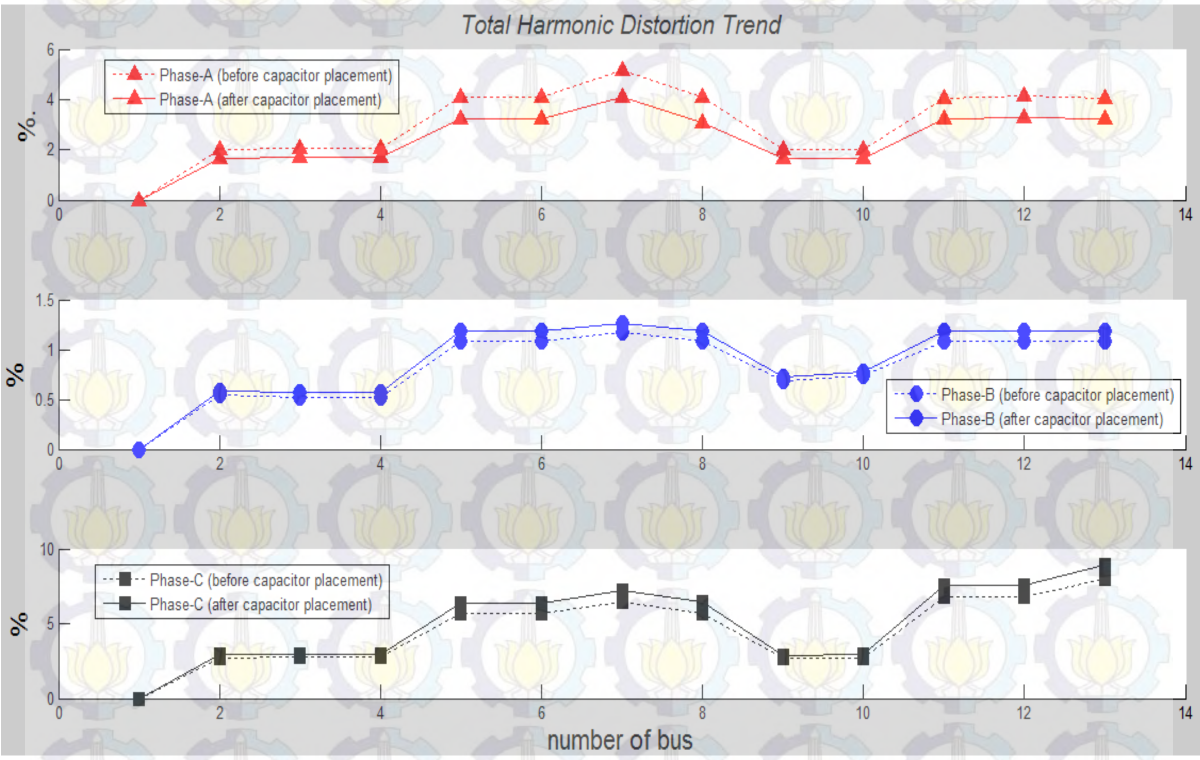

Figure 4.8 THD profile by Placing 900 kVAr at bus-8A

Figure 4.9 depicted that the power losses in third, fifth, seventh, and ninth are slightly decreasing in comparison with the base case system. Meanwhile, power losses in rest order of harmonic are very small. By placing that capacitor, the harmonic power losses is slightly reduced.

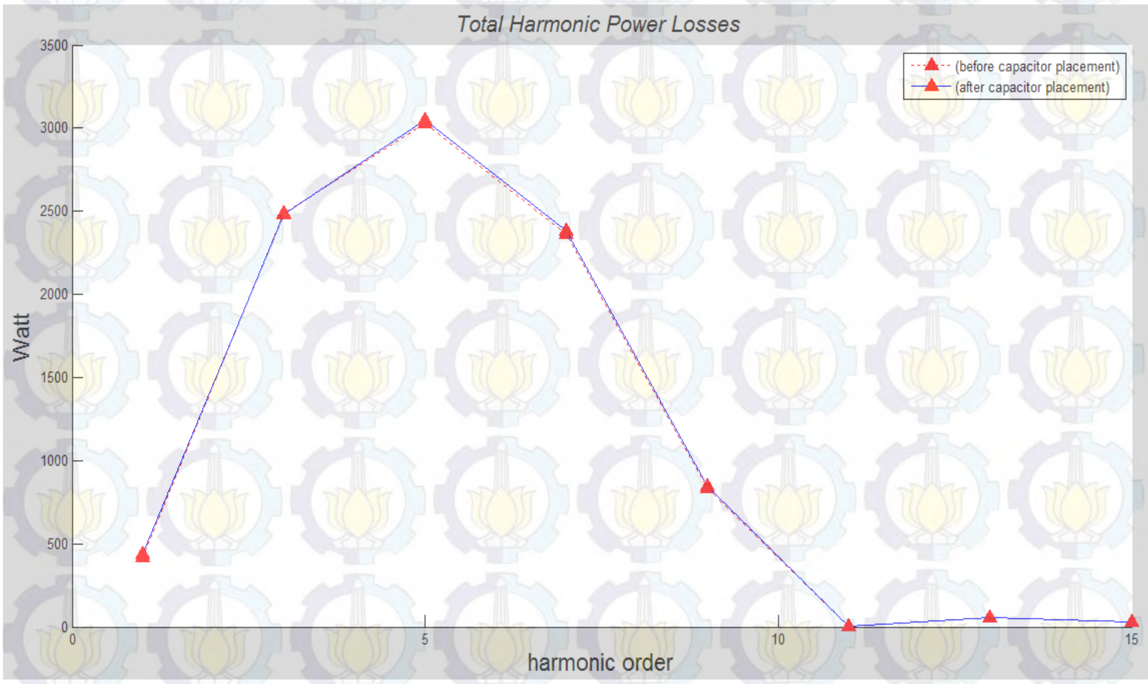

Figure 4.9 Total Harmonic Power Losses Trend

From Figure 4.10, the power losses in third, fifth, seventh, and ninth harmonic frequency in phase-B and phase-C are slightly reduced while power losses in phase-A at fifth, seventh, and ninth harmonic frequency are relatively larger than the other phases. But, in comparison with the base case, there are reduction in power losses at phase-A. The harmonic penetration in phase-A are still higher than the other phases because it is loaded by more harmonic loads.

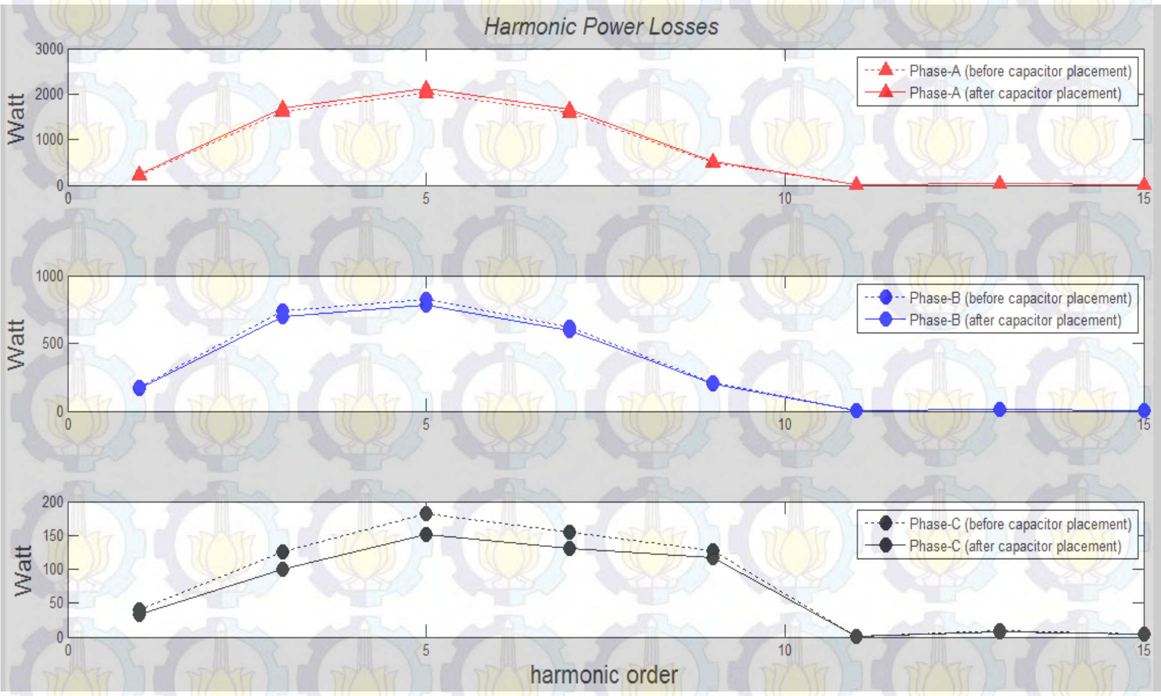

Figure 4.10 Harmonic Power Losses

The second strategy in this following subsection is done by considering LSF for capacitor placement. Besides that, voltage and THD constraint is also applied. The capacitors is placed on proospective bus based on LSF. After that, the minimum objective function is found to know the best size of capacitors. The following steps which has been explained in the flowchart of DSA are as follows:

1. Each bus will be identified by placing multiple capacitor to determine the maximum capacitor that can be installed on the prospective bus. With voltage constraint, the identification will be focus to install the capacitor in bus that has poor voltage profile. The result of the identification will be kept to be within the voltage limit. The maximum loss of system is determined from the total reactive power demand of test system. This uncompensated loss is considered to be maximum loss in the system. the refference that will be taken are as follows:
   i. Total cost of active power losses = 30,311.064 USD/year
   ii. Active power losses = 180.423 kW
   iii. Maximum reactive power limit for capacitor placement = 1,743.0 kVAr
   iv. Maximum Voltage = 1.05 pu
   v. Minimum Voltage = 0.9 pu
   vi. Maximum THD level = 5 %
2. Calculate loss sensitivity factor and sort the prospective bus in descending order. Find prospective buses which is within the constraint $|V_i| \leq V_{min}$ to avoid overcompensated system. The total prospective bus is seven location. First and second column represents the bus-to-bus connection or branch. Third column represents the phase, which is 1,2 and

3 is the index of phase-A, phase-B, and phase-C respectively. The fourth and fifth column show the voltage and LSF calculation. The following result is the prospective bus that will be placed by capacitor.

```
%
send_bus recieve_bus phase V  LSF by aggregated
5   11  3    0.8688    8.0860
2   5   3    0.8894    7.9351
5   6   3    0.8894    7.9351
5   8   3    0.8894    7.9351
6   7   3    0.8754    4.5126
11 13  3    0.8492    4.0141
9   10  3    0.8900    2.9284
```

3. Because there are some options of capacitor size, run the power flow for each capacitor size for all the number of possible prospective buses from step , keep each result on matrix that represent number of prospective buses. Calculate the objective function (3.23). For information, first column represents the size of capacitor and second column represents the bus and index of phase, which is 1,2 and 3 is the index of phase-A, phase-B, and phase-C respectively. The third, fourth and fifth column show the active power losses, net saving as objective function and set of maximum and minimum voltage respectively. The following result is the result after placed by capacitor. According to the option of capacitor bank in Table 3.4, the following result will be the possible solution of capacitor placement. The following result is the result after placed by capacitor. The detailed result is attached at Appendix B Table B.2.

Capacitor_Size	Location	Active_PLoss_kW	Losses_Price_USD	Vmax - Vmin
150	11 - 3	50.407	8468.458	0.981 - 0.885
150	5 - 3	45.399	7626.952	0.981 - 0.872
150	6 - 3	48.317	8117.228	0.981 - 0.872
150	8 - 3	50.571	8495.871	0.981 - 0.872
150	7 - 3	42.944	7214.646	0.980 - 0.872
150	13 - 3	43.098	7240.457	0.981 - 0.897
150	10 - 3	42.677	7169.800	0.985 - 0.860
300	11 - 3	51.654	8677.881	0.977 - 0.912
300	5 - 3	42.256	7098.942	0.977 - 0.894
300	6 - 3	47.846	8038.141	0.977 - 0.894
300	8 - 3	52.592	8835.437	0.977 - 0.893
300	7 - 3	37.539	6306.538	0.976 - 0.894
300	13 - 3	37.833	6355.950	0.977 - 0.912
300	10 - 3	36.663	6159.398	0.982 - 0.871
450	11 - 3	53.348	8962.497	0.974 - 0.922
450	5 - 3	40.426	6791.613	0.974 - 0.914
450	6 - 3	48.482	8145.013	0.974 - 0.914
450	8 - 3	55.808	9375.793	0.977 - 0.912
450	7 - 3	35.088	5894.854	0.974 - 0.914
450	13 - 3	35.968	6042.694	0.979 - 0.921

450	10 - 3	37.738	6340.011	0.990 - 0.880
600	11 - 3	55.133	9262.284	0.993 - 0.922
600	5 - 3	39.708	6670.975	0.978 - 0.920
600	6 - 3	50.053	8408.958	0.978 - 0.920
600	8 - 3	59.949	10071.455	1.003 - 0.921
600	7 - 3	38.098	6400.461	0.977 - 0.928
600	13 - 3	41.022	6891.763	1.014 - 0.924
600	10 - 3	43.296	7273.684	1.019 - 0.888
750	11 - 3	56.741	9532.440	1.019 - 0.922
750	5 - 3	39.937	6709.391	0.988 - 0.919
750	6 - 3	52.419	8806.357	0.988 - 0.919
750	8 - 3	64.806	10887.487	1.028 - 0.920
750	7 - 3	40.422	6790.942	0.994 - 0.927
750	13 - 3	46.902	7879.565	1.047 - 0.924
750	10 - 3	49.369	8294.018	1.045 - 0.896
900	11 - 3	57.966	9738.369	1.044 - 0.922
900	5 - 3	40.976	6883.995	1.006 - 0.918
900	6 - 3	55.462	9317.570	1.006 - 0.918
900	8 - 3	70.216	11796.338	1.051 - 0.919
900	7 - 3	42.286	7104.051	1.014 - 0.927
900	13 - 3	54.010	9073.630	1.077 - 0.925
900	10 - 3	56.304	9459.076	1.069 - 0.894
1050	11 - 3	58.647	9852.622	1.067 - 0.922
1050	5 - 3	42.712	7175.592	1.023 - 0.917
1050	6 - 3	59.084	9926.035	1.023 - 0.917
1050	8 - 3	76.046	12775.809	1.074 - 0.919
1050	7 - 3	43.872	7370.501	1.033 - 0.927
1050	13 - 3	62.647	10524.758	1.105 - 0.926
1050	10 - 3	64.371	10814.312	1.093 - 0.885
1200	11 - 3	58.649	9852.954	1.090 - 0.923
1200	5 - 3	45.047	7567.873	1.039 - 0.917
1200	6 - 3	63.200	10617.615	1.039 - 0.917
1200	8 - 3	82.189	13807.691	1.095 - 0.917
1200	7 - 3	45.332	7615.716	1.051 - 0.921
1200	13 - 3	73.050	12272.401	1.131 - 0.928
1200	10 - 3	73.787	12396.159	1.115 - 0.876
1350	11 - 3	57.863	9721.011	1.111 - 0.924
1350	5 - 3	47.898	8046.821	1.055 - 0.916
1350	6 - 3	67.739	11380.114	1.055 - 0.916
1350	8 - 3	88.552	14876.820	1.116 - 0.910
1350	7 - 3	46.792	7861.053	1.069 - 0.914
1350	13 - 3	85.405	14347.968	1.156 - 0.929

1350	10 - 3	84.729	14234.389	1.136 - 0.867
1500	11 - 3	56.199	9441.436	1.132 - 0.925
1500	5 - 3	51.192	8600.283	1.070 - 0.916
1500	6 - 3	72.636	12202.920	1.070 - 0.916
1500	8 - 3	95.062	15970.407	1.136 - 0.903
1500	7 - 3	48.361	8124.676	1.086 - 0.907
1500	13 - 3	99.863	16776.963	1.180 - 0.927
1500	10 - 3	97.344	16353.713	1.155 - 0.858

4. Find the lowest cost from the previous calculation. Update the minimum objective function reference. The following result is the lowest cost from the selection in the previous step. The result is as follows:

```
min_obj_find =
  6.0087e+003  %

Best Size      = 450
Best Location  = 7 (3)
Max Voltage    = 0.974
Min Voltage    = 0.914
Max THD        = 4.95868
Min THD        = 1.2013
RealPowerLoss = 35.088
```

Figure 4.11 represents the best solution from the 7x10 iteration. The last iteration point out the result from the reference to 6,008.7 USD/year

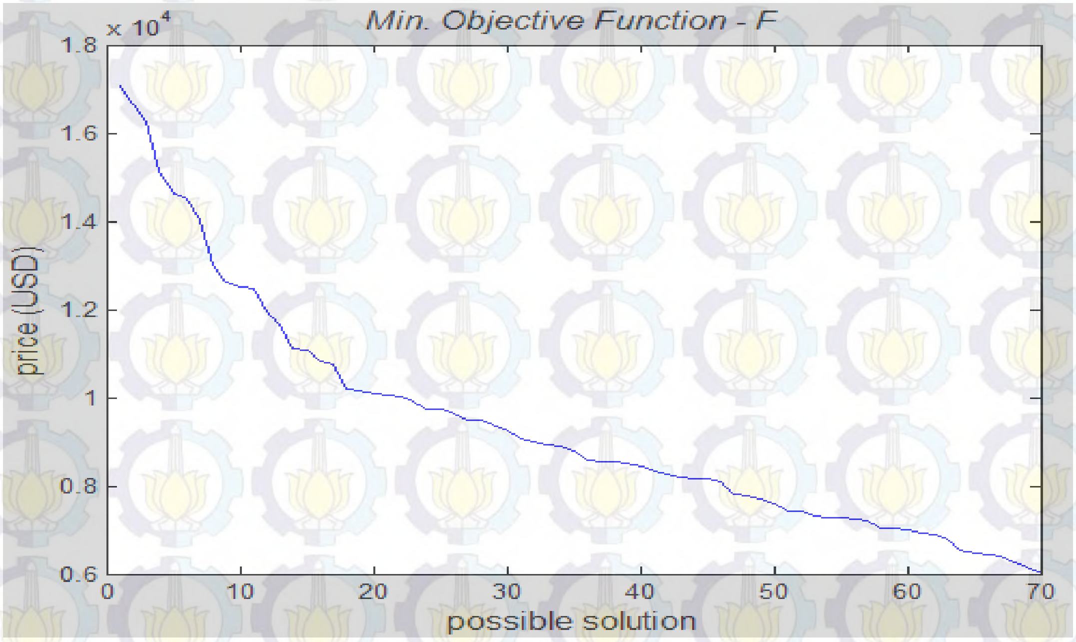

Figure 4.11 Minimum Objective Function by Placing 450 kVAr at bus-7C

Figure 4.12 represents the voltage profile after 450 kVAr placed on bus-7 phase-C. From the figure, the voltage profile at bus-13 phase-C is the lowest voltage and bus-9 phase-A and bus-10 phase-A has the highest voltage. The voltage condition is within the standard.

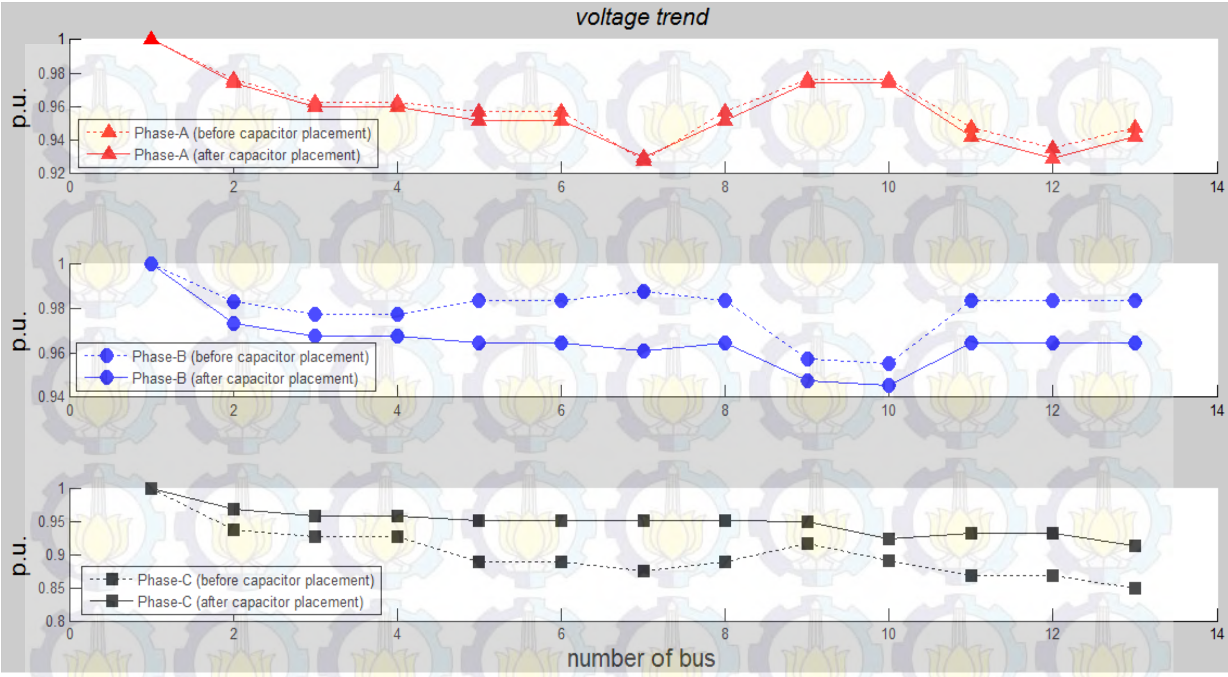

Figure 4.1 Voltage Profile by Placing 450 kVAr at bus-7C

Figure 4.13 depicted that the recent harmonic profile of the system are significantly within the limit. THD level can comply with the constraint, which is not exceeding 5 % after bus-7 phase-C is placed by 450 kVAr.

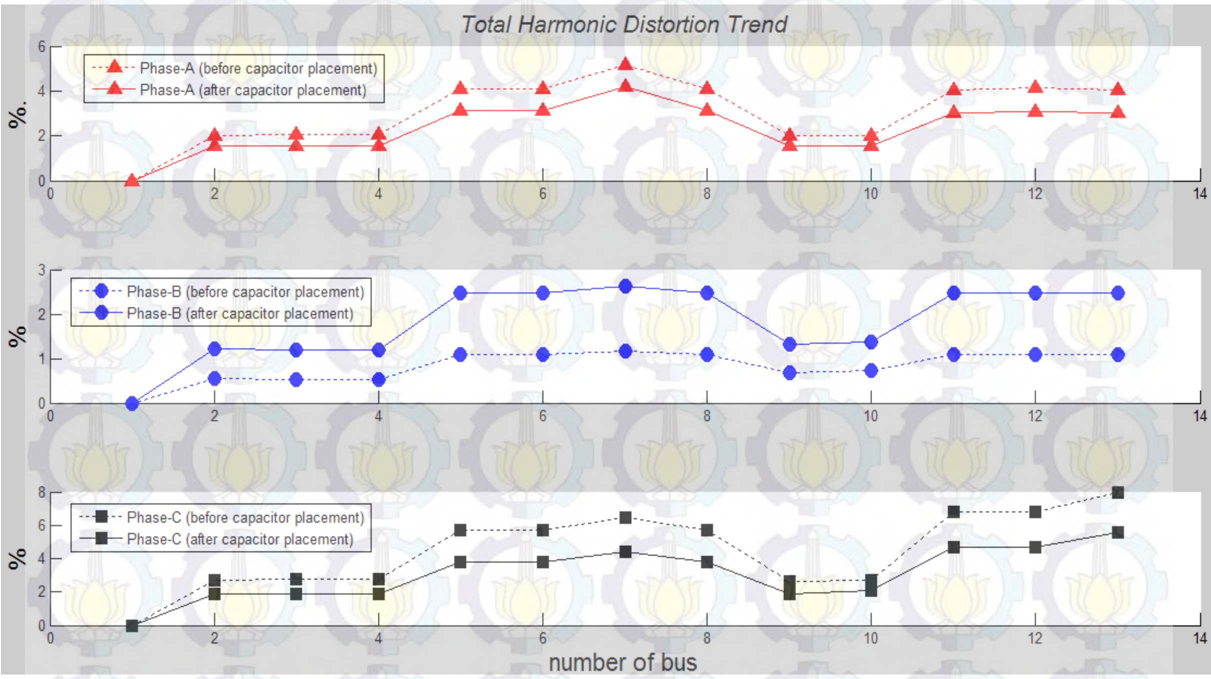

Figure 4.2 THD profile by Placing 450 kVAr at bus-7C

Figure 4.14 depicted that the power losses is similar with the result of previouse strategy. In third, fifth, seventh, and ninth harmonic order, the power losses are significantly decreasing in comparison with the base case system. Meanwhile, power losses in rest order of harmonic are relatively small. By placing that capacitor, the harmonic penetration is reduced.

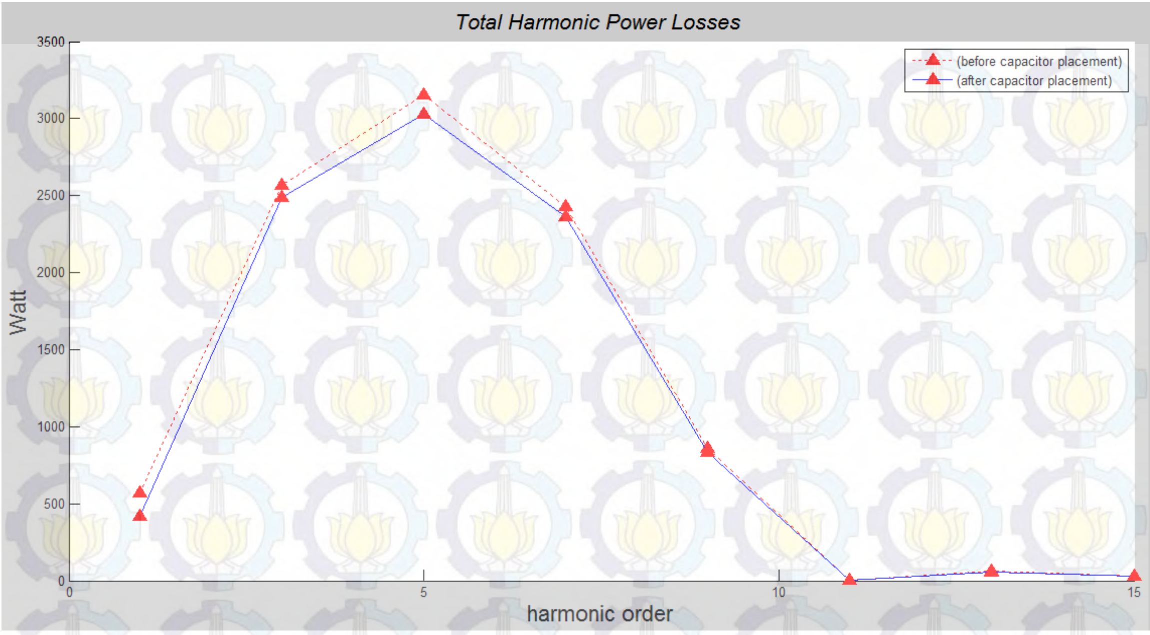

Figure 4.3 Total Harmonic Power Losses Trend

From Figure 4.15, the power losses in third, fifth, seventh, and ninth harmonic frequency in phase-A and phase-C are significantly reduced while power losses in phase-B at fifth, seventh, and ninth harmonic frequency are relatively larger than the other phases. But, in comparison with the base case, there are reduction in power losses at phase-A. The harmonic penetration in phase-B are the highest because it is loaded by heavy harmonic load.

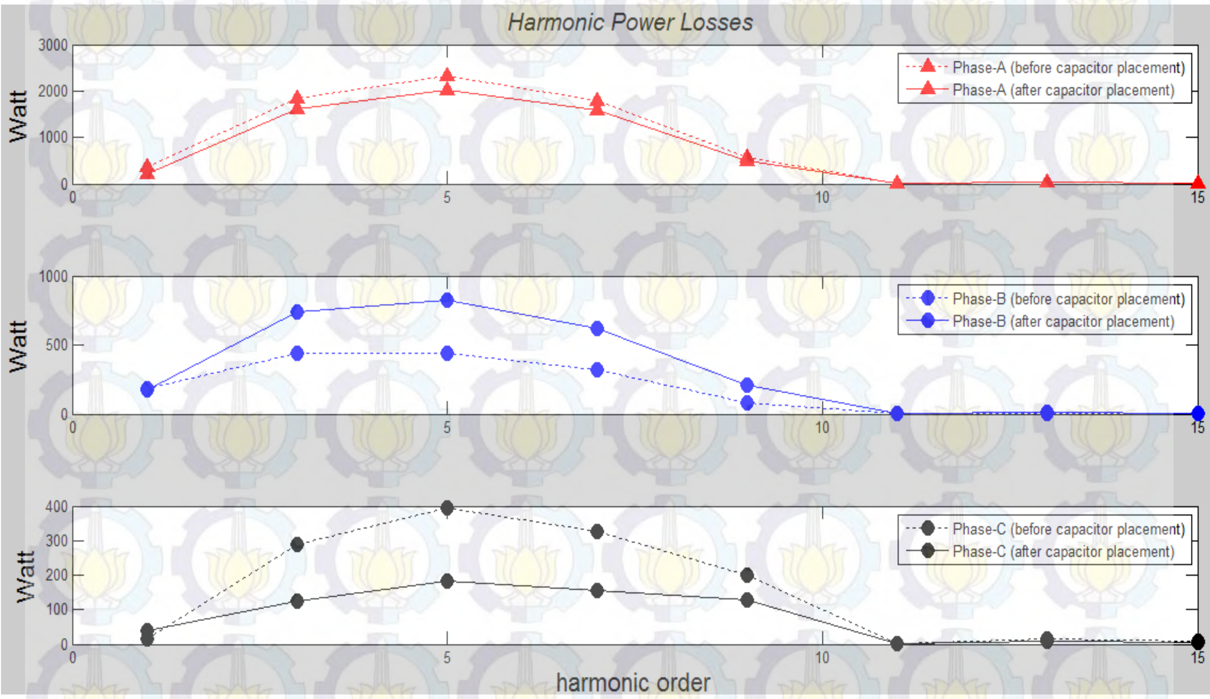

Figure 4.4 Harmonic Power Losses

4.4.3.2. Maximum Size of Capacitor Installation with voltage constraint

The strategy in placing maximum size of capacitor is done with the same step explained in subsection 4.4.3.1. For the placement without LSF, at first, all possible bus is placed with highest capacitor size. After finding the minimum objective function, another size of capacitor is being placed until the total number of location is near the reactive load power.

For the strategy without LSF, the following steps are as follows:

1. Because there are several options of capacitor size, run the power flow for each capacitor size for all the number of possible prospective buses from step, keep each result on matrix that represent number of prospective buses. Calculate the objective function (3.23). For the first step, 29 columns represented from test system branch size will be placed by highest size of capacitor. Then, objective function will determine whether that size has meet the criterion or not. The result will have one column and *n* rows. n rows represents the prospective capacitor sizes. According to the option of capacitor bank in Table 1.

```
location =
2 2 2 3 3 3 4 4 4 5 5 5 6 6 6 7 7 7 8 8 8 9 9 10 10 11 11 12 13
```

While finding the lowest cost from each possible capacitor size, total capacity of capacitor reactive power is upadated. The result is as follows:

```
P_losses = 15.9640e+004
THD_best = 0.9830    4.95357
V_best =    0.9240    0.9993
Obj_res = 2.6984e+004
Capacitor = 450,300, 150, 150, 150, 150, 150
Location = 25,11,7,10,12,28,29 [10-c,5-b,4-a,5-a,5-c,12-a,13-c]
```

The following figure will describe the total harmonic power losses from different order of harmonic frequencies after placement of 1500 kVAr in total for each folowing location. Figure 4.16 represents the best solution from the 8 iterations. The last iteration point out the result from the reference to 26,984 USD/year

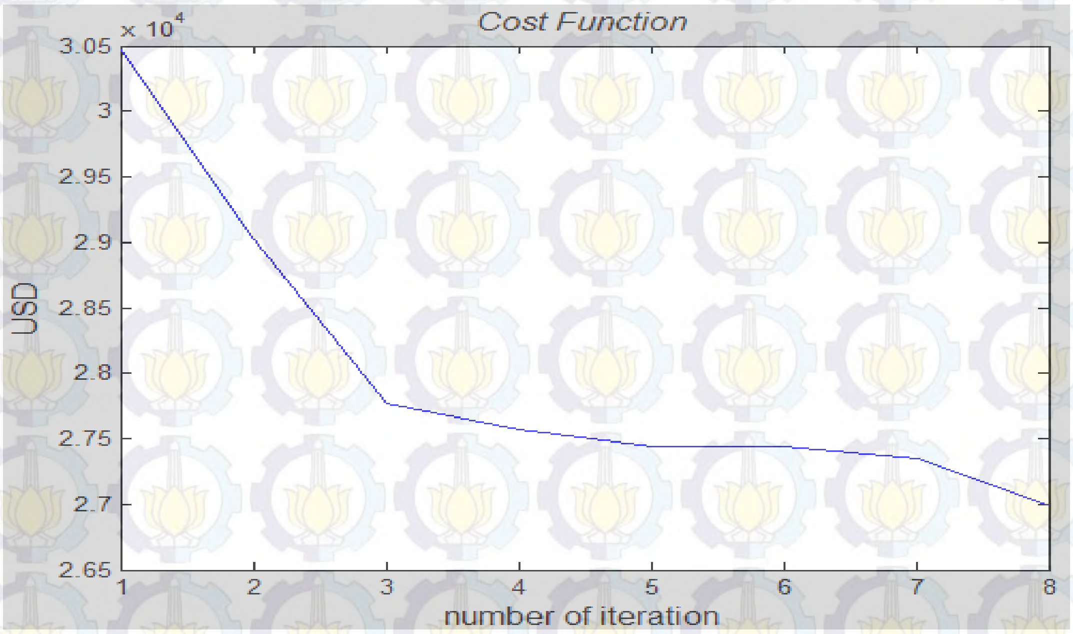

Figure 4.16 Minimum Objective Function by Placing 1500 kVAr

Figure 4.17 represents the voltage profile of system after 1500 kVAr placed. From the figure, the voltage profile at bus-10 phase-B is the lowest voltage and phase-A has the highest voltage. The voltage condition is within the standard.

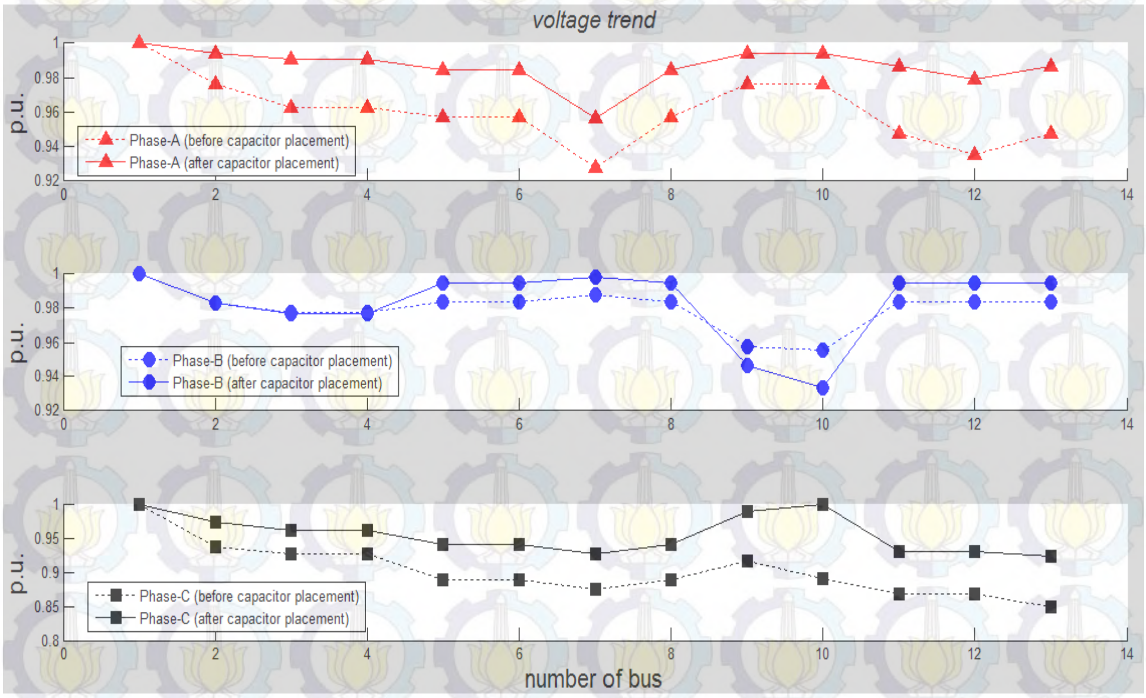

Figure 4.17 Voltage Profile by Placing 1500 kVAr

Figure 4.18depicted that the recent harmonic profile of the system are significantly within the limit with phase-C as exception. Before capacitor placement, THD level of phase-C can not comply with the constraint, meanwhile after the placement, harmonic level is within the limit which is not exceeding 5%.

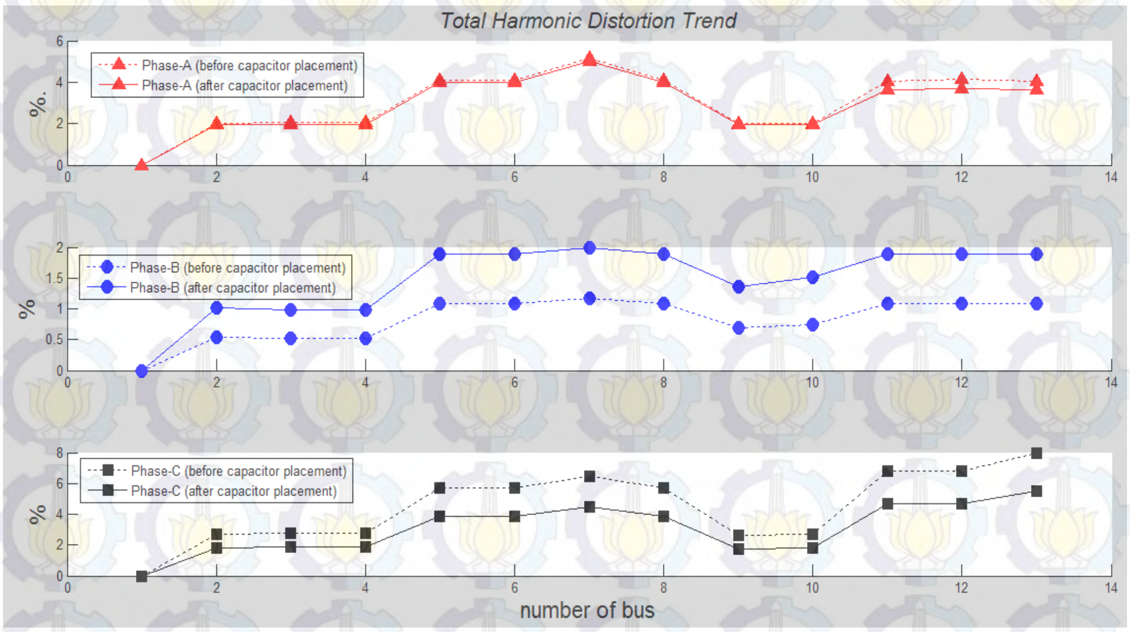

Figure 4.18 THD profile by Placing 1500 kVAr

Figure 4.19 depicted that the power losses in third, fifth, seventh, and ninth are slightly decreasing in comparison with the base case system. Meanwhile, power losses in rest order of harmonic are very small. By placing that capacitor, the harmonic power losses is slightly reduced.

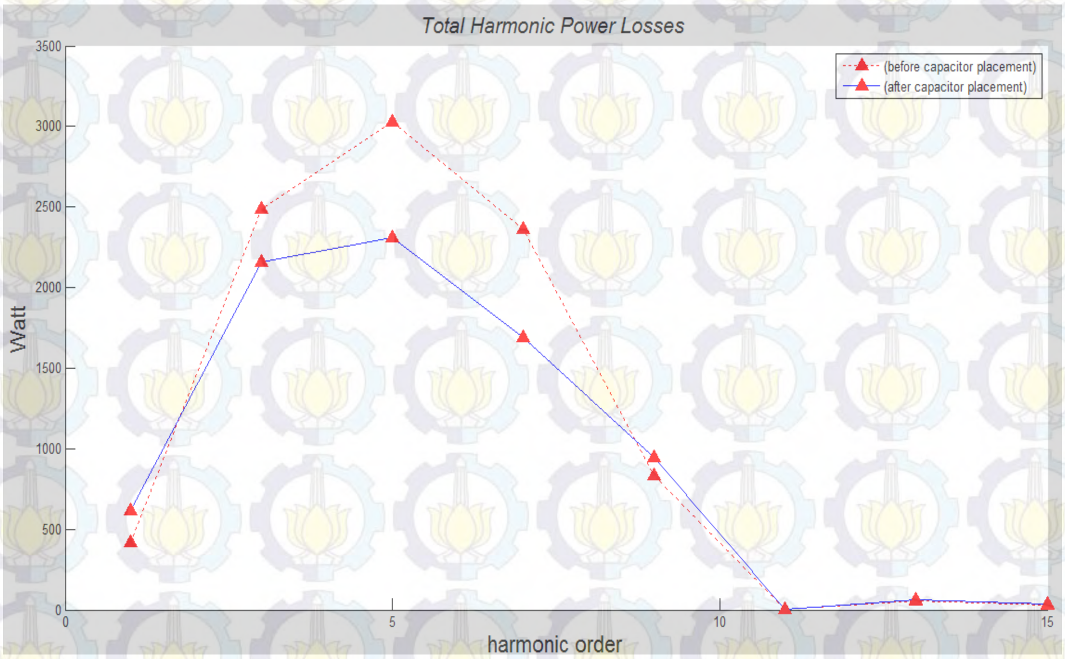

Figure 4.19 Total Harmonic Power Losses Trend

From Figure 4.20, the power losses in third, fifth, seventh, and ninth harmonic frequency in phase-B and phase-C are slightly reduced while power losses in phase-A at fifth, seventh, and ninth harmonic frequency are relatively larger than the other phases. But, in comparison with the base case, there are reduction in power losses at phase-A. The harmonic penetration in phase-A are still higher than the other phases because it is loaded by more harmonic loads.

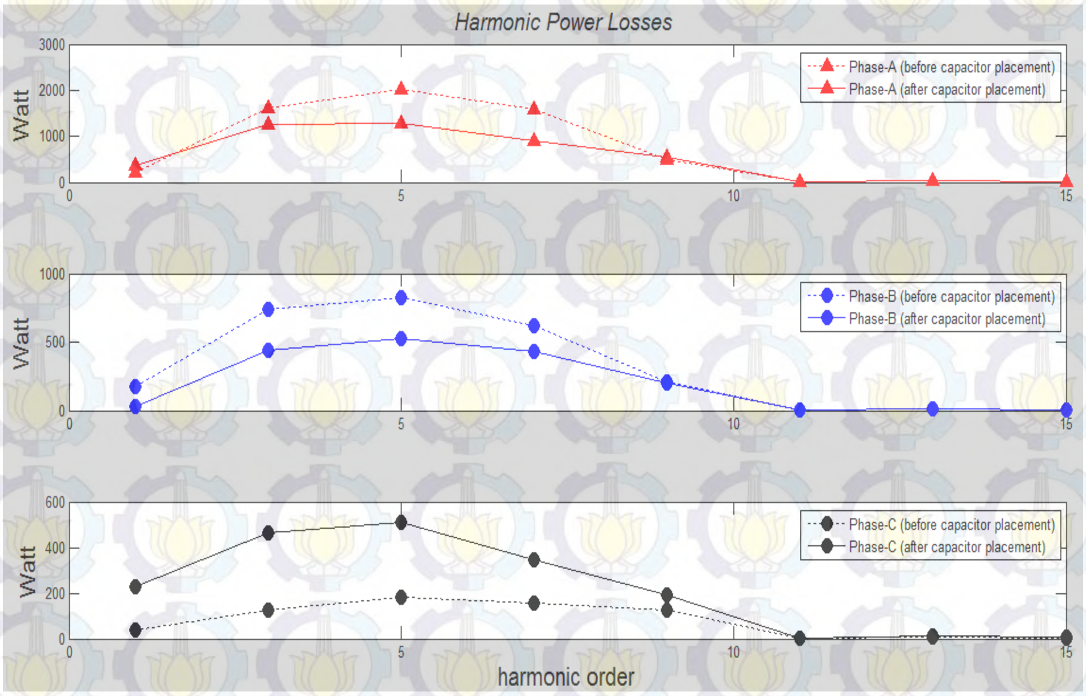

Figure 4.20 Harmonic Power Losses

For the strategy with LSF, the following steps are as follows:

1. Because there are several options of capacitor size, run the power flow for each capacitor size for all the number of possible prospective buses from step, keep each result on matrix that represent number of prospective buses. Calculate the objective function (3.23). For the first step, 15 columns represented from test system branch size which has the highest LSF will be placed by capacitor. Then, objective function will determine whether that size has meet the criterion or not. The result will have one column and *n* rows. n rows represents the prospective capacitor sizes. According to the option of capacitor bank in Table 1.

```
location =
12   7   11   11   5   6   8   9   2   3   4   7   13   10   6
```

While finding the lowest cost from each possible capacitor size, total capacity of capacitor reactive power is upadated. The result is as follows:

```
P_losses =  8.2869e+004
THD_best =     1.2408     5.0015
V_best =    0.9411    0.9977
Obj_res = 1.4533e+004
Capacitor = 600,300, 150, 150, 150, 150, 150
Location = 18,23,13, 14,15, 19,29 [7-c,9-b,6-a,6-b,6-c,8-a,13-c]
```

The following figure will describe the total harmonic power losses from different order of harmonic frequencies after placement of 1650 kVAr in total of 1 unit of 600 kVAr capacitor, i unit of 300 capacitor and 5 units of 150 kVAr capacitor in the following locations. Figure 4.21 represents the best solution from the 8 iteration. The last iteration point out the result from the reference to 14,533 USD/year

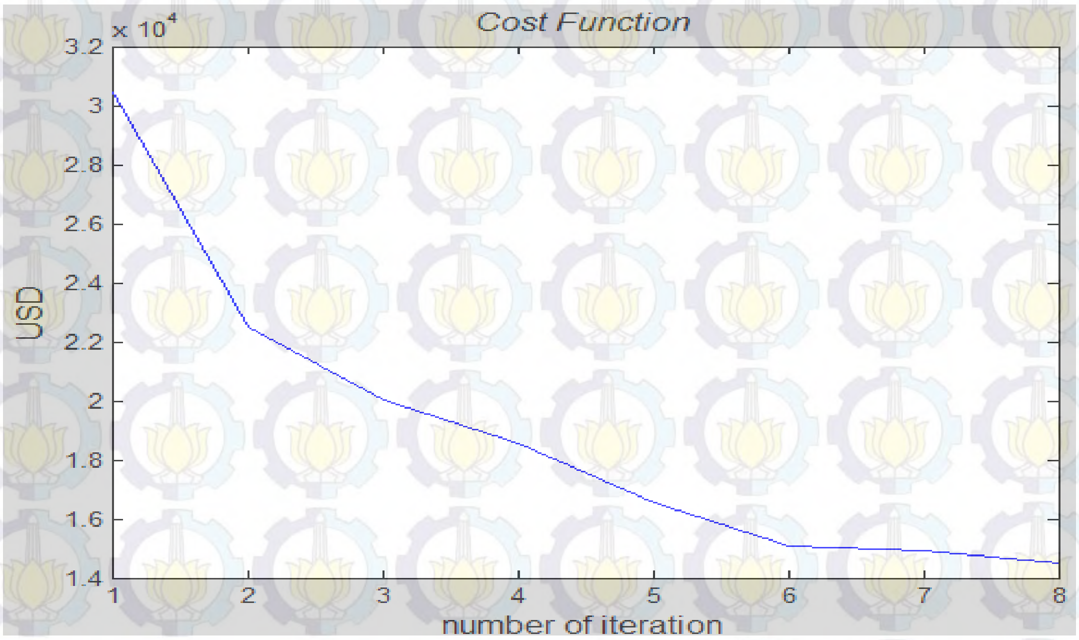

Figure 4.21 Minimum Objective Function by Placing 1650 kVAr

Figure 4.22 represents the voltage profile of bus-8 phase-A after 1650 kVAr placed. From the figure, the voltage profile at bus-10 phase-C is the lowest voltage and bus-7 phase-C has the highest voltage. All phases have the voltage quality that fullfilled the voltage level constraint.

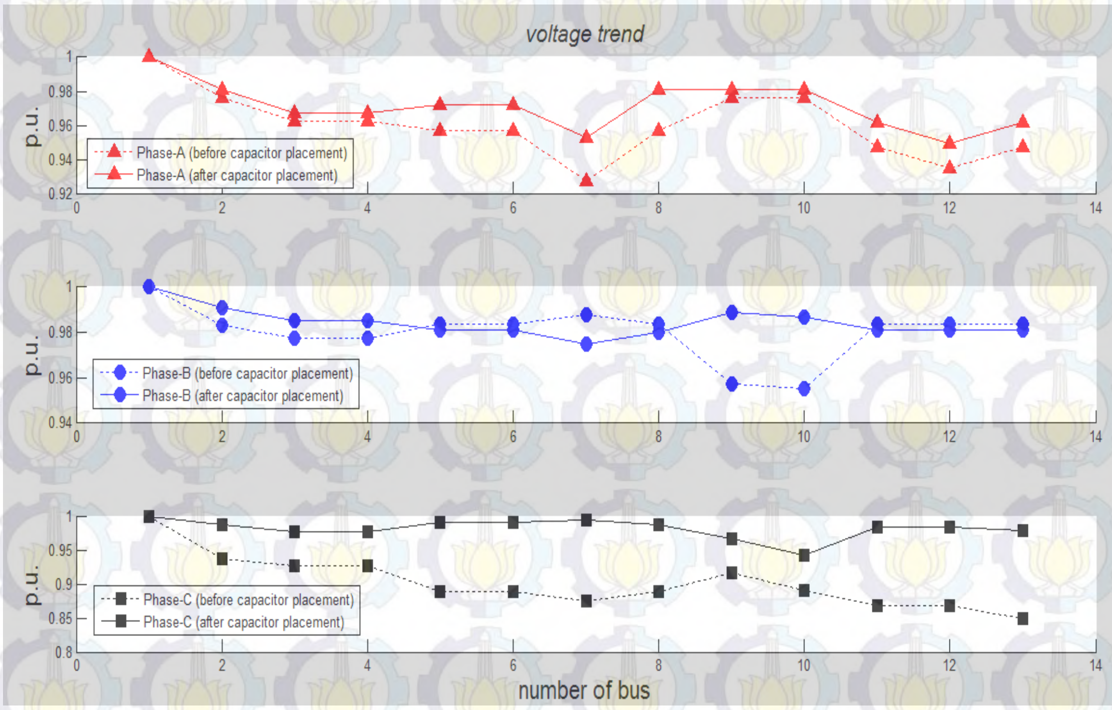

Figure 4.22 Voltage Profile by Placing 1650 kVAr

Figure 4.23 depicted that the recent harmonic profile of the system are significantly within the limit. THD level of each phase can comply with the which is not exceeding 5%.

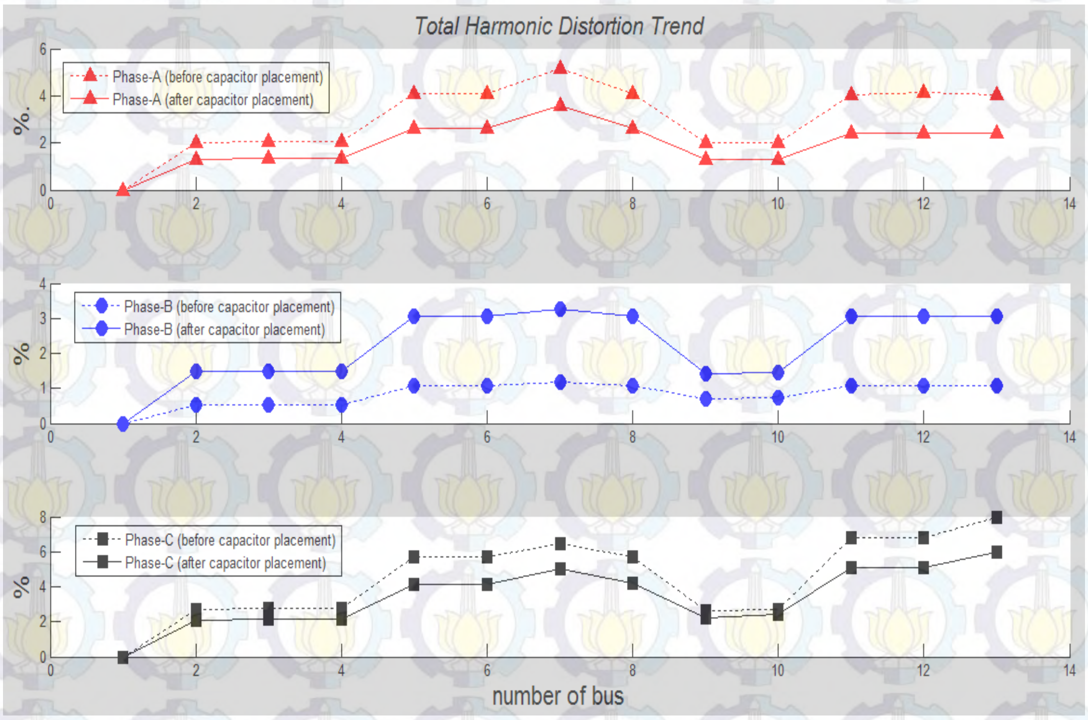

Figure 4.23 THD profile by Placing 1650 kVAr

Figure 4.24 depicted that the power losses in third, fifth, seventh, and ninth are slightly decreasing in comparison with the base case system. Meanwhile, power losses in rest order of harmonic are very small. By placing that capacitor, the harmonic power losses is slightly reduced.

Figure 4.24 Total Harmonic Power Losses Trend

From Figure 4.25, the power losses in third, fifth, seventh, and ninth harmonic frequency in phase-A are slightly reduced while power losses in phase-B at fifth, seventh, and ninth harmonic frequency is relatively having significant reduction of harmonic power losses. The harmonic penetration in phase-C are still high because it is loaded by more harmonic loads.

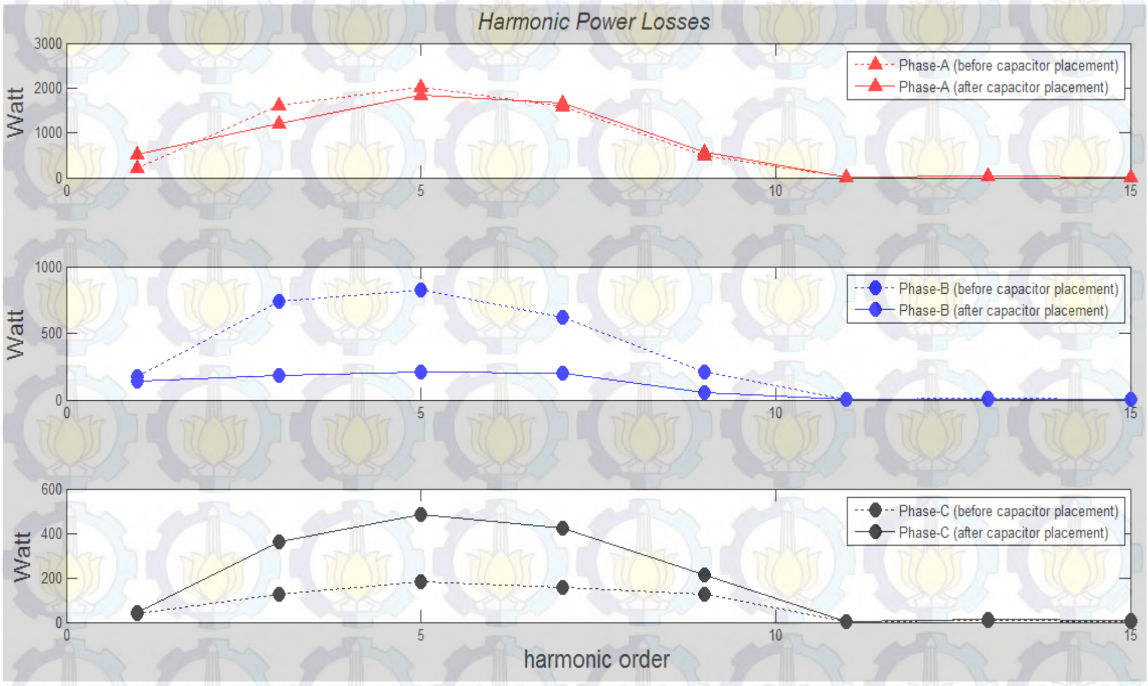

Figure 4.25 Harmonic Power Losses

4.4.3.3. Capacitor Installation with Random Initialization

1. Each bus will be identified by placing a set of capacitor to obtain the first initial condition of prospective bus. This initial condition will be kept as a reference for the next iteration. For the first initialization, the random value of set capacitor will be placed. The

location of the capacitor placement will also be randomly located. Meanwhile, the constraint of the algorithm is similar with the previous subsection B. The maximum losses of system is determined from the total reactive power demand of test system. This uncompensated loss is considered to be maximum loss in the system. the refference that will be taken are as follows:

i. Total cost of active power losses = 30,311.064 USD/year
ii. Active power losses = 180.423 kW
iii. Maximum reactive power limit for capacitor placement = 1,743 kVAr
iv. Maximum Voltage = 1.05 pu
v. Minimum Voltage = 0.9 pu
vi. Maximum THD level = 5 %

Some modification in the constraint is done which are as follows:

```
data_capacitor  = [-150*1e3 150*1e3];
data_location   = [1 36];
num_particle    = 10;  % number of random search particle
iteration_max    = 100;  % Maximum Iteration
num_variable    = 10 ;  % total candidate location
```

data_capacitor is the range of each capacitor size in which capacitor can vary. data_location is the possible location of test system in which capacitor can be installed. Range [1,36] is representation of 36 individual location in which each bus at each phase will be counted as 1 possible location. num_particle represents the number of possible solution which will help maximize the searching process. num_variable represents the number of capacitor location which will be maximized through the searching process. Iteration_max maximum iteration of the searching process.

2. Put the initial range of searching candidate. Because it has been determined to limit only 10 location, the sum of one set of capacitor will not exceed the maximum reactive power limit which is 1,743 kVAr. Each candidate will be varied among data_capacitor range.

position_particle(yy,xx)= abs((data_position(1,1)+(data_position(1,2)- data_position(1,1))*rand));

3. Similar with previous step, the locations will be set in the num_variable. The initial place of the capacitor will be the determined from the random value between data_location which is the total number of bus without slack bus.

position_location(yy,xx)= round(data_location(1,1)+(data_location(1,2)-data_location(1,1))*rand);

1. At the first iteration, with the random initial position of location and size, the possibilities of candidate solution which has size **(num_particle) x (num_variable)** will be as follows.

```
>> position_particle *** in kVAr based

   55.2879   68.5001  136.1521  159.3203   35.3642   21.0342  138.6925   65.9077   77.0508   23.8421
   70.5285  341.3245   69.0446   51.8890  236.4919  214.5820   69.5334  287.4869   99.9997  120.0453
   25.5656   66.2997   22.8659   72.8153   13.6158  177.3984  137.3499  275.5850   69.5320  114.5795
   27.4455   33.0975   43.3062   44.8373   18.3528   53.4137  110.7163  116.7248   68.2843   69.5763
   50.9827   17.9850    5.8714   39.2933   74.9974  174.8063   24.7548   19.2897  250.7143   57.2615
   12.8672   18.3486    6.8317   44.9025    5.3814    0.3290   36.2878   85.5971  118.1532  161.0354
  210.6770   88.5317  178.6875   71.3577  164.7110  195.6544  112.2998  125.1934   41.3906  131.2099
   25.5257   66.4483   52.9715  192.3479  168.6973   55.2270   36.2775  186.6170  195.9172   70.2132
   66.3839  113.2313  241.6151   33.4768  160.6571   52.7339  126.6370  177.5725  109.6706  125.4770
   34.4848   87.3644  144.9357   24.4538   88.7845   37.1283  109.8410  104.3029   32.4009  106.3166
     1          2         3         4         5         6         7         8         9        10
                              candidate set of 10 particles
```

```
position_location =

    13    33    12    14    21     4    27    27    17    30
    26    11    19    30    30     8     5    17    30    15
     6    16    11     9    19    15    26    18    10    26
     7     6    16    11     2     6    10    24    12    26
     9     6    27    28    30    30    10    17    36    16
    26    16    10    34     5    36    14    28     8    30
    19    15    26     2    20     8     9    11    24     4
     2     6    16    23    21     3     8    18     5     5
    16    31     5     2    21    27    14     8    17    11
    18    28    28    21    23     6     8    17    13    22
     1     2     3     4     5     6     7     8     9    10   candidate place
```

By randomize initial position of location, some parts of the set has the same value. This condition will be maintained as the sum of each part of possible position of particle in the same prospective bus due to the following position_location result.

2. Find the highest net savings from the previous calculation. Update the minimum objective function reference. After one iteration, the result which is active power losses of each candidate solution will be kept and sort. The minimum active power losses will be the best fitness from 1 iteration.

```
% reference
REF_P_losses   = 3.6981e+004
% best solution
Fgbest         = 2.9839e+004
```

Table 4.10 represents the result of power losses reduction after the placement of 1 set of 10 shunt capacitors. Y-Axis represents the active power in kW unit while X-axis represents the number of iteration. DSA obtained 29.839 active power losses reduction by placing 750 kVAr capacitor in total at bus: 9A, 3A, 5B, 2B, 7C, 1B, 2A, 3B, and 5C. The maximum active power losses reduction from this capacitor installation is about 16.57 % from the total active power losses of the rest of the system. The convergence criteria is depicted in Figure 4.26

Table 4.10 Result of DSA on placing 1 set of 10 capacitors

Best Capacitor	Location Index	Bus location
150	28	9-A
70	10	3-A
3	28	9-A
65	17	5-B
6	8	2-B
150	24	7-C

150	5	1-B
77	7	2-A
15	11	3-B
80	18	5-C

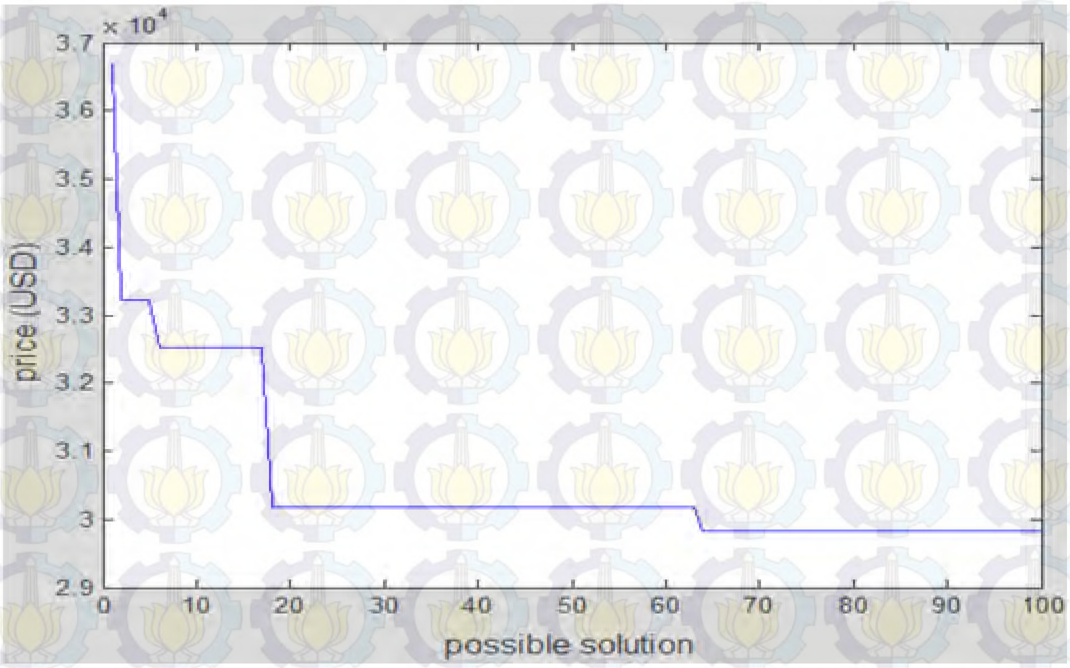

Figure 4.26 Minimum objective function on placing 1 set of 10 capacitors

Figure 4.27 depicted the result of power losses reduction after the placement of 1 set of 3 shunt capacitors. Y-Axis represents the active power in kW unit while X-axis represents the number of iteration. DSA obtained 29.980 kW active power losses reduction by placing 513 kVAr capacitor in total at bus-5 phase-C, bus-6 phase-A, and bus-7 phase-C. The maximum net saving from this capacitor installation is about 16.65 % from the total cost function of base case system.

```
% reference
REF_P_losses  =   3.6981e+004
% best solution
Fgbest        =   2.9980e+004
```

Table 4.1 The result of DSA on placing 1 set of 3 capacitors

Best Capacitor	Location Index	Bus location
240	15	5C
160	16	6A
113	21	7C

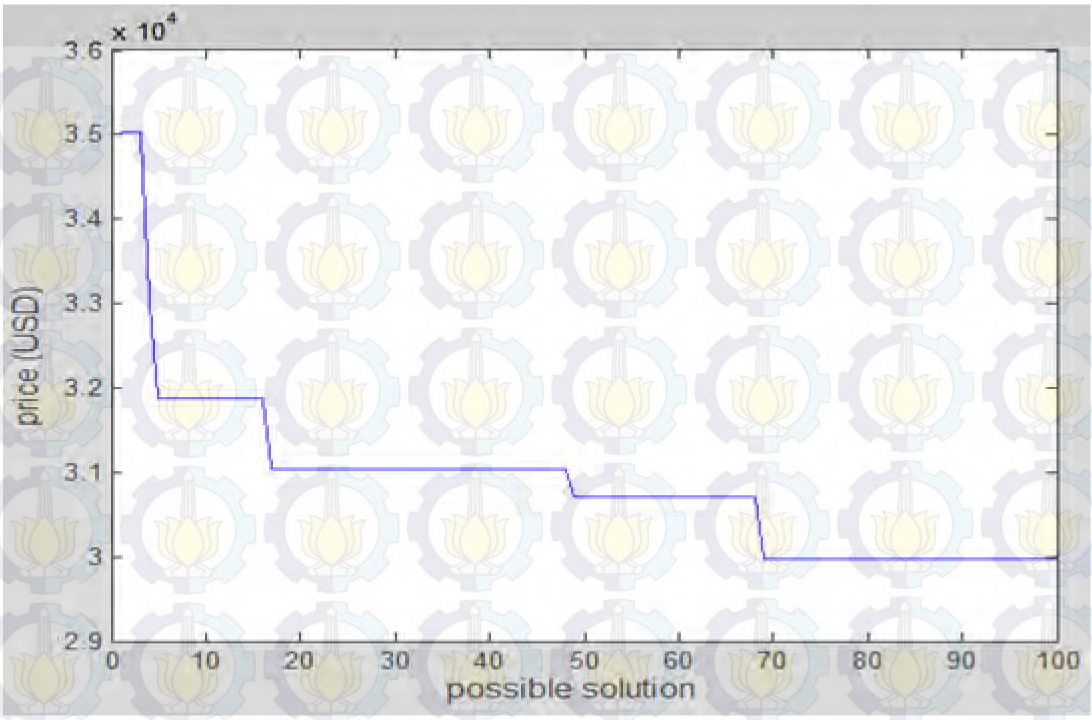

Figure 4.5 Minimum objective function on placing 1 set of 3 capacitors

Another test system is applied in DSA algorithm which is 22-bus Agriculture distribution sytem (Raju, *et al*, 2012). This test sytem represented the small portion of agricultural distribution system of Eastern Power Distribution System in India. This system has 11 kV base voltage. The reactive power load demand in this test system is 657.4 kVAr an active power losses without capacitor compensation is 17.69 kVAr while the active power losses when no reactive power load assumed is 9.14 kW. The following result when DSA is applied for the base case is as follows:

	A	B	C	Total
System Input				
kW	672.429	0.000	0.000	672.429
kVAR	640.519	0.000	0.000	640.519
kVA	928.669	0.000	0.000	928.669
PF	0.724	0.000	0.000	
LOAD				
kW	662.311	0.000	0.000	662.311
kVAR	**657.400**	**0.000**	**0.000**	**657.400**
kVA	933.183	0.000	0.000	933.183
PF	0.710	0.000	0.000	
LOSS				
kW	**10.118**	**0.000**	**0.000**	**10.118**
kVAR	-16.881	0.000	0.000	-16.881
kVA	19.680	0.000	0.000	19.680

TOTAL LOSSES (US$) 1699.782 *** with losses price=168 USD/kW

The active power losses obtained is 10.12 kW while in the reference, the system suffers 17.69 kW active power losses. When the system is assumed without any reactive power demand,

(Q_{system}=0), the active power losses obtained is 9.115 kW as mentioned in the following result.

	A	B	C	Total
System Input				
kW	671.426	0.000	0.000	671.426
kVAR	4.531	0.000	0.000	4.531
kVA	671.441	0.000	0.000	671.441
PF	1.000	0.000	0.000	
LOAD				
kW	662.311	0.000	0.000	662.311
kVAR	0.000	0.000	0.000	0.000
kVA	662.311	0.000	0.000	662.311
PF	1.000	0.000	0.000	
LOSS				
kW	**9.115**	**0.000**	**0.000**	**9.115**
kVAR	4.531	0.000	0.000	4.531
kVA	10.179	0.000	0.000	10.179

TOTAL LOSSES (US$) 1531.352 *** with losses price=168 USD/kW

The following figure 4.28 represents the voltage profile before and after assumptions. After assumption, with all the reactive power demand compensated, voltage profile is much better than the system with any reactive power demand. The voltage can increased from 0.973 pu to 0.981 pu.

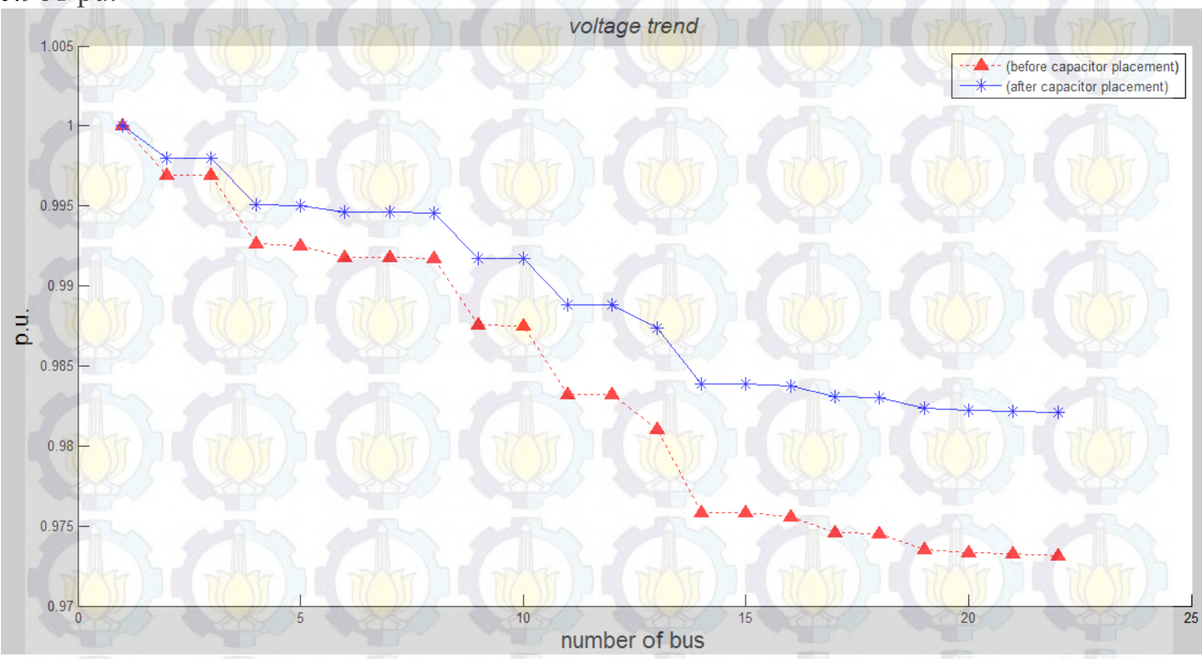

Figure 4.6 Voltage profile of 22-bus Test System

The folowing figure 4.29 represent the THD profile in the test system. THD is significantly reduced when the reactive power is fully compensated.

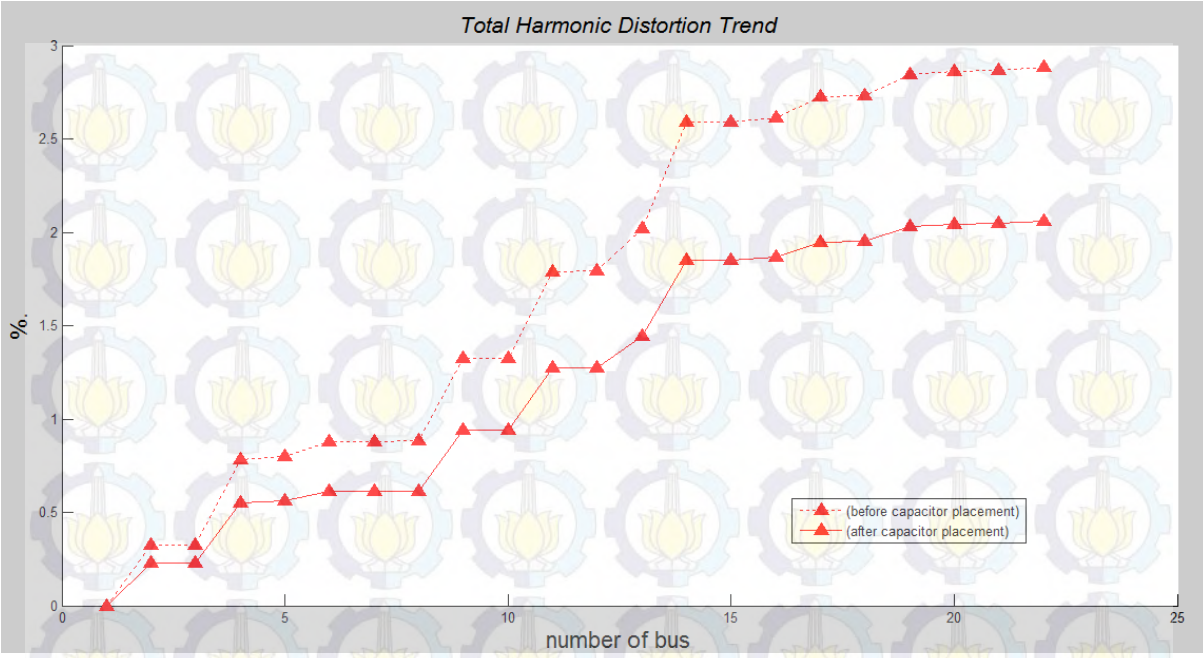

Figure 4.7 THD profile of 22-bus test system

4.5. Discussion

The system has reactive power load 1,743 kVAr in total and the uncompensated active power losses which is about 180.423 kW (due to Table 9 in subsection 4.3). By the strategy done in subsection 4.4, the single size capacitor placement find the maximum net savings which is 4,690 USD/year with real power losses obtained to reduce about 26.937 kW. By using voltage constraint, the capacitor placement find the objective function which is 6,009 USD/year with active power losses obtained 35.088 kW. By using random initialization, the active power losses saving become 29.980 kW and yields 5,037 USD/year net savings.

To compare the effectiveness of the algorithm, a comparison with the result in (Eajal, A.A., El-Hawary, M.E., 2010) is done. The strategies that has been done in this research to identify the effect on how the shunt capacitor allocation affecting the system voltage profile, total harmonic distortion, total active power losses and net savings, the strategy studied which are as follows:

- Case-1 analyzes the system condition with harmonic consideration. Case 1 is taken as the base case or reference which is the system condition without capacitor placement.
- Case-2 analyze the effect of capacitor placement by finding the minimum objective function without limiting the THD level on each prospective bus.
- Case-3 analyze the effect of capacitor placement by finding the optimal net savings and keeping the THD level on each prospective bus within the limit.

Table 4.2 Result of Optimal Capacitor Placing and Location with PSO algorithm
(source: Eajal and El-Hawary, 2010)

	Case-1 (Without Capacitor)	Case-2 (Without THD constraint)	Case-3 (With complete constraint)
Min. Bus Voltage (p.u)	0.8954	0.9555	0.9556
Max. Bus Voltage (p.u)	0.9863	0.9945	0.9947
Max.THD (%)	4.459	19.0335	1.723
Reactive Power Injection (kVAr)	-	(5b) 300	(5c) 600
		(6a) 450	(6a) 450
		(6c) 600	(6b) 300
Active Power Losses (kW)	192.75	164.99	165.22
Cost Function (USD/year)	32,326.69	28,069	28,107
Net Savings (USD/year) Net Savings (%)	-	4,257.69 13.17	4,219.69 13.05

Table 4.11 represents the result of optimal capacitor allocation in (Eajal and El-Hawary, 2010). This reference also used IEEE 13-bus test system and objective function whose goal is to maximize the net savings. With the use of Particle Swarm Optimization (PSO) algorithm, this reference yields 165.216 kW active power losses and cost function reduction from 32.326 USD/year to 28,107 USD/year. The algorithm yields 13.05 % of total cost function. The algorithm considers the THD of each bus to be kept within the allowed THD limit.

Without considering THD limit, the algorithm in reference yields 164.987 kW active power losses and cost function reduction which is about 4,258 USD/year. The active power losses before capacitor installation is 192.75 kW. The cost function decreases about 13.17 % eventhough the maximumm THD reach .

For the comparison, direct search algorithm identified the bus with the help of load sensitivity factor. For achieving the good result, load sensitivity factor must be taken by including aggregated power losses as the reference. By using aggregated power – LSF, DSA obtained about tenth percent difference from the total losses of the system. This result is better than by considering only fundamental power.

The comparison between the performance of direct search algorithm and particle swarm optimization in reference can only be done by comparing the percentage of maximum net savings that achieved. The main difficulties are make the same base case because the load composition is uncertain.

For single placement capacitor without LSF approach, direct search algorithm obtained 26.937 kW active power losses improvement by placing 900 kVAr capacitor at bus-8A. The net saving from this capacitor installation is about 15 percent from total cost function. For single capacitor placement with LSF, direct search algorithm achieved 6,009 USD/year net savings or about 19.4 percent in comparison with the cost function in base case. This net savings is achieved by placing 450 kVAr capacitor in bus-7 phase-C and it yields 35.088 kW active power losses reduction. For more detail understanding, the following Table 4.12 will represent the comparison of optimal capacitor in single capacitor placement.

Table 4.3 Result of Optimal Single Capacitor Placing and Sizing With DSA

Single Capacitor	Base Case	Without LSF	With LSF
Reduction in Real Power Losses (kW)	180.423	26.9	35.1
Reduction Cost Saving (USD/year)	30,253.94	4,690.0	6,008.7
Capacitor size (kVAr)	-	900	450
Location	-	8-A	7-C
Max. Voltage (pu)	0.988	1.106	0.974
Min. Voltage (pu)	0.849	0.808	0.914
Max. THD (%)	8	8.916	4.958
Net Savings (%)		14.9	19.4

Table 4.4 Result of Optimal Multiple Capacitor Placing and Sizing with DSA

Multiple Capacitor	Base Case	Without LSF		With LSF	
Real Power Losses (kW)	180.423	159.6		82.9	
Cost Saving (USD/year)	30,253.94	26,984.0		14,533.0	
Capacitor size (kVAr)		10-C	450	7-C	600
		5-B	300	9-B	300
		4-A	150	6-A	150
		5-A	150	6-B	150
		5-C	150	6-C	150
		12-A	150	8-A	150
		13-C	150	13-C	150
Max. Voltage (pu)	0.988	0.999		0.998	
Min. Voltage (pu)	0.849	0.924		0.941	
Max. THD (%)	8	4.954		5.000	
Net Savings (%)		11.5		54.1	

The following Table 4.13 will represent the comparison of optimal multiple capacitor allocation based on direct search algorithm. For the placement without LSF approach, DSA obtained 159.6 kW real power losses or about 20.82 kW losses reduction by placing 1500 kVAr capacitor in total at following buses. The maximum net saving from this capacitor installation is about 11.5 % from the total cost function of base case system. The voltage and THD profile can be maintained within the standard. For the placement with LSF approach, DSA obtained 82.9 kW real power losses or about 97.5 kW losses reduction by placing 1650 kVAr capacitor in total at following buses. The maximum net saving from this capacitor installation is about half percent from the total cost function of base case system. The voltage and THD profile also can be maintained within the standard.

By the following explaination, direct search algorithm performance is significantly reduction from the algorithm that used in reference. Table 4.14 shown the detail comparison between DSA and reference in base case system.

Table 4.5 Comparison of DSA with reference in Base Case (without capacitor placement)

	13-Bus Test System		22-Test System	
	(Eajal &El-Hawary,2012)	DSA	(Raju, *et al*, 2013)	DSA
Min. Bus Voltage (p.u)	0.8954	0.849	0.9729	0.973
Max. Bus Voltage (p.u)	0.9863	0.988	-	0.9955
Max.THD (%)	4.459	8	-	2.6
Active Power Losses (kW)	192.75	180.423	17.69	10.118
Cost Function (USD/year)	32,326.69	30,253.94	10,302	5,892.30

From the following table, the DSA can obtain 180.423 kW power losses while the PSO obtains 192.75 kW from the applied 13-bus test sytem. The THD of the system before the placement is worse than the result in reference (Eajal &El-Hawary,2012) which is obtained that THD level is 8%. When DSA is applied in 22-Test system, the following result of DSA shows that 22-bus test system already has good voltage profile and the THD level in this system is relatively small in comparison with 13-bus test system. The active power losses obtained with DSA is about 10.12 kW while in reference (Raju, *et al,* 2013), active power losses is about 17.69 kW. Thus, DSA can significantly sense the condition of the system better than the references.

CHAPTER 5
CONCLUSION AND RECOMMENDATIONS

5.1 Conclusion

This research has been gone through the following detail. Application of direct search algorithm in capacitor placement and sizing prediction could achieve significant result of finding the maximum net savings while maintaining the system voltage within the standard and THD limit. Direct search algorithm identified the bus with the help of load sensitivity factor. For achieving the significant result, load sensitivity factor must be taken by including aggregated harmonic power losses as the reference. Direct search algorithm is applied on IEEE 13-bus test system. Three strategies has been done to see the performance of direct search algorithm which are applying single and mutiple fixed shunt capacitor with and without load sensitivity factor. Direct search performance finds more significant net savings when it is combined with load sensitivity factor. The result provide some understanding when the harmonics is taken into account, the system will be secure of the damage caused by hitting the thermal limit due to the less power system losses so that current that flows in the system. It is necessary to concern about harmonic on the system because harmonics can increase the current and when it flowing through branch impedance, the power losses of the system will be higher than normal condition.

5.2 Recommendations

Recommendations for the next research and researcher are as follows:

1. Capacitor placement can be upgraded by using maintenance cost, installation cost, and penalty cost instead of only using aggregated installation cost of capacitor.
2. In distribution power flow, the PQ model can be substituted to be PV model so that the capacitor allocation strategy can solve both passive and active power system that is very suitable for the real condition.
3. This capacitor allocation strategy can be implemented into the real time system which the load composition of the distribution network will be clearly available, especially in harmonic source load. The load composition is very important which can determine the performance of the algorithm.
4. Load modelling can be improved in more detail such as exponential load and composite load for further understanding of the shunt capacitor application effect on distribution network.

REFERENCES

Aman, M.M., Jasmon, G.B., Bakar, A.H.A., Mokhlis, H., Karimi, M., (2014). Optimum Shunt Capacitor Placement In Distribution System-A Review And Comparative Study. Renewable and Sustainable Energy Reviews Vol. 30 pp. 429-439.

Arrillaga, J., Watson, Neville R., (2003). Power System Harmonics. ISBN-10: 0470851295, ISBN-13: 978-0470851296, Second Edition. England: Wiley

Blooming, T.M., Carnovale, D.J, (2008). Capacitor Application Issues. IEEE Transaction on Industry Applications. Vol.44, Issue:4, pp. 1013-1026.

Distribution System Analysis Subcommittee, (2004). IEEE 13 Node Test Feeder. IEEE Power Engineering Society. Power System Analysis, Computing and Economics Committee. The Institute of Electrical and Electronics Engineers. Inc.

Eajal, A.A., El-Hawary, M.E., (2010). Optimal Capacitor Placement and Sizing in Distorted Radial Distribution Systems Part I: System Modeling and Harmonic Power Flow Studies. IEEE conference: 14th International Conference on Harmonics and Quality of Power. E-ISBN: 978-1-4244-7245-1. pp. 1-9

Eajal, A.A., El-Hawary, M.E., (2010). Optimal Capacitor Placement and Sizing in Distorted Radial Distribution Systems Part II: Problem formulation and solution method. IEEE conference: 14th International Conference on Harmonics and Quality of Power. E-ISBN: 978-1-4244-7245-1. pp. 1-6.

Eajal, A.A., El-Hawary, M.E., (2010). Optimal Capacitor Placement and Sizing in Distorted Radial Distribution Systems Part III: Numerical Results. IEEE conference: 14th International Conference on Harmonics and Quality of Power. E-ISBN: 978-1-4244-7245-1. pp. 1-8.

Eajal, A.A., El-Hawary, M.E., (2010). Optimal Capacitor Placement and Sizing in Unbalanced Distribution Systems with Harmonics Consideration Using Particle Swarm Optimization. IEEE Transactions On Power Delivery, Vol. 25, No. 3. pp. 1734-1741.

Elamin, I.M., (1990). Fast decoupled harmonic loadflow method. Industry applications society annual meeting. Conference Record of 1990 IEEE. ISSBN:0-87942-553-9. Vol.2 pp. 1749-1756.

El-Fergany, Attia A., Abdelaziz, A.Y., (2014). Capacitor placement for net saving maximization and system stability enhancement in distribution networks using artificial bee colony-base approach. Electrical Power and Energy Systems Vol. 54 pp. 235-243. ELSEVIER

IEEE standard 519-1992. IEEE recommended practices and requirement for harmonic control in electrical power system. American National Standard (ANSI). Industry Applications Society/Power Engineering Society.

Jordanger, E., Sand, K., Kristensen, R., 2001. Method for calculation of cost of electrical power system losses. Electricity Distribution. CIRED. 16th International Conference and Exhibition on (IEE Conf. Publ) Vol.5, No. 482, pp. 1-4

Kersting, W.H., (2002). Distribution System Modelling and Analysis. USA: CRC Press.

Murthy, K.V.S Ramachandra, Karayat, Mamta, Das, P. K., Shankar, A., Ravi, Rao, G. V.Srihara, (2013). Loss Less Distribution using Optimal Capacitor and Type-3 DG

Placement. International Journal of Engineering Trends in Electrical and Electronics (IJETEE – ISSN: 2320-9569).

Pesonen, M. A., (1981). Harmonics, characteristic parameters, methods of study, estimates of existing values in the network. Electra, Vol.77, PP.35-36.

Raju, M. Ramalinga, Murthy, K.V.S. Ramachandra, Ravindra, K., (2012). Direct search algorithm for capacitive compensation in radial distribution systems. Electrical Power and Energy Systems Vol.42 pp. 24-30, ELSEVIER.

Singh, S.P., Rao, A.R., (2012). Optimal allocation of capacitors in distribution systems using particle swarm optimization. Electrical Power and Energy Systems. Vol. 43. Issue 1, pg.1267-1275. ELSEVIER.

Syai`in, M., Lian K. L., Yang, N., Chen T., (2012). A distribution power flow using particle swarm optimization. Power and Energy Society General Meeting 2012 IEEE. ISSN:1944-9925. pp. 1-7.

Tafreshi, S. M. Moghaddas, Mashhour, E., (2009). Distributed generation modeling for power flow studies and a three-phase unbalanced power flow solution for radial distribution systems considering distributed generation. Electric Power Systems Research, vol. 79, Issue 4, pp. 680-686, ELSEVIER.

Task Force in Harmonics Modelling and Simulation, (1996). Modelling and simulation of the propagation of harmonics in electric power networks part II: Sample Systems and examples”. IEEE Transaction. Power Delivery, Vol. 11, no.1, pp. 466-474.

Task Force in Harmonics Modelling and Simulation, (1996). Modelling and simulation of the propagation of harmonics in electric power networks part I: Concepts, Models and Simulation Techniques”. IEEE Transaction. Power Delivery, Vol. 11, no.1, Jan. pp. 452-465.

Teng, J. H., (2000). A network-topology based three phase load flow for distribution systems. Proceedings of National Science Council ROC (A), Vol. 24, no:4. pp. 259-264.

Teng, J.H., (2003). A Direct Approach for Distribution System Load Flow Solution. IEEE Transactions On Power Delivery, Vol. 18 No.3, ISSN:0885-8977,pp. 882-887.

Teng, J. H., Yang, Chuo-Yean, (2007). Backward/forward sweep-based harmonic analysis method for distribution system. IEEE Transaction on Power Delivery, Vol. 22, no.3, pp. 1665-1672.

Ulinuha, A., Masoum, M.A.S., Islam, S.M., (2007). Unbalance power flow calculation for a radial distribution system using forward-backward propagation algorithm. Power Engineering Conference, AUPEC. ISBN: 978-0-646-49499-1. pp. 1-6

CONCLUSION

This research has been gone through the following detail. Application of direct search algorithm in capacitor placement and sizing prediction could achieve significant result of finding the maximum net savings while maintaining the system voltage within the standard and THD limit. Direct search algorithm identified the bus with the help of load sensitivity factor. For achieving the significant result, load sensitivity factor must be taken by including aggregated harmonic power losses as the reference. Direct search algorithm is applied on IEEE 13-bus test system. Three strategies has been done to see the performance of direct search algorithm which are applying single and mutiple fixed shunt capacitor with and without load sensitivity factor. Direct search performance finds more significant net savings when it is combined with load sensitivity factor. The result provide some understanding when the harmonics is taken into account, the system will be secure of the damage caused by hitting the thermal limit due to the less power system losses so that current that flows in the system. It is necessary to concern about harmonic on the system because harmonics can increase the current and when it flowing through branch impedance, the power losses of the system will be higher than normal condition.

BIOGRAPHY

Nama	:	Happy Aprillia
Tempat, tanggal lahir	:	Samarinda, 11 April 1991
Alamat Rumah	:	Jl. Jakarta Blok BM. No. 23 Perumahan KORPRI Loa Bakung Samarinda 75129 Kalimantan Timur
Kewarganegaraan	:	Indonesia
Agama	:	Islam
Jenis Kelamin	:	Perempuan
Telepon, HP	:	(0541) 6275493 / 085257017790
E-mail	:	heprillia@gmail.com

Setelah menyelesaikan studi Sarjana dari Politeknik Elektronika Negeri Surabaya pada tahun 2012, penulis melanjutkan studi S2 di Institut Teknologi Sepuluh Nopember (ITS). Penulis berkesempatan untuk melanjutkan studi melalui program beasiswa Joint Degree dimana penulis menyelesaikan masa kuliah program master satu tahun di ITS Indonesia dan satu tahun di Asian Institute of Technology (AIT) Thailand. Spesialisasi penulis adalah bidang keahlian Teknik Sistem Tenaga khususnya pada bidang *harmonic power flow*.

APPENDIX

Full Body Matrix (FBM)

1			2			3		
0.3465 + 1.0182i	0 - 0.1382i	0 - 0.2934i	0.7526 + 1.1818i	0 - 0.0345i	0 - 0.0734i	0	0	0
0 - 0.1382i	0.1560 + 0.5020i	0 - 0.2268i	0 - 0.0345i	0.1580 + 0.4240i	0 - 0.0567i	0	0	0
0 - 0.2934i	0 - 0.2268i	0.1580 + 0.4239i	0 - 0.0734i	0 - 0.0567i	0.1560 + 0.5021i	0	0	0
0.3465 + 1.0182i	0 - 0.1382i	0 - 0.2934i	0.7526 + 1.1818i	0 - 0.0345i	0 - 0.0734i	0	0	0
0 - 0.1382i	0.1560 + 0.5020i	0 - 0.2268i	0 - 0.0345i	0.1580 + 0.4240i	0 - 0.0567i	0	0	0
0 - 0.2934i	0 - 0.2268i	0.1580 + 0.4239i	0 - 0.0734i	0 - 0.0567i	0.1560 + 0.5021i	0	0	0
0.3465 + 1.0182i	0 - 0.1382i	0 - 0.2934i	0.7526 + 1.1818i	0 - 0.0345i	0 - 0.0734i	0	0	0
0 - 0.1382i	0.1560 + 0.5020i	0 - 0.2268i	0 - 0.0345i	0.1580 + 0.4240i	0 - 0.0567i	0	0	0
0 - 0.2934i	0 - 0.2268i	0.1580 + 0.4239i	0 - 0.0734i	0 - 0.0567i	0.1560 + 0.5021i	0	0	0
0.3465 + 1.0182i	0 - 0.1382i	0 - 0.2934i	0.7526 + 1.1818i	0 - 0.0345i	0 - 0.0734i	0	0	0
0 - 0.1382i	0.1560 + 0.5020i	0 - 0.2268i	0 - 0.0345i	0.1580 + 0.4240i	0 - 0.0567i	0	0	0
0 - 0.2934i	0 - 0.2268i	0.1580 + 0.4239i	0 - 0.0734i	0 - 0.0567i	0.1560 + 0.5021i	0	0	0
0.3465 + 1.0182i	0 - 0.1382i	0 - 0.2934i	0.7526 + 1.1818i	0 - 0.0345i	0 - 0.0734i	0	0	0
0 - 0.1382i	0.1560 + 0.5020i	0 - 0.2268i	0 - 0.0345i	0.1580 + 0.4240i	0 - 0.0567i	0	0	0
0 - 0.2934i	0 - 0.2268i	0.1580 + 0.4239i	0 - 0.0734i	0 - 0.0567i	0.1560 + 0.5021i	0	0	0
0.3465 + 1.0182i	0 - 0.1382i	0 - 0.2934i	0.7526 + 1.1818i	0 - 0.0345i	0 - 0.0734i	0	0	0
0 - 0.1382i	0.1560 + 0.5020i	0 - 0.2268i	0 - 0.0345i	0.1580 + 0.4240i	0 - 0.0567i	0	0	0
0 - 0.2934i	0 - 0.2268i	0.1580 + 0.4239i	0 - 0.0734i	0 - 0.0567i	0.1560 + 0.5021i	0	0	0
0.3465 + 1.0182i	0 - 0.1382i	0 - 0.2934i	0.7526 + 1.1818i	0 - 0.0345i	0 - 0.0734i	0	0	0
0 - 0.1382i	0.1560 + 0.5020i	0 - 0.2268i	0 - 0.0345i	0.1580 + 0.4240i	0 - 0.0567i	0	0	0
0 - 0.2934i	0 - 0.2268i	0.1580 + 0.4239i	0 - 0.0734i	0 - 0.0567i	0.1560 + 0.5021i	0	0	0
0.3465 + 1.0182i	0 - 0.1382i	0 - 0.2934i	0.7526 + 1.1818i	0 - 0.0345i	0 - 0.0734i	0	0	0
0 - 0.1382i	0.1560 + 0.5020i	0 - 0.2268i	0 - 0.0345i	0.1580 + 0.4240i	0 - 0.0567i	0	0	0
0 - 0.2934i	0 - 0.2268i	0.1580 + 0.4239i	0 - 0.0734i	0 - 0.0567i	0.1560 + 0.5021i	0	0	0
0.3465 + 1.0182i	0 - 0.1382i	0 - 0.2934i	0.7526 + 1.1818i	0 - 0.0345i	0 - 0.0734i	0	0	0
0 - 0.1382i	0.1560 + 0.5020i	0 - 0.2268i	0 - 0.0345i	0.1580 + 0.4240i	0 - 0.0567i	0	0	0
0 - 0.2934i	0 - 0.2268i	0.1580 + 0.4239i	0 - 0.0734i	0 - 0.0567i	0.1560 + 0.5021i	0	0	0
0.3465 + 1.0182i	0 - 0.1382i	0 - 0.2934i	0.7526 + 1.1818i	0 - 0.0345i	0 - 0.0734i	0	0	0
0 - 0.1382i	0.1560 + 0.5020i	0 - 0.2268i	0 - 0.0345i	0.1580 + 0.4240i	0 - 0.0567i	0	0	0
0 - 0.2934i	0 - 0.2268i	0.1580 + 0.4239i	0 - 0.0734i	0 - 0.0567i	0.1560 + 0.5021i	0	0	0
0.3465 + 1.0182i	0 - 0.1382i	0 - 0.2934i	0.7526 + 1.1818i	0 - 0.0345i	0 - 0.0734i	0	0	0
0 - 0.1382i	0.1560 + 0.5020i	0 - 0.2268i	0 - 0.0345i	0.1580 + 0.4240i	0 - 0.0567i	0	0	0
0 - 0.2934i	0 - 0.2268i	0.1580 + 0.4239i	0 - 0.0734i	0 - 0.0567i	0.1560 + 0.5021i	0	0	0
0.3465 + 1.0182i	0 - 0.1382i	0 - 0.2934i	0.7526 + 1.1818i	0 - 0.0345i	0 - 0.0734i	0	0	0
0 - 0.1382i	0.1560 + 0.5020i	0 - 0.2268i	0 - 0.0345i	0.1580 + 0.4240i	0 - 0.0567i	0	0	0
0 - 0.2934i	0 - 0.2268i	0.1580 + 0.4239i	0 - 0.0734i	0 - 0.0567i	0.1560 + 0.5021i	0	0	0

Figure A.1 FBM matrix (column 1-9)

4			5			6		
0	0	0 - 0.0734i	0	0	0 - 0.0440i	0.3465 + 1.0182i	0 - 0.1382i	0 - 0.2934i
0	1.3294 + 1.3475i	0 - 0.0734i	0	1.3294 + 1.3475i	0 - 0.0440i	0 - 0.1382i	0.1560 + 0.5020i	0 - 0.2268i
0 - 0.0734i	0 - 0.0734i	0.2066 + 0.4595i	0 - 0.0440i	0 - 0.0440i	0.2066 + 0.4595i	0 - 0.2934i	0 - 0.2268i	0.1580 + 0.4239i
0	0	0 - 0.0734i	0	0	0 - 0.0440i	0.3465 + 1.0182i	0 - 0.1382i	0 - 0.2934i
0	1.3294 + 1.3475i	0 - 0.0734i	0	1.3294 + 1.3475i	0 - 0.0440i	0 - 0.1382i	0.1560 + 0.5020i	0 - 0.2268i
0 - 0.0734i	0 - 0.0734i	0.2066 + 0.4595i	0 - 0.0440i	0 - 0.0440i	0.2066 + 0.4595i	0 - 0.2934i	0 - 0.2268i	0.1580 + 0.4239i
0	0	0 - 0.0734i	0	0	0 - 0.0440i	0.3465 + 1.0182i	0 - 0.1382i	0 - 0.2934i
0	1.3294 + 1.3475i	0 - 0.0734i	0	1.3294 + 1.3475i	0 - 0.0440i	0 - 0.1382i	0.1560 + 0.5020i	0 - 0.2268i
0 - 0.0734i	0 - 0.0734i	0.2066 + 0.4595i	0 - 0.0440i	0 - 0.0440i	0.2066 + 0.4595i	0 - 0.2934i	0 - 0.2268i	0.1580 + 0.4239i
0	0	0 - 0.0734i	0	0	0 - 0.0440i	0.3465 + 1.0182i	0 - 0.1382i	0 - 0.2934i
0	1.3294 + 1.3475i	0 - 0.0734i	0	1.3294 + 1.3475i	0 - 0.0440i	0 - 0.1382i	0.1560 + 0.5020i	0 - 0.2268i
0 - 0.0734i	0 - 0.0734i	0.2066 + 0.4595i	0 - 0.0440i	0 - 0.0440i	0.2066 + 0.4595i	0 - 0.2934i	0 - 0.2268i	0.1580 + 0.4239i
0	0	0 - 0.0734i	0	0	0 - 0.0440i	0.3465 + 1.0182i	0 - 0.1382i	0 - 0.2934i
0	1.3294 + 1.3475i	0 - 0.0734i	0	1.3294 + 1.3475i	0 - 0.0440i	0 - 0.1382i	0.1560 + 0.5020i	0 - 0.2268i
0 - 0.0734i	0 - 0.0734i	0.2066 + 0.4595i	0 - 0.0440i	0 - 0.0440i	0.2066 + 0.4595i	0 - 0.2934i	0 - 0.2268i	0.1580 + 0.4239i
0	0	0 - 0.0734i	0	0	0 - 0.0440i	0.3465 + 1.0182i	0 - 0.1382i	0 - 0.2934i
0	1.3294 + 1.3475i	0 - 0.0734i	0	1.3294 + 1.3475i	0 - 0.0440i	0 - 0.1382i	0.1560 + 0.5020i	0 - 0.2268i
0 - 0.0734i	0 - 0.0734i	0.2066 + 0.4595i	0 - 0.0440i	0 - 0.0440i	0.2066 + 0.4595i	0 - 0.2934i	0 - 0.2268i	0.1580 + 0.4239i
0	0	0 - 0.0734i	0	0	0 - 0.0440i	0.3465 + 1.0182i	0 - 0.1382i	0 - 0.2934i
0	1.3294 + 1.3475i	0 - 0.0734i	0	1.3294 + 1.3475i	0 - 0.0440i	0 - 0.1382i	0.1560 + 0.5020i	0 - 0.2268i
0 - 0.0734i	0 - 0.0734i	0.2066 + 0.4595i	0 - 0.0440i	0 - 0.0440i	0.2066 + 0.4595i	0 - 0.2934i	0 - 0.2268i	0.1580 + 0.4239i
0	0	0 - 0.0734i	0	0	0 - 0.0440i	0.3465 + 1.0182i	0 - 0.1382i	0 - 0.2934i
0	1.3294 + 1.3475i	0 - 0.0734i	0	1.3294 + 1.3475i	0 - 0.0440i	0 - 0.1382i	0.1560 + 0.5020i	0 - 0.2268i
0 - 0.0734i	0 - 0.0734i	0.2066 + 0.4595i	0 - 0.0440i	0 - 0.0440i	0.2066 + 0.4595i	0 - 0.2934i	0 - 0.2268i	0.1580 + 0.4239i
0	0	0 - 0.0734i	0	0	0 - 0.0440i	0.3465 + 1.0182i	0 - 0.1382i	0 - 0.2934i
0	1.3294 + 1.3475i	0 - 0.0734i	0	1.3294 + 1.3475i	0 - 0.0440i	0 - 0.1382i	0.1560 + 0.5020i	0 - 0.2268i
0 - 0.0734i	0 - 0.0734i	0.2066 + 0.4595i	0 - 0.0440i	0 - 0.0440i	0.2066 + 0.4595i	0 - 0.2934i	0 - 0.2268i	0.1580 + 0.4239i
0	0	0 - 0.0734i	0	0	0 - 0.0440i	0.3465 + 1.0182i	0 - 0.1382i	0 - 0.2934i
0	1.3294 + 1.3475i	0 - 0.0734i	0	1.3294 + 1.3475i	0 - 0.0440i	0 - 0.1382i	0.1560 + 0.5020i	0 - 0.2268i
0 - 0.0734i	0 - 0.0734i	0.2066 + 0.4595i	0 - 0.0440i	0 - 0.0440i	0.2066 + 0.4595i	0 - 0.2934i	0 - 0.2268i	0.1580 + 0.4239i
0	0	0 - 0.0734i	0	0	0 - 0.0440i	0.3465 + 1.0182i	0 - 0.1382i	0 - 0.2934i
0	1.3294 + 1.3475i	0 - 0.0734i	0	1.3294 + 1.3475i	0 - 0.0440i	0 - 0.1382i	0.1560 + 0.5020i	0 - 0.2268i
0 - 0.0734i	0 - 0.0734i	0.2066 + 0.4595i	0 - 0.0440i	0 - 0.0440i	0.2066 + 0.4595i	0 - 0.2934i	0 - 0.2268i	0.1580 + 0.4239i
0	0	0 - 0.0734i	0	0	0 - 0.0440i	0.3465 + 1.0182i	0 - 0.1382i	0 - 0.2934i
0	1.3294 + 1.3475i	0 - 0.0734i	0	1.3294 + 1.3475i	0 - 0.0440i	0 - 0.1382i	0.1560 + 0.5020i	0 - 0.2268i
0 - 0.0734i	0 - 0.0734i	0.2066 + 0.4595i	0 - 0.0440i	0 - 0.0440i	0.2066 + 0.4595i	0 - 0.2934i	0 - 0.2268i	0.1580 + 0.4239i

Figure A.1 FBM matrix (column 10-18)

7			8			9		
0	0	0	0.3465 + 1.0182i	0 - 0.0691i	0 - 0.1467i	0.7982 + 0.4466i	0 - 0.0345i	0 - 0.0734i
0	0	0	0 - 0.0691i	0.1560 + 0.5020i	0 - 0.1134i	0 - 0.0345i	0.3192 + 0.0331i	0 - 0.0567i
0	0	0	0 - 0.1467i	0 - 0.1134i	0.1580 + 0.4239i	0 - 0.0734i	0 - 0.0567i	0.2849 - 0.0140i
0	0	0	0.3465 + 1.0182i	0 - 0.0691i	0 - 0.1467i	0.7982 + 0.4466i	0 - 0.0345i	0 - 0.0734i
0	0	0	0 - 0.0691i	0.1560 + 0.5020i	0 - 0.1134i	0 - 0.0345i	0.3192 + 0.0331i	0 - 0.0567i
0	0	0	0 - 0.1467i	0 - 0.1134i	0.1580 + 0.4239i	0 - 0.0734i	0 - 0.0567i	0.2849 - 0.0140i
0	0	0	0.3465 + 1.0182i	0 - 0.0691i	0 - 0.1467i	0.7982 + 0.4466i	0 - 0.0345i	0 - 0.0734i
0	0	0	0 - 0.0691i	0.1560 + 0.5020i	0 - 0.1134i	0 - 0.0345i	0.3192 + 0.0331i	0 - 0.0567i
0	0	0	0 - 0.1467i	0 - 0.1134i	0.1580 + 0.4239i	0 - 0.0734i	0 - 0.0567i	0.2849 - 0.0140i
0	0	0	0.3465 + 1.0182i	0 - 0.0691i	0 - 0.1467i	0.7982 + 0.4466i	0 - 0.0345i	0 - 0.0734i
0	0	0	0 - 0.0691i	0.1560 + 0.5020i	0 - 0.1134i	0 - 0.0345i	0.3192 + 0.0331i	0 - 0.0567i
0	0	0	0 - 0.1467i	0 - 0.1134i	0.1580 + 0.4239i	0 - 0.0734i	0 - 0.0567i	0.2849 - 0.0140i
0	0	0	0.3465 + 1.0182i	0 - 0.0691i	0 - 0.1467i	0.7982 + 0.4466i	0 - 0.0345i	0 - 0.0734i
0	0	0	0 - 0.0691i	0.1560 + 0.5020i	0 - 0.1134i	0 - 0.0345i	0.3192 + 0.0331i	0 - 0.0567i
0	0	0	0 - 0.1467i	0 - 0.1134i	0.1580 + 0.4239i	0 - 0.0734i	0 - 0.0567i	0.2849 - 0.0140i
0	0	0	0.3465 + 1.0182i	0 - 0.0691i	0 - 0.1467i	0.7982 + 0.4466i	0 - 0.0345i	0 - 0.0734i
0	0	0	0 - 0.0691i	0.1560 + 0.5020i	0 - 0.1134i	0 - 0.0345i	0.3192 + 0.0331i	0 - 0.0567i
0	0	0	0 - 0.1467i	0 - 0.1134i	0.1580 + 0.4239i	0 - 0.0734i	0 - 0.0567i	0.2849 - 0.0140i
0	0	0	0.3465 + 1.0182i	0 - 0.0691i	0 - 0.1467i	0.7982 + 0.4466i	0 - 0.0345i	0 - 0.0734i
0	0	0	0 - 0.0691i	0.1560 + 0.5020i	0 - 0.1134i	0 - 0.0345i	0.3192 + 0.0331i	0 - 0.0567i
0	0	0	0 - 0.1467i	0 - 0.1134i	0.1580 + 0.4239i	0 - 0.0734i	0 - 0.0567i	0.2849 - 0.0140i
0	0	0	0.3465 + 1.0182i	0 - 0.0691i	0 - 0.1467i	0.7982 + 0.4466i	0 - 0.0345i	0 - 0.0734i
0	0	0	0 - 0.0691i	0.1560 + 0.5020i	0 - 0.1134i	0 - 0.0345i	0.3192 + 0.0331i	0 - 0.0567i
0	0	0	0 - 0.1467i	0 - 0.1134i	0.1580 + 0.4239i	0 - 0.0734i	0 - 0.0567i	0.2849 - 0.0140i
0	0	0	0.3465 + 1.0182i	0 - 0.0691i	0 - 0.1467i	0.7982 + 0.4466i	0 - 0.0345i	0 - 0.0734i
0	0	0	0 - 0.0691i	0.1560 + 0.5020i	0 - 0.1134i	0 - 0.0345i	0.3192 + 0.0331i	0 - 0.0567i
0	0	0	0 - 0.1467i	0 - 0.1134i	0.1580 + 0.4239i	0 - 0.0734i	0 - 0.0567i	0.2849 - 0.0140i
0	0	0	0.3465 + 1.0182i	0 - 0.0691i	0 - 0.1467i	0.7982 + 0.4466i	0 - 0.0345i	0 - 0.0734i
0	0	0	0 - 0.0691i	0.1560 + 0.5020i	0 - 0.1134i	0 - 0.0345i	0.3192 + 0.0331i	0 - 0.0567i
0	0	0	0 - 0.1467i	0 - 0.1134i	0.1580 + 0.4239i	0 - 0.0734i	0 - 0.0567i	0.2849 - 0.0140i
0	0	0	0.3465 + 1.0182i	0 - 0.0691i	0 - 0.1467i	0.7982 + 0.4466i	0 - 0.0345i	0 - 0.0734i
0	0	0	0 - 0.0691i	0.1560 + 0.5020i	0 - 0.1134i	0 - 0.0345i	0.3192 + 0.0331i	0 - 0.0567i
0	0	0	0 - 0.1467i	0 - 0.1134i	0.1580 + 0.4239i	0 - 0.0734i	0 - 0.0567i	0.2849 - 0.0140i
0	0	0	0.3465 + 1.0182i	0 - 0.0691i	0 - 0.1467i	0.7982 + 0.4466i	0 - 0.0345i	0 - 0.0734i
0	0	0	0 - 0.0691i	0.1560 + 0.5020i	0 - 0.1134i	0 - 0.0345i	0.3192 + 0.0331i	0 - 0.0567i
0	0	0	0 - 0.1467i	0 - 0.1134i	0.1580 + 0.4239i	0 - 0.0734i	0 - 0.0567i	0.2849 - 0.0140i

Figure A.3 FBM matrix (column 19-27)

10			11			12		
1.3280 + 1.3573i	0 - 0.0440i	0 - 0.0440i	0	0	0 + 0.0042i	1.3425 + 0.5127i	0 + 0.0112i	0
0 - 0.0440i	0	0	0	0	0	0 + 0.0112i	0	0
0 - 0.0440i	0	0.2066 + 0.4595i	0 + 0.0042i	0	1.3292 + 1.3479i	0	0	0
1.3280 + 1.3573i	0 - 0.0440i	0 - 0.0440i	0	0	0 + 0.0042i	1.3425 + 0.5127i	0 + 0.0112i	0
0 - 0.0440i	0	0	0	0	0	0 + 0.0112i	0	0
0 - 0.0440i	0	0.2066 + 0.4595i	0 + 0.0042i	0	1.3292 + 1.3479i	0	0	0
1.3280 + 1.3573i	0 - 0.0440i	0 - 0.0440i	0	0	0 + 0.0042i	1.3425 + 0.5127i	0 + 0.0112i	0
0 - 0.0440i	0	0	0	0	0	0 + 0.0112i	0	0
0 - 0.0440i	0	0.2066 + 0.4595i	0 + 0.0042i	0	1.3292 + 1.3479i	0	0	0
1.3280 + 1.3573i	0 - 0.0440i	0 - 0.0440i	0	0	0 + 0.0042i	1.3425 + 0.5127i	0 + 0.0112i	0
0 - 0.0440i	0	0	0	0	0	0 + 0.0112i	0	0
0 - 0.0440i	0	0.2066 + 0.4595i	0 + 0.0042i	0	1.3292 + 1.3479i	0	0	0
1.3280 + 1.3573i	0 - 0.0440i	0 - 0.0440i	0	0	0 + 0.0042i	1.3425 + 0.5127i	0 + 0.0112i	0
0 - 0.0440i	0	0	0	0	0	0 + 0.0112i	0	0
0 - 0.0440i	0	0.2066 + 0.4595i	0 + 0.0042i	0	1.3292 + 1.3479i	0	0	0
1.3280 + 1.3573i	0 - 0.0440i	0 - 0.0440i	0	0	0 + 0.0042i	1.3425 + 0.5127i	0 + 0.0112i	0
0 - 0.0440i	0	0	0	0	0	0 + 0.0112i	0	0
0 - 0.0440i	0	0.2066 + 0.4595i	0 + 0.0042i	0	1.3292 + 1.3479i	0	0	0
1.3280 + 1.3573i	0 - 0.0440i	0 - 0.0440i	0	0	0 + 0.0042i	1.3425 + 0.5127i	0 + 0.0112i	0
0 - 0.0440i	0	0	0	0	0	0 + 0.0112i	0	0
0 - 0.0440i	0	0.2066 + 0.4595i	0 + 0.0042i	0	1.3292 + 1.3479i	0	0	0
1.3280 + 1.3573i	0 - 0.0440i	0 - 0.0440i	0	0	0 + 0.0042i	1.3425 + 0.5127i	0 + 0.0112i	0
0 - 0.0440i	0	0	0	0	0	0 + 0.0112i	0	0
0 - 0.0440i	0	0.2066 + 0.4595i	0 + 0.0042i	0	1.3292 + 1.3479i	0	0	0
1.3280 + 1.3573i	0 - 0.0440i	0 - 0.0440i	0	0	0 + 0.0042i	1.3425 + 0.5127i	0 + 0.0112i	0
0 - 0.0440i	0	0	0	0	0	0 + 0.0112i	0	0
0 - 0.0440i	0	0.2066 + 0.4595i	0 + 0.0042i	0	1.3292 + 1.3479i	0	0	0
1.3280 + 1.3573i	0 - 0.0440i	0 - 0.0440i	0	0	0 + 0.0042i	1.3425 + 0.5127i	0 + 0.0112i	0
0 - 0.0440i	0	0	0	0	0	0 + 0.0112i	0	0
0 - 0.0440i	0	0.2066 + 0.4595i	0 + 0.0042i	0	1.3292 + 1.3479i	0	0	0
1.3280 + 1.3573i	0 - 0.0440i	0 - 0.0440i	0	0	0 + 0.0042i	1.3425 + 0.5127i	0 + 0.0112i	0
0 - 0.0440i	0	0	0	0	0	0 + 0.0112i	0	0
0 - 0.0440i	0	0.2066 + 0.4595i	0 + 0.0042i	0	1.3292 + 1.3479i	0	0	0
1.3280 + 1.3573i	0 - 0.0440i	0 - 0.0440i	0	0	0 + 0.0042i	1.3425 + 0.5127i	0 + 0.0112i	0
0 - 0.0440i	0	0	0	0	0	0 + 0.0112i	0	0
0 - 0.0440i	0	0.2066 + 0.4595i	0 + 0.0042i	0	1.3292 + 1.3479i	0	0	0

Figure A.2 FBM matrix (column 27-36)

Branch Current to Bus Voltage Matrix (BCBV Matrix)

1			2			3		
0.3465 + 1.0182i	0 - 0.1382i	0 - 0.2934i	0	0	0	0	0	0
0 - 0.1382i	0.1560 + 0.5020i	0 - 0.2268i	0	0	0	0	0	0
0 - 0.2934i	0 - 0.2268i	0.1580 + 0.4239i	0	0	0	0	0	0
0.3465 + 1.0182i	0 - 0.1382i	0 - 0.2934i	0.7526 + 1.1818i	0 - 0.0345i	0 - 0.0734i	0	0	0
0 - 0.1382i	0.1560 + 0.5020i	0 - 0.2268i	0 - 0.0345i	0.1580 + 0.4240i	0 - 0.0567i	0	0	0
0 - 0.2934i	0 - 0.2268i	0.1580 + 0.4239i	0 - 0.0734i	0 - 0.0567i	0.1560 + 0.5021i	0	0	0
0.3465 + 1.0182i	0 - 0.1382i	0 - 0.2934i	0.7526 + 1.1818i	0 - 0.0345i	0 - 0.0734i	0	0	0
0 - 0.1382i	0.1560 + 0.5020i	0 - 0.2268i	0 - 0.0345i	0.1580 + 0.4240i	0 - 0.0567i	0	0	0
0 - 0.2934i	0 - 0.2268i	0.1580 + 0.4239i	0 - 0.0734i	0 - 0.0567i	0.1560 + 0.5021i	0	0	0
0.3465 + 1.0182i	0 - 0.1382i	0 - 0.2934i	0	0	0	0	0	0
0 - 0.1382i	0.1560 + 0.5020i	0 - 0.2268i	0	0	0	0	0	0
0 - 0.2934i	0 - 0.2268i	0.1580 + 0.4239i	0	0	0	0	0	0
0.3465 + 1.0182i	0 - 0.1382i	0 - 0.2934i	0	0	0	0	0	0
0 - 0.1382i	0.1560 + 0.5020i	0 - 0.2268i	0	0	0	0	0	0
0 - 0.2934i	0 - 0.2268i	0.1580 + 0.4239i	0	0	0	0	0	0
0.3465 + 1.0182i	0 - 0.1382i	0 - 0.2934i	0	0	0	0	0	0
0 - 0.1382i	0.1560 + 0.5020i	0 - 0.2268i	0	0	0	0	0	0
0 - 0.2934i	0 - 0.2268i	0.1580 + 0.4239i	0	0	0	0	0	0
0.3465 + 1.0182i	0 - 0.1382i	0 - 0.2934i	0	0	0	0	0	0
0 - 0.1382i	0.1560 + 0.5020i	0 - 0.2268i	0	0	0	0	0	0
0 - 0.2934i	0 - 0.2268i	0.1580 + 0.4239i	0	0	0	0	0	0
0.3465 + 1.0182i	0 - 0.1382i	0 - 0.2934i	0	0	0	0	0	0
0 - 0.1382i	0.1560 + 0.5020i	0 - 0.2268i	0	0	0	0	0	0
0 - 0.2934i	0 - 0.2268i	0.1580 + 0.4239i	0	0	0	0	0	0
0.3465 + 1.0182i	0 - 0.1382i	0 - 0.2934i	0	0	0	0	0	0
0 - 0.1382i	0.1560 + 0.5020i	0 - 0.2268i	0	0	0	0	0	0
0 - 0.2934i	0 - 0.2268i	0.1580 + 0.4239i	0	0	0	0	0	0
0.3465 + 1.0182i	0 - 0.1382i	0 - 0.2934i	0	0	0	0	0	0
0 - 0.1382i	0.1560 + 0.5020i	0 - 0.2268i	0	0	0	0	0	0
0 - 0.2934i	0 - 0.2268i	0.1580 + 0.4239i	0	0	0	0	0	0
0.3465 + 1.0182i	0 - 0.1382i	0 - 0.2934i	0	0	0	0	0	0
0 - 0.1382i	0.1560 + 0.5020i	0 - 0.2268i	0	0	0	0	0	0
0 - 0.2934i	0 - 0.2268i	0.1580 + 0.4239i	0	0	0	0	0	0
0.3465 + 1.0182i	0 - 0.1382i	0 - 0.2934i	0	0	0	0	0	0
0 - 0.1382i	0.1560 + 0.5020i	0 - 0.2268i	0	0	0	0	0	0
0 - 0.2934i	0 - 0.2268i	0.1580 + 0.4239i	0	0	0	0	0	0

Figure A.5 BCBV matrix (column 1-9)

4			5			6		
0	0	0	0	0	0	0	0	0
0	0	0	0	0	0	0	0	0
0	0	0	0	0	0	0	0	0
0	0	0	0	0	0	0	0	0
0	0	0	0	0	0	0	0	0
0	0	0	0	0	0	0	0	0
0	0	0	0	0	0	0	0	0
0	0	0	0	0	0	0	0	0
0	0	0	0	0	0	0	0	0
0	0	0 - 0.0734i	0	0	0	0	0	0
0	1.3294 + 1.3475i	0 - 0.0734i	0	0	0	0	0	0
0 - 0.0734i	0 - 0.0734i	0.2066 + 0.4595i	0	0	0	0	0	0
0	0	0 - 0.0734i	0	0	0 - 0.0440i	0	0	0
0	1.3294 + 1.3475i	0 - 0.0734i	0	1.3294 + 1.3475i	0 - 0.0440i	0	0	0
0 - 0.0734i	0 - 0.0734i	0.2066 + 0.4595i	0 - 0.0440i	0 - 0.0440i	0.2066 + 0.4595i	0	0	0
0	0	0 - 0.0734i	0	0	0 - 0.0440i	0.3465 + 1.0182i	0 - 0.1382i	0 - 0.2934i
0	1.3294 + 1.3475i	0 - 0.0734i	0	1.3294 + 1.3475i	0 - 0.0440i	0 - 0.1382i	0.1560 + 0.5020i	0 - 0.2268i
0 - 0.0734i	0 - 0.0734i	0.2066 + 0.4595i	0 - 0.0440i	0 - 0.0440i	0.2066 + 0.4595i	0 - 0.2934i	0 - 0.2268i	0.1580 + 0.4239i
0	0	0 - 0.0734i	0	0	0	0	0	0
0	1.3294 + 1.3475i	0 - 0.0734i	0	0	0	0	0	0
0 - 0.0734i	0 - 0.0734i	0.2066 + 0.4595i	0	0	0	0	0	0
0	0	0	0	0	0	0	0	0
0	0	0	0	0	0	0	0	0
0	0	0	0	0	0	0	0	0
0	0	0	0	0	0	0	0	0
0	0	0	0	0	0	0	0	0
0	0	0	0	0	0	0	0	0
0	0	0 - 0.0734i	0	0	0	0	0	0
0	1.3294 + 1.3475i	0 - 0.0734i	0	0	0	0	0	0
0 - 0.0734i	0 - 0.0734i	0.2066 + 0.4595i	0	0	0	0	0	0
0	0	0 - 0.0734i	0	0	0	0	0	0
0	1.3294 + 1.3475i	0 - 0.0734i	0	0	0	0	0	0
0 - 0.0734i	0 - 0.0734i	0.2066 + 0.4595i	0	0	0	0	0	0
0	0	0 - 0.0734i	0	0	0	0	0	0
0	1.3294 + 1.3475i	0 - 0.0734i	0	0	0	0	0	0
0 - 0.0734i	0 - 0.0734i	0.2066 + 0.4595i	0	0	0	0	0	0

Figure A.6 BCBV matrix (column 10-18)

7			8			9		
0	0	0	0	0	0	0	0	0
0	0	0	0	0	0	0	0	0
0	0	0	0	0	0	0	0	0
0	0	0	0	0	0	0	0	0
0	0	0	0	0	0	0	0	0
0	0	0	0	0	0	0	0	0
0	0	0	0	0	0	0	0	0
0	0	0	0	0	0	0	0	0
0	0	0	0	0	0	0	0	0
0	0	0	0	0	0	0	0	0
0	0	0	0	0	0	0	0	0
0	0	0	0	0	0	0	0	0
0	0	0	0	0	0	0	0	0
0	0	0	0	0	0	0	0	0
0	0	0	0	0	0	0	0	0
0	0	0	0	0	0	0	0	0
0	0	0	0	0	0	0	0	0
0	0	0	0	0	0	0	0	0
0	0	0	0	0	0	0	0	0
0	0	0	0	0	0	0	0	0
0	0	0	0	0	0	0	0	0
0	0	0	0	0	0	0	0	0
0	0	0	0	0.1560 + 0.5020i	0 - 0.1134i	0	0	0
0	0	0	0	0 - 0.1134i	0.1580 + 0.4239i	0	0	0
0	0	0	0	0	0	0	0	0
0	0	0	0	0.1560 + 0.5020i	0 - 0.1134i	0	0.3192 + 0.0331i	0 - 0.0567i
0	0	0	0	0 - 0.1134i	0.1580 + 0.4239i	0	0 - 0.0567i	0.2849 - 0.0140i
0	0	0	0	0	0	0	0	0
0	0	0	0	0	0	0	0	0
0	0	0	0	0	0	0	0	0
0	0	0	0	0	0	0	0	0
0	0	0	0	0	0	0	0	0
0	0	0	0	0	0	0	0	0
0	0	0	0	0	0	0	0	0
0	0	0	0	0	0	0	0	0
0	0	0	0	0	0	0	0	0

Figure A.7 BCBV matrix (column 19-27)

10			11			12		
0	0	0	0	0	0	0	0	0
0	0	0	0	0	0	0	0	0
0	0	0	0	0	0	0	0	0
0	0	0	0	0	0	0	0	0
0	0	0	0	0	0	0	0	0
0	0	0	0	0	0	0	0	0
0	0	0	0	0	0	0	0	0
0	0	0	0	0	0	0	0	0
0	0	0	0	0	0	0	0	0
0	0	0	0	0	0	0	0	0
0	0	0	0	0	0	0	0	0
0	0	0	0	0	0	0	0	0
0	0	0	0	0	0	0	0	0
0	0	0	0	0	0	0	0	0
0	0	0	0	0	0	0	0	0
0	0	0	0	0	0	0	0	0
0	0	0	0	0	0	0	0	0
0	0	0	0	0	0	0	0	0
0	0	0	0	0	0	0	0	0
0	0	0	0	0	0	0	0	0
0	0	0	0	0	0	0	0	0
0	0	0	0	0	0	0	0	0
0	0	0	0	0	0	0	0	0
0	0	0	0	0	0	0	0	0
0	0	0	0	0	0	0	0	0
0	0	0	0	0	0	0	0	0
0	0	0	0	0	0	0	0	0
1.3280 + 1.3573i	0	0 - 0.0440i	0	0	0	0	0	0
0	0	0	0	0	0	0	0	0
0 - 0.0440i	0	0.2066 + 0.4595i	0	0	0	0	0	0
1.3280 + 1.3573i	0	0 - 0.0440i	0	0	0	0	0	0
0	0	0	0	0	0	0	0	0
0 - 0.0440i	0	0.2066 + 0.4595i	0	0	1.3292 + 1.3479i	0	0	0
1.3280 + 1.3573i	0	0 - 0.0440i	0	0	0	1.3425 + 0.5127i	0	0
0	0	0	0	0	0	0	0	0
0 - 0.0440i	0	0.2066 + 0.4595i	0	0	0	0	0	0

Figure A.8 BCBV matrix (column 28-36)

Distribution Load Flow Matrix (DLF Matrix)

1			2			3		
0.3465 + 1.0182i	0 - 0.1382i	0 - 0.2934i	0.3465 + 1.0182i	0 - 0.1382i	0 - 0.2934i	0.3465 + 1.0182i	0 - 0.1382i	0 - 0.2934i
0 - 0.1382i	0.1560 + 0.5020i	0 - 0.2268i	0 - 0.1382i	0.1560 + 0.5020i	0 - 0.2268i	0 - 0.1382i	0.1560 + 0.5020i	0 - 0.2268i
0 - 0.2934i	0 - 0.2268i	0.1580 + 0.4239i	0 - 0.2934i	0 - 0.2268i	0.1580 + 0.4239i	0 - 0.2934i	0 - 0.2268i	0.1580 + 0.4239i
0.3465 + 1.0182i	0 - 0.1382i	0 - 0.2934i	1.0991 + 2.1999i	0 - 0.1727i	0 - 0.3668i	1.0991 + 2.1999i	0 - 0.1727i	0 - 0.3668i
0 - 0.1382i	0.1560 + 0.5020i	0 - 0.2268i	0 - 0.1727i	0.3140 + 0.9259i	0 - 0.2835i	0 - 0.1727i	0.3140 + 0.9259i	0 - 0.2835i
0 - 0.2934i	0 - 0.2268i	0.1580 + 0.4239i	0 - 0.3668i	0 - 0.2835i	0.3140 + 0.9259i	0 - 0.3668i	0 - 0.2835i	0.3140 + 0.9259i
0.3465 + 1.0182i	0 - 0.1382i	0 - 0.2934i	1.0991 + 2.1999i	0 - 0.1727i	0 - 0.3668i	1.0991 + 2.1999i	0 - 0.1727i	0 - 0.3668i
0 - 0.1382i	0.1560 + 0.5020i	0 - 0.2268i	0 - 0.1727i	0.3140 + 0.9259i	0 - 0.2835i	0 - 0.1727i	0.3140 + 0.9259i	0 - 0.2835i
0 - 0.2934i	0 - 0.2268i	0.1580 + 0.4239i	0 - 0.3668i	0 - 0.2835i	0.3140 + 0.9259i	0 - 0.3668i	0 - 0.2835i	0.3140 + 0.9259i
0.3465 + 1.0182i	0 - 0.1382i	0 - 0.2934i	0.3465 + 1.0182i	0 - 0.1382i	0 - 0.2934i	0.3465 + 1.0182i	0 - 0.1382i	0 - 0.2934i
0 - 0.1382i	0.1560 + 0.5020i	0 - 0.2268i	0 - 0.1382i	0.1560 + 0.5020i	0 - 0.2268i	0 - 0.1382i	0.1560 + 0.5020i	0 - 0.2268i
0 - 0.2934i	0 - 0.2268i	0.1580 + 0.4239i	0 - 0.2934i	0 - 0.2268i	0.1580 + 0.4239i	0 - 0.2934i	0 - 0.2268i	0.1580 + 0.4239i
0.3465 + 1.0182i	0 - 0.1382i	0 - 0.2934i	0.3465 + 1.0182i	0 - 0.1382i	0 - 0.2934i	0.3465 + 1.0182i	0 - 0.1382i	0 - 0.2934i
0 - 0.1382i	0.1560 + 0.5020i	0 - 0.2268i	0 - 0.1382i	0.1560 + 0.5020i	0 - 0.2268i	0 - 0.1382i	0.1560 + 0.5020i	0 - 0.2268i
0 - 0.2934i	0 - 0.2268i	0.1580 + 0.4239i	0 - 0.2934i	0 - 0.2268i	0.1580 + 0.4239i	0 - 0.2934i	0 - 0.2268i	0.1580 + 0.4239i
0.3465 + 1.0182i	0 - 0.1382i	0 - 0.2934i	0.3465 + 1.0182i	0 - 0.1382i	0 - 0.2934i	0.3465 + 1.0182i	0 - 0.1382i	0 - 0.2934i
0 - 0.1382i	0.1560 + 0.5020i	0 - 0.2268i	0 - 0.1382i	0.1560 + 0.5020i	0 - 0.2268i	0 - 0.1382i	0.1560 + 0.5020i	0 - 0.2268i
0 - 0.2934i	0 - 0.2268i	0.1580 + 0.4239i	0 - 0.2934i	0 - 0.2268i	0.1580 + 0.4239i	0 - 0.2934i	0 - 0.2268i	0.1580 + 0.4239i
0.3465 + 1.0182i	0 - 0.1382i	0 - 0.2934i	0.3465 + 1.0182i	0 - 0.1382i	0 - 0.2934i	0.3465 + 1.0182i	0 - 0.1382i	0 - 0.2934i
0 - 0.1382i	0.1560 + 0.5020i	0 - 0.2268i	0 - 0.1382i	0.1560 + 0.5020i	0 - 0.2268i	0 - 0.1382i	0.1560 + 0.5020i	0 - 0.2268i
0 - 0.2934i	0 - 0.2268i	0.1580 + 0.4239i	0 - 0.2934i	0 - 0.2268i	0.1580 + 0.4239i	0 - 0.2934i	0 - 0.2268i	0.1580 + 0.4239i
0.3465 + 1.0182i	0 - 0.1382i	0 - 0.2934i	0.3465 + 1.0182i	0 - 0.1382i	0 - 0.2934i	0.3465 + 1.0182i	0 - 0.1382i	0 - 0.2934i
0 - 0.1382i	0.1560 + 0.5020i	0 - 0.2268i	0 - 0.1382i	0.1560 + 0.5020i	0 - 0.2268i	0 - 0.1382i	0.1560 + 0.5020i	0 - 0.2268i
0 - 0.2934i	0 - 0.2268i	0.1580 + 0.4239i	0 - 0.2934i	0 - 0.2268i	0.1580 + 0.4239i	0 - 0.2934i	0 - 0.2268i	0.1580 + 0.4239i
0.3465 + 1.0182i	0 - 0.1382i	0 - 0.2934i	0.3465 + 1.0182i	0 - 0.1382i	0 - 0.2934i	0.3465 + 1.0182i	0 - 0.1382i	0 - 0.2934i
0 - 0.1382i	0.1560 + 0.5020i	0 - 0.2268i	0 - 0.1382i	0.1560 + 0.5020i	0 - 0.2268i	0 - 0.1382i	0.1560 + 0.5020i	0 - 0.2268i
0 - 0.2934i	0 - 0.2268i	0.1580 + 0.4239i	0 - 0.2934i	0 - 0.2268i	0.1580 + 0.4239i	0 - 0.2934i	0 - 0.2268i	0.1580 + 0.4239i
0.3465 + 1.0182i	0 - 0.1382i	0 - 0.2934i	0.3465 + 1.0182i	0 - 0.1382i	0 - 0.2934i	0.3465 + 1.0182i	0 - 0.1382i	0 - 0.2934i
0 - 0.1382i	0.1560 + 0.5020i	0 - 0.2268i	0 - 0.1382i	0.1560 + 0.5020i	0 - 0.2268i	0 - 0.1382i	0.1560 + 0.5020i	0 - 0.2268i
0 - 0.2934i	0 - 0.2268i	0.1580 + 0.4239i	0 - 0.2934i	0 - 0.2268i	0.1580 + 0.4239i	0 - 0.2934i	0 - 0.2268i	0.1580 + 0.4239i
0.3465 + 1.0182i	0 - 0.1382i	0 - 0.2934i	0.3465 + 1.0182i	0 - 0.1382i	0 - 0.2934i	0.3465 + 1.0182i	0 - 0.1382i	0 - 0.2934i
0 - 0.1382i	0.1560 + 0.5020i	0 - 0.2268i	0 - 0.1382i	0.1560 + 0.5020i	0 - 0.2268i	0 - 0.1382i	0.1560 + 0.5020i	0 - 0.2268i
0 - 0.2934i	0 - 0.2268i	0.1580 + 0.4239i	0 - 0.2934i	0 - 0.2268i	0.1580 + 0.4239i	0 - 0.2934i	0 - 0.2268i	0.1580 + 0.4239i
0.3465 + 1.0182i	0 - 0.1382i	0 - 0.2934i	0.3465 + 1.0182i	0 - 0.1382i	0 - 0.2934i	0.3465 + 1.0182i	0 - 0.1382i	0 - 0.2934i
0 - 0.1382i	0.1560 + 0.5020i	0 - 0.2268i	0 - 0.1382i	0.1560 + 0.5020i	0 - 0.2268i	0 - 0.1382i	0.1560 + 0.5020i	0 - 0.2268i
0 - 0.2934i	0 - 0.2268i	0.1580 + 0.4239i	0 - 0.2934i	0 - 0.2268i	0.1580 + 0.4239i	0 - 0.2934i	0 - 0.2268i	0.1580 + 0.4239i

Figure A.9 DLF matrix (column 1-9)

4			5			6		
0.3465 + 1.0182i	0 - 0.1382i	0 - 0.2934i	0.3465 + 1.0182i	0 - 0.1382i	0 - 0.2934i	0.3465 + 1.0182i	0 - 0.1382i	0 - 0.2934i
0 - 0.1382i	0.1560 + 0.5020i	0 - 0.2268i	0 - 0.1382i	0.1560 + 0.5020i	0 - 0.2268i	0 - 0.1382i	0.1560 + 0.5020i	0 - 0.2268i
0 - 0.2934i	0 - 0.2268i	0.1580 + 0.4239i	0 - 0.2934i	0 - 0.2268i	0.1580 + 0.4239i	0 - 0.2934i	0 - 0.2268i	0.1580 + 0.4239i
0.3465 + 1.0182i	0 - 0.1382i	0 - 0.2934i	0.3465 + 1.0182i	0 - 0.1382i	0 - 0.2934i	0.3465 + 1.0182i	0 - 0.1382i	0 - 0.2934i
0 - 0.1382i	0.1560 + 0.5020i	0 - 0.2268i	0 - 0.1382i	0.1560 + 0.5020i	0 - 0.2268i	0 - 0.1382i	0.1560 + 0.5020i	0 - 0.2268i
0 - 0.2934i	0 - 0.2268i	0.1580 + 0.4239i	0 - 0.2934i	0 - 0.2268i	0.1580 + 0.4239i	0 - 0.2934i	0 - 0.2268i	0.1580 + 0.4239i
0.3465 + 1.0182i	0 - 0.1382i	0 - 0.2934i	0.3465 + 1.0182i	0 - 0.1382i	0 - 0.2934i	0.3465 + 1.0182i	0 - 0.1382i	0 - 0.2934i
0 - 0.1382i	0.1560 + 0.5020i	0 - 0.2268i	0 - 0.1382i	0.1560 + 0.5020i	0 - 0.2268i	0 - 0.1382i	0.1560 + 0.5020i	0 - 0.2268i
0 - 0.2934i	0 - 0.2268i	0.1580 + 0.4239i	0 - 0.2934i	0 - 0.2268i	0.1580 + 0.4239i	0 - 0.2934i	0 - 0.2268i	0.1580 + 0.4239i
0.3465 + 1.0182i	0 - 0.1382i	0 - 0.3668i	0.3465 + 1.0182i	0 - 0.1382i	0 - 0.3668i	0.3465 + 1.0182i	0 - 0.1382i	0 - 0.3668i
0 - 0.1382i	1.4854 + 1.8495i	0 - 0.3002i	0 - 0.1382i	1.4854 + 1.8495i	0 - 0.3002i	0 - 0.1382i	1.4854 + 1.8495i	0 - 0.3002i
0 - 0.3668i	0 - 0.3002i	0.3646 + 0.8834i	0 - 0.3668i	0 - 0.3002i	0.3646 + 0.8834i	0 - 0.3668i	0 - 0.3002i	0.3646 + 0.8834i
0.3465 + 1.0182i	0 - 0.1382i	0 - 0.3668i	0.3465 + 1.0182i	0 - 0.1382i	0 - 0.4108i	0.3465 + 1.0182i	0 - 0.1382i	0 - 0.4108i
0 - 0.1382i	1.4854 + 1.8495i	0 - 0.3002i	0 - 0.1382i	2.8148 + 3.1970i	0 - 0.3442i	0 - 0.1382i	2.8148 + 3.1970i	0 - 0.3442i
0 - 0.3668i	0 - 0.3002i	0.3646 + 0.8834i	0 - 0.4108i	0 - 0.3442i	0.5712 + 1.3429i	0 - 0.4108i	0 - 0.3442i	0.5712 + 1.3429i
0.3465 + 1.0182i	0 - 0.1382i	0 - 0.3668i	0.3465 + 1.0182i	0 - 0.1382i	0 - 0.4108i	0.6930 + 2.0363i	0 - 0.2763i	0 - 0.7042i
0 - 0.1382i	1.4854 + 1.8495i	0 - 0.3002i	0 - 0.1382i	2.8148 + 3.1970i	0 - 0.3442i	0 - 0.2763i	2.9708 + 3.6989i	0 - 0.5710i
0 - 0.3668i	0 - 0.3002i	0.3646 + 0.8834i	0 - 0.4108i	0 - 0.3442i	0.5712 + 1.3429i	0 - 0.7042i	0 - 0.5710i	0.7292 + 1.7667i
0.3465 + 1.0182i	0 - 0.1382i	0 - 0.3668i	0.3465 + 1.0182i	0 - 0.1382i	0 - 0.3668i	0.3465 + 1.0182i	0 - 0.1382i	0 - 0.3668i
0 - 0.1382i	1.4854 + 1.8495i	0 - 0.3002i	0 - 0.1382i	1.4854 + 1.8495i	0 - 0.3002i	0 - 0.1382i	1.4854 + 1.8495i	0 - 0.3002i
0 - 0.3668i	0 - 0.3002i	0.3646 + 0.8834i	0 - 0.3668i	0 - 0.3002i	0.3646 + 0.8834i	0 - 0.3668i	0 - 0.3002i	0.3646 + 0.8834i
0.3465 + 1.0182i	0 - 0.1382i	0 - 0.2934i	0.3465 + 1.0182i	0 - 0.1382i	0 - 0.2934i	0.3465 + 1.0182i	0 - 0.1382i	0 - 0.2934i
0 - 0.1382i	0.1560 + 0.5020i	0 - 0.2268i	0 - 0.1382i	0.1560 + 0.5020i	0 - 0.2268i	0 - 0.1382i	0.1560 + 0.5020i	0 - 0.2268i
0 - 0.2934i	0 - 0.2268i	0.1580 + 0.4239i	0 - 0.2934i	0 - 0.2268i	0.1580 + 0.4239i	0 - 0.2934i	0 - 0.2268i	0.1580 + 0.4239i
0.3465 + 1.0182i	0 - 0.1382i	0 - 0.2934i	0.3465 + 1.0182i	0 - 0.1382i	0 - 0.2934i	0.3465 + 1.0182i	0 - 0.1382i	0 - 0.2934i
0 - 0.1382i	0.1560 + 0.5020i	0 - 0.2268i	0 - 0.1382i	0.1560 + 0.5020i	0 - 0.2268i	0 - 0.1382i	0.1560 + 0.5020i	0 - 0.2268i
0 - 0.2934i	0 - 0.2268i	0.1580 + 0.4239i	0 - 0.2934i	0 - 0.2268i	0.1580 + 0.4239i	0 - 0.2934i	0 - 0.2268i	0.1580 + 0.4239i
0.3465 + 1.0182i	0 - 0.1382i	0 - 0.3668i	0.3465 + 1.0182i	0 - 0.1382i	0 - 0.3668i	0.3465 + 1.0182i	0 - 0.1382i	0 - 0.3668i
0 - 0.1382i	1.4854 + 1.8495i	0 - 0.3002i	0 - 0.1382i	1.4854 + 1.8495i	0 - 0.3002i	0 - 0.1382i	1.4854 + 1.8495i	0 - 0.3002i
0 - 0.3668i	0 - 0.3002i	0.3646 + 0.8834i	0 - 0.3668i	0 - 0.3002i	0.3646 + 0.8834i	0 - 0.3668i	0 - 0.3002i	0.3646 + 0.8834i
0.3465 + 1.0182i	0 - 0.1382i	0 - 0.3668i	0.3465 + 1.0182i	0 - 0.1382i	0 - 0.3668i	0.3465 + 1.0182i	0 - 0.1382i	0 - 0.3668i
0 - 0.1382i	1.4854 + 1.8495i	0 - 0.3002i	0 - 0.1382i	1.4854 + 1.8495i	0 - 0.3002i	0 - 0.1382i	1.4854 + 1.8495i	0 - 0.3002i
0 - 0.3668i	0 - 0.3002i	0.3646 + 0.8834i	0 - 0.3668i	0 - 0.3002i	0.3646 + 0.8834i	0 - 0.3668i	0 - 0.3002i	0.3646 + 0.8834i
0.3465 + 1.0182i	0 - 0.1382i	0 - 0.3668i	0.3465 + 1.0182i	0 - 0.1382i	0 - 0.3668i	0.3465 + 1.0182i	0 - 0.1382i	0 - 0.3668i
0 - 0.1382i	1.4854 + 1.8495i	0 - 0.3002i	0 - 0.1382i	1.4854 + 1.8495i	0 - 0.3002i	0 - 0.1382i	1.4854 + 1.8495i	0 - 0.3002i
0 - 0.3668i	0 - 0.3002i	0.3646 + 0.8834i	0 - 0.3668i	0 - 0.3002i	0.3646 + 0.8834i	0 - 0.3668i	0 - 0.3002i	0.3646 + 0.8834i

Figure A.10 DLF matrix (column 10-18)

7			8			9		
0.3465 + 1.0182i	0 - 0.1382i	0 - 0.2934i	0.3465 + 1.0182i	0 - 0.1382i	0 - 0.2934i	0.3465 + 1.0182i	0 - 0.1382i	0 - 0.2934i
0 - 0.1382i	0.1560 + 0.5020i	0 - 0.2268i	0 - 0.1382i	0.1560 + 0.5020i	0 - 0.2268i	0 - 0.1382i	0.1560 + 0.5020i	0 - 0.2268i
0 - 0.2934i	0 - 0.2268i	0.1580 + 0.4239i	0 - 0.2934i	0 - 0.2268i	0.1580 + 0.4239i	0 - 0.2934i	0 - 0.2268i	0.1580 + 0.4239i
0.3465 + 1.0182i	0 - 0.1382i	0 - 0.2934i	0.3465 + 1.0182i	0 - 0.1382i	0 - 0.2934i	0.3465 + 1.0182i	0 - 0.1382i	0 - 0.2934i
0 - 0.1382i	0.1560 + 0.5020i	0 - 0.2268i	0 - 0.1382i	0.1560 + 0.5020i	0 - 0.2268i	0 - 0.1382i	0.1560 + 0.5020i	0 - 0.2268i
0 - 0.2934i	0 - 0.2268i	0.1580 + 0.4239i	0 - 0.2934i	0 - 0.2268i	0.1580 + 0.4239i	0 - 0.2934i	0 - 0.2268i	0.1580 + 0.4239i
0.3465 + 1.0182i	0 - 0.1382i	0 - 0.2934i	0.3465 + 1.0182i	0 - 0.1382i	0 - 0.2934i	0.3465 + 1.0182i	0 - 0.1382i	0 - 0.2934i
0 - 0.1382i	0.1560 + 0.5020i	0 - 0.2268i	0 - 0.1382i	0.1560 + 0.5020i	0 - 0.2268i	0 - 0.1382i	0.1560 + 0.5020i	0 - 0.2268i
0 - 0.2934i	0 - 0.2268i	0.1580 + 0.4239i	0 - 0.2934i	0 - 0.2268i	0.1580 + 0.4239i	0 - 0.2934i	0 - 0.2268i	0.1580 + 0.4239i
0.3465 + 1.0182i	0 - 0.1382i	0 - 0.3668i	0.3465 + 1.0182i	0 - 0.1382i	0 - 0.2934i	0.3465 + 1.0182i	0 - 0.1382i	0 - 0.2934i
0 - 0.1382i	1.4854 + 1.8495i	0 - 0.3002i	0 - 0.1382i	0.1560 + 0.5020i	0 - 0.2268i	0 - 0.1382i	0.1560 + 0.5020i	0 - 0.2268i
0 - 0.3668i	0 - 0.3002i	0.3646 + 0.8834i	0 - 0.2934i	0 - 0.2268i	0.1580 + 0.4239i	0 - 0.2934i	0 - 0.2268i	0.1580 + 0.4239i
0.3465 + 1.0182i	0 - 0.1382i	0 - 0.3668i	0.3465 + 1.0182i	0 - 0.1382i	0 - 0.2934i	0.3465 + 1.0182i	0 - 0.1382i	0 - 0.2934i
0 - 0.1382i	1.4854 + 1.8495i	0 - 0.3002i	0 - 0.1382i	0.1560 + 0.5020i	0 - 0.2268i	0 - 0.1382i	0.1560 + 0.5020i	0 - 0.2268i
0 - 0.3668i	0 - 0.3002i	0.3646 + 0.8834i	0 - 0.2934i	0 - 0.2268i	0.1580 + 0.4239i	0 - 0.2934i	0 - 0.2268i	0.1580 + 0.4239i
0.3465 + 1.0182i	0 - 0.1382i	0 - 0.3668i	0.3465 + 1.0182i	0 - 0.1382i	0 - 0.2934i	0.3465 + 1.0182i	0 - 0.1382i	0 - 0.2934i
0 - 0.1382i	1.4854 + 1.8495i	0 - 0.3002i	0 - 0.1382i	0.1560 + 0.5020i	0 - 0.2268i	0 - 0.1382i	0.1560 + 0.5020i	0 - 0.2268i
0 - 0.3668i	0 - 0.3002i	0.3646 + 0.8834i	0 - 0.2934i	0 - 0.2268i	0.1580 + 0.4239i	0 - 0.2934i	0 - 0.2268i	0.1580 + 0.4239i
0.3465 + 1.0182i	0 - 0.1382i	0 - 0.3668i	0.3465 + 1.0182i	0 - 0.1382i	0 - 0.2934i	0.3465 + 1.0182i	0 - 0.1382i	0 - 0.2934i
0 - 0.1382i	1.4854 + 1.8495i	0 - 0.3002i	0 - 0.1382i	0.1560 + 0.5020i	0 - 0.2268i	0 - 0.1382i	0.1560 + 0.5020i	0 - 0.2268i
0 - 0.3668i	0 - 0.3002i	0.3646 + 0.8834i	0 - 0.2934i	0 - 0.2268i	0.1580 + 0.4239i	0 - 0.2934i	0 - 0.2268i	0.1580 + 0.4239i
0.3465 + 1.0182i	0 - 0.1382i	0 - 0.2934i	0.3465 + 1.0182i	0 - 0.1382i	0 - 0.2934i	0.3465 + 1.0182i	0 - 0.1382i	0 - 0.2934i
0 - 0.1382i	0.1560 + 0.5020i	0 - 0.2268i	0 - 0.1382i	0.3120 + 1.0039i	0 - 0.3402i	0 - 0.1382i	0.3120 + 1.0039i	0 - 0.3402i
0 - 0.2934i	0 - 0.2268i	0.1580 + 0.4239i	0 - 0.2934i	0 - 0.3402i	0.3160 + 0.8477i	0 - 0.2934i	0 - 0.3402i	0.3160 + 0.8477i
0.3465 + 1.0182i	0 - 0.1382i	0 - 0.2934i	0.3465 + 1.0182i	0 - 0.1382i	0 - 0.2934i	0.3465 + 1.0182i	0 - 0.1382i	0 - 0.2934i
0 - 0.1382i	0.1560 + 0.5020i	0 - 0.2268i	0 - 0.1382i	0.3120 + 1.0039i	0 - 0.3402i	0 - 0.1382i	0.6312 + 1.0371i	0 - 0.3969i
0 - 0.2934i	0 - 0.2268i	0.1580 + 0.4239i	0 - 0.2934i	0 - 0.3402i	0.3160 + 0.8477i	0 - 0.2934i	0 - 0.3969i	0.6009 + 0.8338i
0.3465 + 1.0182i	0 - 0.1382i	0 - 0.3668i	0.3465 + 1.0182i	0 - 0.1382i	0 - 0.2934i	0.3465 + 1.0182i	0 - 0.1382i	0 - 0.2934i
0 - 0.1382i	1.4854 + 1.8495i	0 - 0.3002i	0 - 0.1382i	0.1560 + 0.5020i	0 - 0.2268i	0 - 0.1382i	0.1560 + 0.5020i	0 - 0.2268i
0 - 0.3668i	0 - 0.3002i	0.3646 + 0.8834i	0 - 0.2934i	0 - 0.2268i	0.1580 + 0.4239i	0 - 0.2934i	0 - 0.2268i	0.1580 + 0.4239i
0.3465 + 1.0182i	0 - 0.1382i	0 - 0.3668i	0.3465 + 1.0182i	0 - 0.1382i	0 - 0.2934i	0.3465 + 1.0182i	0 - 0.1382i	0 - 0.2934i
0 - 0.1382i	1.4854 + 1.8495i	0 - 0.3002i	0 - 0.1382i	0.1560 + 0.5020i	0 - 0.2268i	0 - 0.1382i	0.1560 + 0.5020i	0 - 0.2268i
0 - 0.3668i	0 - 0.3002i	0.3646 + 0.8834i	0 - 0.2934i	0 - 0.2268i	0.1580 + 0.4239i	0 - 0.2934i	0 - 0.2268i	0.1580 + 0.4239i
0.3465 + 1.0182i	0 - 0.1382i	0 - 0.3668i	0.3465 + 1.0182i	0 - 0.1382i	0 - 0.2934i	0.3465 + 1.0182i	0 - 0.1382i	0 - 0.2934i
0 - 0.1382i	1.4854 + 1.8495i	0 - 0.3002i	0 - 0.1382i	0.1560 + 0.5020i	0 - 0.2268i	0 - 0.1382i	0.1560 + 0.5020i	0 - 0.2268i
0 - 0.3668i	0 - 0.3002i	0.3646 + 0.8834i	0 - 0.2934i	0 - 0.2268i	0.1580 + 0.4239i	0 - 0.2934i	0 - 0.2268i	0.1580 + 0.4239i

Figure A.11 DLF matrix (column 19-27)

10			11			12		
0.3465 + 1.0182i	0 - 0.1382i	0 - 0.2934i	0.3465 + 1.0182i	0 - 0.1382i	0 - 0.2934i	0.3465 + 1.0182i	0 - 0.1382i	0 - 0.2934i
0 - 0.1382i	0.1560 + 0.5020i	0 - 0.2268i	0 - 0.1382i	0.1560 + 0.5020i	0 - 0.2268i	0 - 0.1382i	0.1560 + 0.5020i	0 - 0.2268i
0 - 0.2934i	0 - 0.2268i	0.1580 + 0.4239i	0 - 0.2934i	0 - 0.2268i	0.1580 + 0.4239i	0 - 0.2934i	0 - 0.2268i	0.1580 + 0.4239i
0.3465 + 1.0182i	0 - 0.1382i	0 - 0.2934i	0.3465 + 1.0182i	0 - 0.1382i	0 - 0.2934i	0.3465 + 1.0182i	0 - 0.1382i	0 - 0.2934i
0 - 0.1382i	0.1560 + 0.5020i	0 - 0.2268i	0 - 0.1382i	0.1560 + 0.5020i	0 - 0.2268i	0 - 0.1382i	0.1560 + 0.5020i	0 - 0.2268i
0 - 0.2934i	0 - 0.2268i	0.1580 + 0.4239i	0 - 0.2934i	0 - 0.2268i	0.1580 + 0.4239i	0 - 0.2934i	0 - 0.2268i	0.1580 + 0.4239i
0.3465 + 1.0182i	0 - 0.1382i	0 - 0.2934i	0.3465 + 1.0182i	0 - 0.1382i	0 - 0.2934i	0.3465 + 1.0182i	0 - 0.1382i	0 - 0.2934i
0 - 0.1382i	0.1560 + 0.5020i	0 - 0.2268i	0 - 0.1382i	0.1560 + 0.5020i	0 - 0.2268i	0 - 0.1382i	0.1560 + 0.5020i	0 - 0.2268i
0 - 0.2934i	0 - 0.2268i	0.1580 + 0.4239i	0 - 0.2934i	0 - 0.2268i	0.1580 + 0.4239i	0 - 0.2934i	0 - 0.2268i	0.1580 + 0.4239i
0.3465 + 1.0182i	0 - 0.1382i	0 - 0.3668i	0.3465 + 1.0182i	0 - 0.1382i	0 - 0.3668i	0.3465 + 1.0182i	0 - 0.1382i	0 - 0.3668i
0 - 0.1382i	1.4854 + 1.8495i	0 - 0.3002i	0 - 0.1382i	1.4854 + 1.8495i	0 - 0.3002i	0 - 0.1382i	1.4854 + 1.8495i	0 - 0.3002i
0 - 0.3668i	0 - 0.3002i	0.3646 + 0.8834i	0 - 0.3668i	0 - 0.3002i	0.3646 + 0.8834i	0 - 0.3668i	0 - 0.3002i	0.3646 + 0.8834i
0.3465 + 1.0182i	0 - 0.1382i	0 - 0.3668i	0.3465 + 1.0182i	0 - 0.1382i	0 - 0.3668i	0.3465 + 1.0182i	0 - 0.1382i	0 - 0.3668i
0 - 0.1382i	1.4854 + 1.8495i	0 - 0.3002i	0 - 0.1382i	1.4854 + 1.8495i	0 - 0.3002i	0 - 0.1382i	1.4854 + 1.8495i	0 - 0.3002i
0 - 0.3668i	0 - 0.3002i	0.3646 + 0.8834i	0 - 0.3668i	0 - 0.3002i	0.3646 + 0.8834i	0 - 0.3668i	0 - 0.3002i	0.3646 + 0.8834i
0.3465 + 1.0182i	0 - 0.1382i	0 - 0.3668i	0.3465 + 1.0182i	0 - 0.1382i	0 - 0.3668i	0.3465 + 1.0182i	0 - 0.1382i	0 - 0.3668i
0 - 0.1382i	1.4854 + 1.8495i	0 - 0.3002i	0 - 0.1382i	1.4854 + 1.8495i	0 - 0.3002i	0 - 0.1382i	1.4854 + 1.8495i	0 - 0.3002i
0 - 0.3668i	0 - 0.3002i	0.3646 + 0.8834i	0 - 0.3668i	0 - 0.3002i	0.3646 + 0.8834i	0 - 0.3668i	0 - 0.3002i	0.3646 + 0.8834i
0.3465 + 1.0182i	0 - 0.1382i	0 - 0.3668i	0.3465 + 1.0182i	0 - 0.1382i	0 - 0.3668i	0.3465 + 1.0182i	0 - 0.1382i	0 - 0.3668i
0 - 0.1382i	1.4854 + 1.8495i	0 - 0.3002i	0 - 0.1382i	1.4854 + 1.8495i	0 - 0.3002i	0 - 0.1382i	1.4854 + 1.8495i	0 - 0.3002i
0 - 0.3668i	0 - 0.3002i	0.3646 + 0.8834i	0 - 0.3668i	0 - 0.3002i	0.3646 + 0.8834i	0 - 0.3668i	0 - 0.3002i	0.3646 + 0.8834i
0.3465 + 1.0182i	0 - 0.1382i	0 - 0.2934i	0.3465 + 1.0182i	0 - 0.1382i	0 - 0.2934i	0.3465 + 1.0182i	0 - 0.1382i	0 - 0.2934i
0 - 0.1382i	0.1560 + 0.5020i	0 - 0.2268i	0 - 0.1382i	0.1560 + 0.5020i	0 - 0.2268i	0 - 0.1382i	0.1560 + 0.5020i	0 - 0.2268i
0 - 0.2934i	0 - 0.2268i	0.1580 + 0.4239i	0 - 0.2934i	0 - 0.2268i	0.1580 + 0.4239i	0 - 0.2934i	0 - 0.2268i	0.1580 + 0.4239i
0.3465 + 1.0182i	0 - 0.1382i	0 - 0.2934i	0.3465 + 1.0182i	0 - 0.1382i	0 - 0.2934i	0.3465 + 1.0182i	0 - 0.1382i	0 - 0.2934i
0 - 0.1382i	0.1560 + 0.5020i	0 - 0.2268i	0 - 0.1382i	0.1560 + 0.5020i	0 - 0.2268i	0 - 0.1382i	0.1560 + 0.5020i	0 - 0.2268i
0 - 0.2934i	0 - 0.2268i	0.1580 + 0.4239i	0 - 0.2934i	0 - 0.2268i	0.1580 + 0.4239i	0 - 0.2934i	0 - 0.2268i	0.1580 + 0.4239i
1.6745 + 2.3755i	0 - 0.1382i	0 - 0.4108i	1.6745 + 2.3755i	0 - 0.1382i	0 - 0.4108i	1.6745 + 2.3755i	0 - 0.1382i	0 - 0.4108i
0 - 0.1382i	1.4854 + 1.8495i	0 - 0.3002i	0 - 0.1382i	1.4854 + 1.8495i	0 - 0.3002i	0 - 0.1382i	1.4854 + 1.8495i	0 - 0.3002i
0 - 0.4108i	0 - 0.3002i	0.5712 + 1.3429i	0 - 0.4108i	0 - 0.3002i	0.5712 + 1.3429i	0 - 0.4108i	0 - 0.3002i	0.5712 + 1.3429i
1.6745 + 2.3755i	0 - 0.1382i	0 - 0.4108i	1.6745 + 2.3755i	0 - 0.1382i	0 - 0.4108i	1.6745 + 2.3755i	0 - 0.1382i	0 - 0.4108i
0 - 0.1382i	1.4854 + 1.8495i	0 - 0.3002i	0 - 0.1382i	1.4854 + 1.8495i	0 - 0.3002i	0 - 0.1382i	1.4854 + 1.8495i	0 - 0.3002i
0 - 0.4108i	0 - 0.3002i	0.5712 + 1.3429i	0 - 0.4108i	0 - 0.3002i	1.9004 + 2.6908i	0 - 0.4108i	0 - 0.3002i	0.5712 + 1.3429i
1.6745 + 2.3755i	0 - 0.1382i	0 - 0.4108i	1.6745 + 2.3755i	0 - 0.1382i	0 - 0.4108i	3.0170 + 2.8882i	0 - 0.1382i	0 - 0.4108i
0 - 0.1382i	1.4854 + 1.8495i	0 - 0.3002i	0 - 0.1382i	1.4854 + 1.8495i	0 - 0.3002i	0 - 0.1382i	1.4854 + 1.8495i	0 - 0.3002i
0 - 0.4108i	0 - 0.3002i	0.5712 + 1.3429i	0 - 0.4108i	0 - 0.3002i	0.5712 + 1.3429i	0 - 0.4108i	0 - 0.3002i	0.5712 + 1.3429i

Figure A.12 DLF matrix (column 28-36)

Harmonic Analysis Matrix (HA matrix)

0.3465 +15.2724i	0 - 2.0726i	0 - 4.4015i	0.3465 +15.2724i	0 - 2.0726i	0 - 4.4015i	0.3465 +15.2724i	0 - 2.0726i	0 - 4.4015i
0 - 2.0726i	0.1560 + 7.5294i	0 - 3.4021i	0 - 2.0726i	0.1560 + 7.5294i	0 - 3.4021i	0 - 2.0726i	0.1560 + 7.5294i	0 - 3.4021i
0 - 4.4015i	0 - 3.4021i	0.1580 + 6.3579i	0 - 4.4015i	0 - 3.4021i	0.1580 + 6.3579i	0 - 4.4015i	0 - 3.4021i	0.1580 + 6.3579i
0.3465 +15.2724i	0 - 2.0726i	0 - 4.4015i	0.3465 +15.2724i	0 - 2.0726i	0 - 4.4015i	0.3465 +15.2724i	0 - 2.0726i	0 - 4.4015i
0 - 2.0726i	0.1560 + 7.5294i	0 - 3.4021i	0 - 2.0726i	0.1560 + 7.5294i	0 - 3.4021i	0 - 2.0726i	0.1560 + 7.5294i	0 - 3.4021i
0 - 4.4015i	0 - 3.4021i	0.1580 + 6.3579i	0 - 4.4015i	0 - 3.4021i	0.1580 + 6.3579i	0 - 4.4015i	0 - 3.4021i	0.1580 + 6.3579i
0.3465 +15.2724i	0 - 2.0726i	0 - 4.4015i	0.3465 +15.2724i	0 - 2.0726i	0 - 4.4015i	0.3465 +15.2724i	0 - 2.0726i	0 - 4.4015i
0 - 2.0726i	0.1560 + 7.5294i	0 - 3.4021i	0 - 2.0726i	0.1560 + 7.5294i	0 - 3.4021i	0 - 2.0726i	0.1560 + 7.5294i	0 - 3.4021i
0 - 4.4015i	0 - 3.4021i	0.1580 + 6.3579i	0 - 4.4015i	0 - 3.4021i	0.1580 + 6.3579i	0 - 4.4015i	0 - 3.4021i	0.1580 + 6.3579i
0.3465 +15.2724i	0 - 2.0726i	0 - 4.4015i	0.3465 +15.2724i	0 - 2.0726i	0 - 4.4015i	0.3465 +15.2724i	0 - 2.0726i	0 - 5.5019i
0 - 2.0726i	0.1560 + 7.5294i	0 - 3.4021i	0 - 2.0726i	0.1560 + 7.5294i	0 - 3.4021i	0 - 2.0726i	1.4854 +27.7420i	0 - 4.5025i
0 - 4.4015i	0 - 3.4021i	0.1580 + 6.3579i	0 - 4.4015i	0 - 3.4021i	0.1580 + 6.3579i	0 - 5.5019i	0 - 4.5025i	0.3646 +13.2505i
0.3465 +15.2724i	0 - 2.0726i	0 - 4.4015i	0.3465 +15.2724i	0 - 2.0726i	0 - 4.4015i	0.3465 +15.2724i	0 - 2.0726i	0 - 5.5019i
0 - 2.0726i	0.1560 + 7.5294i	0 - 3.4021i	0 - 2.0726i	0.1560 + 7.5294i	0 - 3.4021i	0 - 2.0726i	1.4854 +27.7420i	0 - 4.5025i
0 - 4.4015i	0 - 3.4021i	0.1580 + 6.3579i	0 - 4.4015i	0 - 3.4021i	0.1580 + 6.3579i	0 - 5.5019i	0 - 4.5025i	0.3646 +13.2505i
0.3465 +15.2724i	0 - 2.0726i	0 - 4.4015i	0.3465 +15.2724i	0 - 2.0726i	0 - 4.4015i	0.3465 +15.2724i	0 - 2.0726i	0 - 5.5019i
0 - 2.0726i	0.1560 + 7.5294i	0 - 3.4021i	0 - 2.0726i	0.1560 + 7.5294i	0 - 3.4021i	0 - 2.0726i	1.4854 +27.7420i	0 - 4.5025i
0 - 4.4015i	0 - 3.4021i	0.1580 + 6.3579i	0 - 4.4015i	0 - 3.4021i	0.1580 + 6.3579i	0 - 5.5019i	0 - 4.5025i	0.3646 +13.2505i
0.3465 +15.2724i	0 - 2.0726i	0 - 4.4015i	0.3465 +15.2724i	0 - 2.0726i	0 - 4.4015i	0.3465 +15.2724i	0 - 2.0726i	0 - 5.5019i
0 - 2.0726i	0.1560 + 7.5294i	0 - 3.4021i	0 - 2.0726i	0.1560 + 7.5294i	0 - 3.4021i	0 - 2.0726i	1.4854 +27.7420i	0 - 4.5025i
0 - 4.4015i	0 - 3.4021i	0.1580 + 6.3579i	0 - 4.4015i	0 - 3.4021i	0.1580 + 6.3579i	0 - 5.5019i	0 - 4.5025i	0.3646 +13.2505i
0.3465 +15.2724i	0 - 2.0726i	0 - 4.4015i	0.3465 +15.2724i	0 - 2.0726i	0 - 4.4015i	0.3465 +15.2724i	0 - 2.0726i	0 - 4.4015i
0 - 2.0726i	0.3120 +15.0588i	0 - 5.1031i	0 - 2.0726i	0.3120 +15.0588i	0 - 5.1031i	0 - 2.0726i	0.1560 + 7.5294i	0 - 3.4021i
0 - 4.4015i	0 - 5.1031i	0.3160 +12.7158i	0 - 4.4015i	0 - 5.1031i	0.3160 +12.7158i	0 - 4.4015i	0 - 3.4021i	0.1580 + 6.3579i
0.3465 +15.2724i	0 - 2.0726i	0 - 4.4015i	0.3465 +15.2724i	0 - 2.0726i	0 - 4.4015i	0.3465 +15.2724i	0 - 2.0726i	0 - 4.4015i
0 - 2.0726i	0.3120 +15.0588i	0 - 5.1031i	0 - 2.0726i	0.6312 +15.5559i	0 - 5.9537i	0 - 2.0726i	0.1560 + 7.5294i	0 - 3.4021i
0 - 4.4015i	0 - 5.1031i	0.3160 +12.7158i	0 - 4.4015i	0 - 5.9537i	0.6009 +12.5064i	0 - 4.4015i	0 - 3.4021i	0.1580 + 6.3579i
0.3465 +15.2724i	0 - 2.0726i	0 - 4.4015i	0.3465 +15.2724i	0 - 2.0726i	0 - 4.4015i	1.6745 +35.6320i	0 - 2.0726i	0 - 6.1621i
0 - 2.0726i	0.1560 + 7.5294i	0 - 3.4021i	0 - 2.0726i	0.1560 + 7.5294i	0 - 3.4021i	0 - 2.0726i	1.4854 +27.7420i	0 - 4.5025i
0 - 4.4015i	0 - 3.4021i	0.1580 + 6.3579i	0 - 4.4015i	0 - 3.4021i	0.1580 + 6.3579i	0 - 6.1621i	0 - 4.5025i	0.5712 +20.1432i
0.3465 +15.2724i	0 - 2.0726i	0 - 4.4015i	0.3465 +15.2724i	0 - 2.0726i	0 - 4.4015i	1.6745 +35.6320i	0 - 2.0726i	0 - 6.1621i
0 - 2.0726i	0.1560 + 7.5294i	0 - 3.4021i	0 - 2.0726i	0.1560 + 7.5294i	0 - 3.4021i	0 - 2.0726i	1.4854 +27.7420i	0 - 4.5025i
0 - 4.4015i	0 - 3.4021i	0.1580 + 6.3579i	0 - 4.4015i	0 - 3.4021i	0.1580 + 6.3579i	0 - 6.1621i	0 - 4.5025i	0.5712 +20.1432i
0.3465 +15.2724i	0 - 2.0726i	0 - 4.4015i	0.3465 +15.2724i	0 - 2.0726i	0 - 4.4015i	1.6745 +35.6320i	0 - 2.0726i	0 - 6.1621i
0 - 2.0726i	0.1560 + 7.5294i	0 - 3.4021i	0 - 2.0726i	0.1560 + 7.5294i	0 - 3.4021i	0 - 2.0726i	1.4854 +27.7420i	0 - 4.5025i
0 - 4.4015i	0 - 3.4021i	0.1580 + 6.3579i	0 - 4.4015i	0 - 3.4021i	0.1580 + 6.3579i	0 - 6.1621i	0 - 4.5025i	0.5712 +20.1432i

Figure A.13 HA-matrix (column 1-9)

0.3465 +15.2724i	0 - 2.0726i	0 - 4.4015i	0.3465 +15.2724i	0 - 2.0726i	0 - 4.4015i	0.3465 +15.2724i	0 - 2.0726i	0 - 4.4015i
0 - 2.0726i	0.1560 + 7.5294i	0 - 3.4021i	0 - 2.0726i	0.1560 + 7.5294i	0 - 3.4021i	0 - 2.0726i	0.1560 + 7.5294i	0 - 3.4021i
0 - 4.4015i	0 - 3.4021i	0.1580 + 6.3579i	0 - 4.4015i	0 - 3.4021i	0.1580 + 6.3579i	0 - 4.4015i	0 - 3.4021i	0.1580 + 6.3579i
0.3465 +15.2724i	0 - 2.0726i	0 - 4.4015i	0.3465 +15.2724i	0 - 2.0726i	0 - 4.4015i	0.3465 +15.2724i	0 - 2.0726i	0 - 4.4015i
0 - 2.0726i	0.1560 + 7.5294i	0 - 3.4021i	0 - 2.0726i	0.1560 + 7.5294i	0 - 3.4021i	0 - 2.0726i	0.1560 + 7.5294i	0 - 3.4021i
0 - 4.4015i	0 - 3.4021i	0.1580 + 6.3579i	0 - 4.4015i	0 - 3.4021i	0.1580 + 6.3579i	0 - 4.4015i	0 - 3.4021i	0.1580 + 6.3579i
0.3465 +15.2724i	0 - 2.0726i	0 - 4.4015i	0.3465 +15.2724i	0 - 2.0726i	0 - 4.4015i	0.3465 +15.2724i	0 - 2.0726i	0 - 4.4015i
0 - 2.0726i	0.1560 + 7.5294i	0 - 3.4021i	0 - 2.0726i	0.1560 + 7.5294i	0 - 3.4021i	0 - 2.0726i	0.1560 + 7.5294i	0 - 3.4021i
0 - 4.4015i	0 - 3.4021i	0.1580 + 6.3579i	0 - 4.4015i	0 - 3.4021i	0.1580 + 6.3579i	0 - 4.4015i	0 - 3.4021i	0.1580 + 6.3579i
0.3465 +15.2724i	0 - 2.0726i	0 - 5.5019i	0.3465 +15.2724i	0 - 2.0726i	0 - 5.5019i	0.3465 +15.2724i	0 - 2.0726i	0 - 5.5019i
0 - 2.0726i	1.4854 +27.7420i	0 - 4.5025i	0 - 2.0726i	1.4854 +27.7420i	0 - 4.5025i	0 - 2.0726i	1.4854 +27.7420i	0 - 4.5025i
0 - 5.5019i	0 - 4.5025i	0.3646 +13.2505i	0 - 5.5019i	0 - 4.5025i	0.3646 +13.2505i	0 - 5.5019i	0 - 4.5025i	0.3646 +13.2505i
0.3465 +15.2724i	0 - 2.0726i	0 - 5.5019i	0.3465 +15.2724i	0 - 2.0726i	0 - 5.5019i	0.3465 +15.2724i	0 - 2.0726i	0 - 5.5019i
0 - 2.0726i	1.4854 +27.7420i	0 - 4.5025i	0 - 2.0726i	1.4854 +27.7420i	0 - 4.5025i	0 - 2.0726i	1.4854 +27.7420i	0 - 4.5025i
0 - 5.5019i	0 - 4.5025i	0.3646 +13.2505i	0 - 5.5019i	0 - 4.5025i	0.3646 +13.2505i	0 - 5.5019i	0 - 4.5025i	0.3646 +13.2505i
0.3465 +15.2724i	0 - 2.0726i	0 - 5.5019i	0.3465 +15.2724i	0 - 2.0726i	0 - 5.5019i	0.3465 +15.2724i	0 - 2.0726i	0 - 5.5019i
0 - 2.0726i	1.4854 +27.7420i	0 - 4.5025i	0 - 2.0726i	1.4854 +27.7420i	0 - 4.5025i	0 - 2.0726i	1.4854 +27.7420i	0 - 4.5025i
0 - 5.5019i	0 - 4.5025i	0.3646 +13.2505i	0 - 5.5019i	0 - 4.5025i	0.3646 +13.2505i	0 - 5.5019i	0 - 4.5025i	0.3646 +13.2505i
0.3465 +15.2724i	0 - 2.0726i	0 - 5.5019i	0.3465 +15.2724i	0 - 2.0726i	0 - 5.5019i	0.3465 +15.2724i	0 - 2.0726i	0 - 5.5019i
0 - 2.0726i	1.4854 +27.7420i	0 - 4.5025i	0 - 2.0726i	1.4854 +27.7420i	0 - 4.5025i	0 - 2.0726i	1.4854 +27.7420i	0 - 4.5025i
0 - 5.5019i	0 - 4.5025i	0.3646 +13.2505i	0 - 5.5019i	0 - 4.5025i	0.3646 +13.2505i	0 - 5.5019i	0 - 4.5025i	0.3646 +13.2505i
0.3465 +15.2724i	0 - 2.0726i	0 - 4.4015i	0.3465 +15.2724i	0 - 2.0726i	0 - 4.4015i	0.3465 +15.2724i	0 - 2.0726i	0 - 4.4015i
0 - 2.0726i	0.1560 + 7.5294i	0 - 3.4021i	0 - 2.0726i	0.1560 + 7.5294i	0 - 3.4021i	0 - 2.0726i	0.1560 + 7.5294i	0 - 3.4021i
0 - 4.4015i	0 - 3.4021i	0.1580 + 6.3579i	0 - 4.4015i	0 - 3.4021i	0.1580 + 6.3579i	0 - 4.4015i	0 - 3.4021i	0.1580 + 6.3579i
0.3465 +15.2724i	0 - 2.0726i	0 - 4.4015i	0.3465 +15.2724i	0 - 2.0726i	0 - 4.4015i	0.3465 +15.2724i	0 - 2.0726i	0 - 4.4015i
0 - 2.0726i	0.1560 + 7.5294i	0 - 3.4021i	0 - 2.0726i	0.1560 + 7.5294i	0 - 3.4021i	0 - 2.0726i	0.1560 + 7.5294i	0 - 3.4021i
0 - 4.4015i	0 - 3.4021i	0.1580 + 6.3579i	0 - 4.4015i	0 - 3.4021i	0.1580 + 6.3579i	0 - 4.4015i	0 - 3.4021i	0.1580 + 6.3579i
1.6745 +35.6320i	0 - 2.0726i	0 - 6.1621i	1.6745 +35.6320i	0 - 2.0726i	0 - 6.1621i	0.3465 +15.2724i	0 - 2.0726i	0 - 5.5019i
0 - 2.0726i	1.4854 +27.7420i	0 - 4.5025i	0 - 2.0726i	1.4854 +27.7420i	0 - 4.5025i	0 - 2.0726i	1.4854 +27.7420i	0 - 4.5025i
0 - 6.1621i	0 - 4.5025i	0.5712 +20.1432i	0 - 6.1621i	0 - 4.5025i	0.5712 +20.1432i	0 - 5.5019i	0 - 4.5025i	0.3646 +13.2505i
1.6745 +35.6320i	0 - 2.0726i	0 - 6.1621i	1.6745 +35.6320i	0 - 2.0726i	0 - 6.1621i	0.3465 +15.2724i	0 - 2.0726i	0 - 5.5019i
0 - 2.0726i	1.4854 +27.7420i	0 - 4.5025i	0 - 2.0726i	1.4854 +27.7420i	0 - 4.5025i	0 - 2.0726i	1.4854 +27.7420i	0 - 4.5025i
0 - 6.1621i	0 - 4.5025i	1.9004 +40.3618i	0 - 6.1621i	0 - 4.5025i	0.5712 +20.1432i	0 - 5.5019i	0 - 4.5025i	0.3646 +13.2505i
1.6745 +35.6320i	0 - 2.0726i	0 - 6.1621i	3.0170 +43.3231i	0 - 2.0726i	0 - 6.1621i	0.3465 +15.2724i	0 - 2.0726i	0 - 5.5019i
0 - 2.0726i	1.4854 +27.7420i	0 - 4.5025i	0 - 2.0726i	1.4854 +27.7420i	0 - 4.5025i	0 - 2.0726i	1.4854 +27.7420i	0 - 4.5025i
0 - 6.1621i	0 - 4.5025i	0.5712 +20.1432i	0 - 6.1621i	0 - 4.5025i	0.5712 +20.1432i	0 - 5.5019i	0 - 4.5025i	0.3646 +13.2505i

Figure A.14 HA-matrix (column 10-18)

Table B.1 Result of Capacitor Placement by Load Sensitivity Factor

Capacitor_Size	Location	Active_PLoss_kW	Losses_Price_USD	Vmax - Vmin
150	12 - 1	46.881	7876.052	0.986 - 0.838
150	10 - 2	47.721	8017.163	0.998 - 0.849
150	7 - 1	44.530	7481.080	0.988 - 0.842
150	7 - 2	49.795	8365.577	1.010 - 0.848
150	2 - 1	49.725	8353.740	0.987 - 0.846
150	5 - 1	47.473	7975.529	0.986 - 0.842
150	6 - 1	49.316	8285.095	0.986 - 0.842
150	8 - 1	49.091	8247.324	0.986 - 0.842
150	3 - 1	49.270	8277.353	0.987 - 0.845
150	11 - 1	48.567	8159.260	0.986 - 0.838
150	4 - 1	46.654	7837.792	0.987 - 0.845
150	2 - 2	49.672	8344.942	0.998 - 0.849
150	5 - 2	50.909	8552.683	1.007 - 0.848
150	6 - 2	48.994	8230.943	1.007 - 0.848
150	8 - 2	48.550	8156.387	1.011 - 0.848
150	3 - 2	48.888	8213.135	0.998 - 0.849
150	9 - 2	51.115	8587.255	0.998 - 0.849
150	4 - 2	50.381	8464.078	0.998 - 0.849
150	11 - 3	50.407	8468.458	0.981 - 0.885
150	5 - 3	45.399	7626.952	0.981 - 0.872
150	6 - 3	48.317	8117.228	0.981 - 0.872
150	8 - 3	50.571	8495.871	0.981 - 0.872
150	9 - 3	50.313	8452.636	0.985 - 0.860
150	4 - 3	46.915	7881.638	0.985 - 0.861
150	2 - 3	49.679	8346.099	0.985 - 0.860
150	3 - 3	50.405	8468.112	0.985 - 0.861
150	7 - 3	42.944	7214.646	0.980 - 0.872
150	13 - 3	43.098	7240.457	0.981 - 0.897
150	10 - 3	42.677	7169.800	0.985 - 0.860
300	12 - 1	40.736	6843.569	1.008 - 0.826
300	10 - 2	44.647	7500.649	1.019 - 0.848
300	7 - 1	38.041	6390.892	0.995 - 0.834
300	7 - 2	47.219	7932.819	1.031 - 0.848
300	2 - 1	48.990	8230.251	0.995 - 0.842
300	5 - 1	44.220	7428.896	0.995 - 0.834
300	6 - 1	47.716	8016.328	0.995 - 0.834
300	8 - 1	46.847	7870.336	1.012 - 0.834
300	3 - 1	47.305	7947.298	1.002 - 0.842
300	11 - 1	44.846	7534.112	1.009 - 0.827
300	4 - 1	41.774	7018.042	1.004 - 0.842
300	2 - 2	48.321	8118.012	1.007 - 0.848

300	5 - 2	49.950	8391.597	1.025 - 0.847
300	6 - 2	46.153	7753.779	1.025 - 0.847
300	8 - 2	44.514	7478.416	1.038 - 0.847
300	3 - 2	45.665	7671.694	1.016 - 0.848
300	9 - 2	49.684	8346.872	1.007 - 0.848
300	4 - 2	47.560	7990.021	1.025 - 0.848
300	11 - 3	51.654	8677.881	0.977 - 0.912
300	5 - 3	42.256	7098.942	0.977 - 0.894
300	6 - 3	47.846	8038.141	0.977 - 0.894
300	8 - 3	52.592	8835.437	0.977 - 0.893
300	9 - 3	51.121	8588.247	0.982 - 0.871
300	4 - 3	45.447	7635.023	0.982 - 0.871
300	2 - 3	49.874	8378.786	0.982 - 0.871
300	3 - 3	51.694	8684.514	0.982 - 0.871
300	7 - 3	37.539	6306.538	0.976 - 0.894
300	13 - 3	37.833	6355.950	0.977 - 0.912
300	10 - 3	36.663	6159.398	0.982 - 0.871
450	12 - 1	31.805	5343.271	1.035 - 0.816
450	10 - 2	53.355	8963.672	1.047 - 0.849
450	7 - 1	30.604	5141.515	1.013 - 0.827
450	7 - 2	45.043	7567.302	1.052 - 0.848
450	2 - 1	47.909	8048.667	1.004 - 0.838
450	5 - 1	40.360	6780.481	1.013 - 0.827
450	6 - 1	45.347	7618.250	1.013 - 0.827
450	8 - 1	43.452	7299.970	1.037 - 0.827
450	3 - 1	44.249	7433.783	1.020 - 0.838
450	11 - 1	39.085	6566.256	1.036 - 0.816
450	4 - 1	35.463	5957.707	1.032 - 0.838
450	2 - 2	46.103	7745.312	1.016 - 0.848
450	5 - 2	47.399	7963.078	1.043 - 0.847
450	6 - 2	45.680	7674.323	1.043 - 0.847
450	8 - 2	49.090	8247.043	1.063 - 0.847
450	3 - 2	46.441	7802.051	1.035 - 0.848
450	9 - 2	46.123	7748.675	1.020 - 0.848
450	4 - 2	44.959	7553.121	1.052 - 0.848
450	11 - 3	53.348	8962.497	0.974 - 0.922
450	5 - 3	40.426	6791.613	0.974 - 0.914
450	6 - 3	48.482	8145.013	0.974 - 0.914
450	8 - 3	55.808	9375.793	0.977 - 0.912
450	9 - 3	52.251	8778.223	0.982 - 0.881
450	4 - 3	45.133	7582.425	1.006 - 0.881
450	2 - 3	50.643	8507.956	0.979 - 0.882
450	3 - 3	53.754	9030.749	0.988 - 0.881
450	7 - 3	35.088	5894.854	0.974 - 0.914
450	13 - 3	35.968	6042.694	0.979 - 0.921
450	10 - 3	37.738	6340.011	0.990 - 0.880

600	12 - 1	30.365	5101.257	1.064 - 0.805
600	10 - 2	64.359	10812.250	1.073 - 0.849
600	7 - 1	28.561	4798.301	1.030 - 0.819
600	7 - 2	51.737	8691.737	1.071 - 0.848
600	2 - 1	46.487	7809.764	1.013 - 0.835
600	5 - 1	35.906	6032.197	1.030 - 0.820
600	6 - 1	42.239	7096.158	1.030 - 0.820
600	8 - 1	38.968	6546.665	1.061 - 0.821
600	3 - 1	40.131	6742.028	1.038 - 0.835
600	11 - 1	31.402	5275.561	1.063 - 0.805
600	4 - 1	27.729	4658.487	1.058 - 0.835
600	2 - 2	44.032	7397.382	1.025 - 0.847
600	5 - 2	44.285	7439.818	1.060 - 0.846
600	6 - 2	51.756	8694.943	1.060 - 0.846
600	8 - 2	57.412	9645.187	1.086 - 0.847
600	3 - 2	53.217	8940.486	1.053 - 0.848
600	9 - 2	45.956	7720.660	1.038 - 0.848
600	4 - 2	52.769	8865.128	1.078 - 0.848
600	11 - 3	55.133	9262.284	0.993 - 0.922
600	5 - 3	39.708	6670.975	0.978 - 0.920
600	6 - 3	50.053	8408.958	0.978 - 0.920
600	8 - 3	59.949	10071.455	1.003 - 0.921
600	9 - 3	53.485	8985.424	1.002 - 0.890
600	4 - 3	45.559	7653.875	1.033 - 0.890
600	2 - 3	51.941	8726.046	0.977 - 0.892
600	3 - 3	56.411	9477.105	1.007 - 0.891
600	7 - 3	38.098	6400.461	0.977 - 0.928
600	13 - 3	41.022	6891.763	1.014 - 0.924
600	10 - 3	43.296	7273.684	1.019 - 0.888
750	12 - 1	45.658	7670.488	1.090 - 0.794
750	10 - 2	77.200	12969.535	1.098 - 0.849
750	7 - 1	39.280	6599.024	1.046 - 0.812
750	7 - 2	60.005	10080.898	1.090 - 0.848
750	2 - 1	44.728	7514.279	1.022 - 0.831
750	5 - 1	30.868	5185.830	1.047 - 0.813
750	6 - 1	38.420	6454.620	1.047 - 0.813
750	8 - 1	33.448	5619.260	1.084 - 0.814
750	3 - 1	34.982	5876.896	1.055 - 0.831
750	11 - 1	30.137	5062.946	1.087 - 0.795
750	4 - 1	30.617	5143.592	1.082 - 0.831
750	2 - 2	47.973	8059.446	1.034 - 0.847
750	5 - 2	49.858	8376.083	1.076 - 0.846
750	6 - 2	59.127	9933.271	1.076 - 0.846
750	8 - 2	67.408	11324.581	1.109 - 0.847
750	3 - 2	61.451	10323.745	1.070 - 0.848
750	9 - 2	53.045	8911.563	1.056 - 0.848
750	4 - 2	62.501	10500.141	1.102 - 0.848
750	11 - 3	56.741	9532.440	1.019 - 0.922

750	5 - 3	39.937	6709.391	0.988 - 0.919
750	6 - 3	52.419	8806.357	0.988 - 0.919
750	8 - 3	64.806	10887.487	1.028 - 0.920
750	9 - 3	54.642	9179.806	1.020 - 0.899
750	4 - 3	46.408	7796.534	1.058 - 0.898
750	2 - 3	53.728	9026.227	0.986 - 0.903
750	3 - 3	59.519	9999.158	1.024 - 0.900
750	7 - 3	40.422	6790.942	0.994 - 0.927
750	13 - 3	46.902	7879.565	1.047 - 0.924
750	10 - 3	49.369	8294.018	1.045 - 0.896
900	12 - 1	63.249	10625.838	1.115 - 0.784
900	10 - 2	91.492	15370.609	1.121 - 0.850
900	7 - 1	50.949	8559.430	1.061 - 0.805
900	7 - 2	69.687	11707.340	1.108 - 0.849
900	2 - 1	42.636	7162.911	1.030 - 0.828
900	5 - 1	27.929	4692.024	1.063 - 0.806
900	6 - 1	33.915	5697.638	1.063 - 0.806
900	8 - 1	26.937	4525.382	1.106 - 0.808
900	3 - 1	28.827	4842.941	1.072 - 0.828
900	11 - 1	42.637	7162.966	1.111 - 0.785
900	4 - 1	41.856	7031.763	1.106 - 0.828
900	2 - 2	52.661	8846.995	1.043 - 0.847
900	5 - 2	56.649	9517.111	1.092 - 0.846
900	6 - 2	67.693	11372.413	1.092 - 0.846
900	8 - 2	78.907	13256.386	1.131 - 0.847
900	3 - 2	71.012	11929.956	1.086 - 0.848
900	9 - 2	61.600	10348.719	1.074 - 0.848
900	4 - 2	73.905	12416.105	1.126 - 0.848
900	11 - 3	57.966	9738.369	1.044 - 0.922
900	5 - 3	40.976	6883.995	1.006 - 0.918
900	6 - 3	55.462	9317.570	1.006 - 0.918
900	8 - 3	70.216	11796.338	1.051 - 0.919
900	9 - 3	55.575	9336.631	1.038 - 0.908
900	4 - 3	47.437	7969.342	1.083 - 0.906
900	2 - 3	55.966	9402.308	0.995 - 0.912
900	3 - 3	62.956	10576.528	1.042 - 0.909
900	7 - 3	42.286	7104.051	1.014 - 0.927
900	13 - 3	54.010	9073.630	1.077 - 0.925
900	10 - 3	56.304	9459.076	1.069 - 0.894
1050	12 - 1	82.996	13943.250	1.138 - 0.774
1050	10 - 2	106.900	17959.281	1.144 - 0.850
1050	7 - 1	63.567	10679.267	1.076 - 0.799
1050	7 - 2	80.637	13547.097	1.125 - 0.849
1050	2 - 1	40.216	6756.325	1.039 - 0.824
1050	5 - 1	35.388	5945.192	1.079 - 0.800
1050	6 - 1	28.743	4828.755	1.079 - 0.800

1050	8 - 1	34.518	5798.950	1.127 - 0.801
1050	3 - 1	29.224	4909.711	1.088 - 0.824
1050	11 - 1	56.754	9534.747	1.133 - 0.775
1050	4 - 1	54.414	9141.561	1.128 - 0.825
1050	2 - 2	58.063	9754.532	1.052 - 0.846
1050	5 - 2	64.571	10847.862	1.108 - 0.846
1050	6 - 2	77.367	12997.599	1.108 - 0.846
1050	8 - 2	91.764	15416.315	1.152 - 0.847
1050	3 - 2	81.786	13739.992	1.102 - 0.848
1050	9 - 2	71.456	12004.593	1.090 - 0.848
1050	4 - 2	86.771	14577.609	1.148 - 0.848
1050	11 - 3	58.647	9852.622	1.067 - 0.922
1050	5 - 3	42.712	7175.592	1.023 - 0.917
1050	6 - 3	59.084	9926.035	1.023 - 0.917
1050	8 - 3	76.046	12775.809	1.074 - 0.919
1050	9 - 3	56.162	9435.216	1.055 - 0.909
1050	4 - 3	48.450	8139.645	1.106 - 0.914
1050	2 - 3	58.623	9848.648	1.004 - 0.920
1050	3 - 3	66.619	11191.994	1.058 - 0.917
1050	7 - 3	43.872	7370.501	1.033 - 0.927
1050	13 - 3	62.647	10524.758	1.105 - 0.926
1050	10 - 3	64.371	10814.312	1.093 - 0.885
1200	12 - 1	104.753	17598.584	1.160 - 0.763
1200	10 - 2	123.131	20685.927	1.165 - 0.851
1200	7 - 1	77.128	12957.502	1.093 - 0.792
1200	7 - 2	92.732	15579.006	1.142 - 0.850
1200	2 - 1	37.471	6295.158	1.047 - 0.821
1200	5 - 1	43.389	7289.351	1.094 - 0.793
1200	6 - 1	32.814	5512.815	1.094 - 0.793
1200	8 - 1	44.049	7400.174	1.148 - 0.795
1200	3 - 1	38.075	6396.536	1.103 - 0.821
1200	11 - 1	72.418	12166.265	1.155 - 0.766
1200	4 - 1	68.262	11467.959	1.150 - 0.822
1200	2 - 2	64.149	10776.970	1.060 - 0.846
1200	5 - 2	73.542	12355.079	1.123 - 0.846
1200	6 - 2	88.070	14795.801	1.123 - 0.846
1200	8 - 2	105.855	17783.634	1.173 - 0.847
1200	3 - 2	93.672	15736.963	1.118 - 0.848
1200	9 - 2	82.469	13854.771	1.106 - 0.849
1200	4 - 2	100.919	16954.343	1.170 - 0.849
1200	11 - 3	58.649	9852.954	1.090 - 0.923
1200	5 - 3	45.047	7567.873	1.039 - 0.917
1200	6 - 3	63.200	10617.615	1.039 - 0.917
1200	8 - 3	82.189	13807.691	1.095 - 0.917
1200	9 - 3	56.298	9458.043	1.072 - 0.903
1200	4 - 3	49.292	8280.973	1.128 - 0.921
1200	2 - 3	61.667	10360.094	1.013 - 0.919
1200	3 - 3	70.422	11830.842	1.075 - 0.919

1200	7 - 3	45.332	7615.716	1.051 - 0.921
1200	13 - 3	73.050	12272.401	1.131 - 0.928
1200	10 - 3	73.787	12396.159	1.115 - 0.876
1350	12 - 1	128.379	21567.646	1.181 - 0.753
1350	10 - 2	139.917	23505.973	1.185 - 0.852
1350	7 - 1	91.622	15392.528	1.110 - 0.785
1350	7 - 2	105.858	17784.191	1.158 - 0.845
1350	2 - 1	34.405	5780.020	1.055 - 0.817
1350	5 - 1	51.925	8723.410	1.109 - 0.787
1350	6 - 1	40.521	6807.610	1.109 - 0.787
1350	8 - 1	54.444	9146.639	1.168 - 0.789
1350	3 - 1	47.843	8037.609	1.118 - 0.818
1350	11 - 1	89.561	15046.321	1.176 - 0.756
1350	4 - 1	83.367	14005.667	1.170 - 0.819
1350	2 - 2	70.890	11909.580	1.069 - 0.846
1350	5 - 2	83.494	14026.983	1.137 - 0.846
1350	6 - 2	99.735	16755.445	1.137 - 0.846
1350	8 - 2	121.074	20340.429	1.193 - 0.848
1350	3 - 2	106.582	17905.835	1.133 - 0.848
1350	9 - 2	94.508	15877.388	1.122 - 0.849
1350	4 - 2	116.190	19519.992	1.190 - 0.849
1350	11 - 3	57.863	9721.011	1.111 - 0.924
1350	5 - 3	47.898	8046.821	1.055 - 0.916
1350	6 - 3	67.739	11380.114	1.055 - 0.916
1350	8 - 3	88.552	14876.820	1.116 - 0.910
1350	9 - 3	55.894	9390.109	1.088 - 0.897
1350	4 - 3	49.830	8371.520	1.149 - 0.916
1350	2 - 3	65.071	10931.920	1.021 - 0.919
1350	3 - 3	74.288	12480.383	1.090 - 0.914
1350	7 - 3	46.792	7861.053	1.069 - 0.914
1350	13 - 3	85.405	14347.968	1.156 - 0.929
1350	10 - 3	84.729	14234.389	1.136 - 0.867
1500	12 - 1	153.727	25826.165	1.200 - 0.743
1500	10 - 2	157.017	26378.787	1.204 - 0.853
1500	7 - 1	107.038	17982.308	1.126 - 0.778
1500	7 - 2	119.915	20145.667	1.174 - 0.836
1500	2 - 1	31.021	5211.494	1.063 - 0.814
1500	5 - 1	60.990	10246.302	1.123 - 0.780
1500	6 - 1	48.833	8204.007	1.123 - 0.780
1500	8 - 1	65.678	11033.934	1.187 - 0.783
1500	3 - 1	58.509	9829.483	1.133 - 0.815
1500	11 - 1	108.121	18164.395	1.196 - 0.747
1500	4 - 1	99.698	16749.252	1.190 - 0.815
1500	2 - 2	78.262	13147.959	1.077 - 0.846
1500	5 - 2	94.363	15853.042	1.152 - 0.847
1500	6 - 2	112.299	18866.171	1.152 - 0.847

1500	8 - 2	137.328	23071.061	1.212 - 0.848
1500	3 - 2	120.435	20233.125	1.148 - 0.848
1500	9 - 2	107.456	18052.684	1.137 - 0.850
1500	4 - 2	132.449	22251.431	1.210 - 0.850
1500	11 - 3	56.199	9441.436	1.132 - 0.925
1500	5 - 3	51.192	8600.283	1.070 - 0.916
1500	6 - 3	72.636	12202.920	1.070 - 0.916
1500	8 - 3	95.062	15970.407	1.136 - 0.903
1500	9 - 3	54.872	9218.443	1.103 - 0.891
1500	4 - 3	49.959	8393.078	1.170 - 0.911
1500	2 - 3	68.808	11559.774	1.030 - 0.918
1500	3 - 3	78.152	13129.575	1.105 - 0.909
1500	7 - 3	48.361	8124.676	1.086 - 0.907
1500	13 - 3	99.863	16776.963	1.180 - 0.927
1500	10 - 3	97.344	16353.713	1.155 - 0.858

Table B.2 **Result of Single Size Capacitor Installation**

Capacitor_Size	Location	Active_PLoss_kW	Losses_Price_USD	Vmax - Vmin
150	12 - 1	46.881	7876.052	0.986 - 0.838
150	10 - 2	47.721	8017.163	0.998 - 0.849
150	7 - 1	44.530	7481.080	0.988 - 0.842
150	7 - 2	49.795	8365.577	1.010 - 0.848
150	2 - 1	49.725	8353.740	0.987 - 0.846
150	5 - 1	47.473	7975.529	0.986 - 0.842
150	6 - 1	49.316	8285.095	0.986 - 0.842
150	8 - 1	49.091	8247.324	0.986 - 0.842
150	3 - 1	49.270	8277.353	0.987 - 0.845
150	11 - 1	48.567	8159.260	0.986 - 0.838
150	4 - 1	46.654	7837.792	0.987 - 0.845
150	2 - 2	49.672	8344.942	0.998 - 0.849
150	5 - 2	50.909	8552.683	1.007 - 0.848
150	6 - 2	48.994	8230.943	1.007 - 0.848
150	8 - 2	48.550	8156.387	1.011 - 0.848
150	3 - 2	48.888	8213.135	0.998 - 0.849
150	9 - 2	51.115	8587.255	0.998 - 0.849
150	4 - 2	50.381	8464.078	0.998 - 0.849
150	11 - 3	50.407	8468.458	0.981 - 0.885
150	5 - 3	45.399	7626.952	0.981 - 0.872
150	6 - 3	48.317	8117.228	0.981 - 0.872
150	8 - 3	50.571	8495.871	0.981 - 0.872
150	9 - 3	50.313	8452.636	0.985 - 0.860
150	4 - 3	46.915	7881.638	0.985 - 0.861
150	2 - 3	49.679	8346.099	0.985 - 0.860
150	3 - 3	50.405	8468.112	0.985 - 0.861
150	7 - 3	42.944	7214.646	0.980 - 0.872
150	13 - 3	43.098	7240.457	0.981 - 0.897
150	10 - 3	42.677	7169.800	0.985 - 0.860
300	12 - 1	40.736	6843.569	1.008 - 0.826
300	10 - 2	44.647	7500.649	1.019 - 0.848
300	7 - 1	38.041	6390.892	0.995 - 0.834
300	7 - 2	47.219	7932.819	1.031 - 0.848
300	2 - 1	48.990	8230.251	0.995 - 0.842
300	5 - 1	44.220	7428.896	0.995 - 0.834
300	6 - 1	47.716	8016.328	0.995 - 0.834
300	8 - 1	46.847	7870.336	1.012 - 0.834
300	3 - 1	47.305	7947.298	1.002 - 0.842
300	11 - 1	44.846	7534.112	1.009 - 0.827
300	4 - 1	41.774	7018.042	1.004 - 0.842
300	2 - 2	48.321	8118.012	1.007 - 0.848
300	5 - 2	49.950	8391.597	1.025 - 0.847

300	6 - 2	46.153	7753.779	1.025 - 0.847
300	8 - 2	44.514	7478.416	1.038 - 0.847
300	3 - 2	45.665	7671.694	1.016 - 0.848
300	9 - 2	49.684	8346.872	1.007 - 0.848
300	4 - 2	47.560	7990.021	1.025 - 0.848
300	11 - 3	51.654	8677.881	0.977 - 0.912
300	5 - 3	42.256	7098.942	0.977 - 0.894
300	6 - 3	47.846	8038.141	0.977 - 0.894
300	8 - 3	52.592	8835.437	0.977 - 0.893
300	9 - 3	51.121	8588.247	0.982 - 0.871
300	4 - 3	45.447	7635.023	0.982 - 0.871
300	2 - 3	49.874	8378.786	0.982 - 0.871
300	3 - 3	51.694	8684.514	0.982 - 0.871
300	7 - 3	37.539	6306.538	0.976 - 0.894
300	13 - 3	37.833	6355.950	0.977 - 0.912
300	10 - 3	36.663	6159.398	0.982 - 0.871
450	12 - 1	31.805	5343.271	1.035 - 0.816
450	10 - 2	53.355	8963.672	1.047 - 0.849
450	7 - 1	30.604	5141.515	1.013 - 0.827
450	7 - 2	45.043	7567.302	1.052 - 0.848
450	2 - 1	47.909	8048.667	1.004 - 0.838
450	5 - 1	40.360	6780.481	1.013 - 0.827
450	6 - 1	45.347	7618.250	1.013 - 0.827
450	8 - 1	43.452	7299.970	1.037 - 0.827
450	3 - 1	44.249	7433.783	1.020 - 0.838
450	11 - 1	39.085	6566.256	1.036 - 0.816
450	4 - 1	35.463	5957.707	1.032 - 0.838
450	2 - 2	46.103	7745.312	1.016 - 0.848
450	5 - 2	47.399	7963.078	1.043 - 0.847
450	6 - 2	45.680	7674.323	1.043 - 0.847
450	8 - 2	49.090	8247.043	1.063 - 0.847
450	3 - 2	46.441	7802.051	1.035 - 0.848
450	9 - 2	46.123	7748.675	1.020 - 0.848
450	4 - 2	44.959	7553.121	1.052 - 0.848
450	11 - 3	53.348	8962.497	0.974 - 0.922
450	5 - 3	40.426	6791.613	0.974 - 0.914
450	6 - 3	48.482	8145.013	0.974 - 0.914
450	8 - 3	55.808	9375.793	0.977 - 0.912
450	9 - 3	52.251	8778.223	0.982 - 0.881
450	4 - 3	45.133	7582.425	1.006 - 0.881
450	2 - 3	50.643	8507.956	0.979 - 0.882
450	3 - 3	53.754	9030.749	0.988 - 0.881
450	7 - 3	35.088	5894.854	0.974 - 0.914
450	13 - 3	35.968	6042.694	0.979 - 0.921
450	10 - 3	37.738	6340.011	0.990 - 0.880
600	12 - 1	30.365	5101.257	1.064 - 0.805

600	10 - 2	64.359	10812.250	1.073 - 0.849
600	7 - 1	28.561	4798.301	1.030 - 0.819
600	7 - 2	51.737	8691.737	1.071 - 0.848
600	2 - 1	46.487	7809.764	1.013 - 0.835
600	5 - 1	35.906	6032.197	1.030 - 0.820
600	6 - 1	42.239	7096.158	1.030 - 0.820
600	8 - 1	38.968	6546.665	1.061 - 0.821
600	3 - 1	40.131	6742.028	1.038 - 0.835
600	11 - 1	31.402	5275.561	1.063 - 0.805
600	4 - 1	27.729	4658.487	1.058 - 0.835
600	2 - 2	44.032	7397.382	1.025 - 0.847
600	5 - 2	44.285	7439.818	1.060 - 0.846
600	6 - 2	51.756	8694.943	1.060 - 0.846
600	8 - 2	57.412	9645.187	1.086 - 0.847
600	3 - 2	53.217	8940.486	1.053 - 0.848
600	9 - 2	45.956	7720.660	1.038 - 0.848
600	4 - 2	52.769	8865.128	1.078 - 0.848
600	11 - 3	55.133	9262.284	0.993 - 0.922
600	5 - 3	39.708	6670.975	0.978 - 0.920
600	6 - 3	50.053	8408.958	0.978 - 0.920
600	8 - 3	59.949	10071.455	1.003 - 0.921
600	9 - 3	53.485	8985.424	1.002 - 0.890
600	4 - 3	45.559	7653.875	1.033 - 0.890
600	2 - 3	51.941	8726.046	0.977 - 0.892
600	3 - 3	56.411	9477.105	1.007 - 0.891
600	7 - 3	38.098	6400.461	0.977 - 0.928
600	13 - 3	41.022	6891.763	1.014 - 0.924
600	10 - 3	43.296	7273.684	1.019 - 0.888
750	12 - 1	45.658	7670.488	1.090 - 0.794
750	10 - 2	77.200	12969.535	1.098 - 0.849
750	7 - 1	39.280	6599.024	1.046 - 0.812
750	7 - 2	60.005	10080.898	1.090 - 0.848
750	2 - 1	44.728	7514.279	1.022 - 0.831
750	5 - 1	30.868	5185.830	1.047 - 0.813
750	6 - 1	38.420	6454.620	1.047 - 0.813
750	8 - 1	33.448	5619.260	1.084 - 0.814
750	3 - 1	34.982	5876.896	1.055 - 0.831
750	11 - 1	30.137	5062.946	1.087 - 0.795
750	4 - 1	30.617	5143.592	1.082 - 0.831
750	2 - 2	47.973	8059.446	1.034 - 0.847
750	5 - 2	49.858	8376.083	1.076 - 0.846
750	6 - 2	59.127	9933.271	1.076 - 0.846
750	8 - 2	67.408	11324.581	1.109 - 0.847
750	3 - 2	61.451	10323.745	1.070 - 0.848
750	9 - 2	53.045	8911.563	1.056 - 0.848
750	4 - 2	62.501	10500.141	1.102 - 0.848
750	11 - 3	56.741	9532.440	1.019 - 0.922
750	5 - 3	39.937	6709.391	0.988 - 0.919

750	6 - 3	52.419	8806.357	0.988 - 0.919
750	8 - 3	64.806	10887.487	1.028 - 0.920
750	9 - 3	54.642	9179.806	1.020 - 0.899
750	4 - 3	46.408	7796.534	1.058 - 0.898
750	2 - 3	53.728	9026.227	0.986 - 0.903
750	3 - 3	59.519	9999.158	1.024 - 0.900
750	7 - 3	40.422	6790.942	0.994 - 0.927
750	13 - 3	46.902	7879.565	1.047 - 0.924
750	10 - 3	49.369	8294.018	1.045 - 0.896
900	12 - 1	63.249	10625.838	1.115 - 0.784
900	10 - 2	91.492	15370.609	1.121 - 0.850
900	7 - 1	50.949	8559.430	1.061 - 0.805
900	7 - 2	69.687	11707.340	1.108 - 0.849
900	2 - 1	42.636	7162.911	1.030 - 0.828
900	5 - 1	27.929	4692.024	1.063 - 0.806
900	6 - 1	33.915	5697.638	1.063 - 0.806
900	8 - 1	26.937	4525.382	1.106 - 0.808
900	3 - 1	28.827	4842.941	1.072 - 0.828
900	11 - 1	42.637	7162.966	1.111 - 0.785
900	4 - 1	41.856	7031.763	1.106 - 0.828
900	2 - 2	52.661	8846.995	1.043 - 0.847
900	5 - 2	56.649	9517.111	1.092 - 0.846
900	6 - 2	67.693	11372.413	1.092 - 0.846
900	8 - 2	78.907	13256.386	1.131 - 0.847
900	3 - 2	71.012	11929.956	1.086 - 0.848
900	9 - 2	61.600	10348.719	1.074 - 0.848
900	4 - 2	73.905	12416.105	1.126 - 0.848
900	11 - 3	57.966	9738.369	1.044 - 0.922
900	5 - 3	40.976	6883.995	1.006 - 0.918
900	6 - 3	55.462	9317.570	1.006 - 0.918
900	8 - 3	70.216	11796.338	1.051 - 0.919
900	9 - 3	55.575	9336.631	1.038 - 0.908
900	4 - 3	47.437	7969.342	1.083 - 0.906
900	2 - 3	55.966	9402.308	0.995 - 0.912
900	3 - 3	62.956	10576.528	1.042 - 0.909
900	7 - 3	42.286	7104.051	1.014 - 0.927
900	13 - 3	54.010	9073.630	1.077 - 0.925
900	10 - 3	56.304	9459.076	1.069 - 0.894
1050	12 - 1	82.996	13943.250	1.138 - 0.774
1050	10 - 2	106.900	17959.281	1.144 - 0.850
1050	7 - 1	63.567	10679.267	1.076 - 0.799
1050	7 - 2	80.637	13547.097	1.125 - 0.849
1050	2 - 1	40.216	6756.325	1.039 - 0.824
1050	5 - 1	35.388	5945.192	1.079 - 0.800
1050	6 - 1	28.743	4828.755	1.079 - 0.800
1050	8 - 1	34.518	5798.950	1.127 - 0.801

1050	3 - 1	29.224	4909.711	1.088 - 0.824
1050	11 - 1	56.754	9534.747	1.133 - 0.775
1050	4 - 1	54.414	9141.561	1.128 - 0.825
1050	2 - 2	58.063	9754.532	1.052 - 0.846
1050	5 - 2	64.571	10847.862	1.108 - 0.846
1050	6 - 2	77.367	12997.599	1.108 - 0.846
1050	8 - 2	91.764	15416.315	1.152 - 0.847
1050	3 - 2	81.786	13739.992	1.102 - 0.848
1050	9 - 2	71.456	12004.593	1.090 - 0.848
1050	4 - 2	86.771	14577.609	1.148 - 0.848
1050	11 - 3	58.647	9852.622	1.067 - 0.922
1050	5 - 3	42.712	7175.592	1.023 - 0.917
1050	6 - 3	59.084	9926.035	1.023 - 0.917
1050	8 - 3	76.046	12775.809	1.074 - 0.919
1050	9 - 3	56.162	9435.216	1.055 - 0.909
1050	4 - 3	48.450	8139.645	1.106 - 0.914
1050	2 - 3	58.623	9848.648	1.004 - 0.920
1050	3 - 3	66.619	11191.994	1.058 - 0.917
1050	7 - 3	43.872	7370.501	1.033 - 0.927
1050	13 - 3	62.647	10524.758	1.105 - 0.926
1050	10 - 3	64.371	10814.312	1.093 - 0.885
1200	12 - 1	104.753	17598.584	1.160 - 0.763
1200	10 - 2	123.131	20685.927	1.165 - 0.851
1200	7 - 1	77.128	12957.502	1.093 - 0.792
1200	7 - 2	92.732	15579.006	1.142 - 0.850
1200	2 - 1	37.471	6295.158	1.047 - 0.821
1200	5 - 1	43.389	7289.351	1.094 - 0.793
1200	6 - 1	32.814	5512.815	1.094 - 0.793
1200	8 - 1	44.049	7400.174	1.148 - 0.795
1200	3 - 1	38.075	6396.536	1.103 - 0.821
1200	11 - 1	72.418	12166.265	1.155 - 0.766
1200	4 - 1	68.262	11467.959	1.150 - 0.822
1200	2 - 2	64.149	10776.970	1.060 - 0.846
1200	5 - 2	73.542	12355.079	1.123 - 0.846
1200	6 - 2	88.070	14795.801	1.123 - 0.846
1200	8 - 2	105.855	17783.634	1.173 - 0.847
1200	3 - 2	93.672	15736.963	1.118 - 0.848
1200	9 - 2	82.469	13854.771	1.106 - 0.849
1200	4 - 2	100.919	16954.343	1.170 - 0.849
1200	11 - 3	58.649	9852.954	1.090 - 0.923
1200	5 - 3	45.047	7567.873	1.039 - 0.917
1200	6 - 3	63.200	10617.615	1.039 - 0.917
1200	8 - 3	82.189	13807.691	1.095 - 0.917
1200	9 - 3	56.298	9458.043	1.072 - 0.903
1200	4 - 3	49.292	8280.973	1.128 - 0.921
1200	2 - 3	61.667	10360.094	1.013 - 0.919
1200	3 - 3	70.422	11830.842	1.075 - 0.919
1200	7 - 3	45.332	7615.716	1.051 - 0.921

1200	13 - 3	73.050	12272.401	1.131 - 0.928
1200	10 - 3	73.787	12396.159	1.115 - 0.876
1350	12 - 1	128.379	21567.646	1.181 - 0.753
1350	10 - 2	139.917	23505.973	1.185 - 0.852
1350	7 - 1	91.622	15392.528	1.110 - 0.785
1350	7 - 2	105.858	17784.191	1.158 - 0.845
1350	2 - 1	34.405	5780.020	1.055 - 0.817
1350	5 - 1	51.925	8723.410	1.109 - 0.787
1350	6 - 1	40.521	6807.610	1.109 - 0.787
1350	8 - 1	54.444	9146.639	1.168 - 0.789
1350	3 - 1	47.843	8037.609	1.118 - 0.818
1350	11 - 1	89.561	15046.321	1.176 - 0.756
1350	4 - 1	83.367	14005.667	1.170 - 0.819
1350	2 - 2	70.890	11909.580	1.069 - 0.846
1350	5 - 2	83.494	14026.983	1.137 - 0.846
1350	6 - 2	99.735	16755.445	1.137 - 0.846
1350	8 - 2	121.074	20340.429	1.193 - 0.848
1350	3 - 2	106.582	17905.835	1.133 - 0.848
1350	9 - 2	94.508	15877.388	1.122 - 0.849
1350	4 - 2	116.190	19519.992	1.190 - 0.849
1350	11 - 3	57.863	9721.011	1.111 - 0.924
1350	5 - 3	47.898	8046.821	1.055 - 0.916
1350	6 - 3	67.739	11380.114	1.055 - 0.916
1350	8 - 3	88.552	14876.820	1.116 - 0.910
1350	9 - 3	55.894	9390.109	1.088 - 0.897
1350	4 - 3	49.830	8371.520	1.149 - 0.916
1350	2 - 3	65.071	10931.920	1.021 - 0.919
1350	3 - 3	74.288	12480.383	1.090 - 0.914
1350	7 - 3	46.792	7861.053	1.069 - 0.914
1350	13 - 3	85.405	14347.968	1.156 - 0.929
1350	10 - 3	84.729	14234.389	1.136 - 0.867
1500	12 - 1	153.727	25826.165	1.200 - 0.743
1500	10 - 2	157.017	26378.787	1.204 - 0.853
1500	7 - 1	107.038	17982.308	1.126 - 0.778
1500	7 - 2	119.915	20145.667	1.174 - 0.836
1500	2 - 1	31.021	5211.494	1.063 - 0.814
1500	5 - 1	60.990	10246.302	1.123 - 0.780
1500	6 - 1	48.833	8204.007	1.123 - 0.780
1500	8 - 1	65.678	11033.934	1.187 - 0.783
1500	3 - 1	58.509	9829.483	1.133 - 0.815
1500	11 - 1	108.121	18164.395	1.196 - 0.747
1500	4 - 1	99.698	16749.252	1.190 - 0.815
1500	2 - 2	78.262	13147.959	1.077 - 0.846
1500	5 - 2	94.363	15853.042	1.152 - 0.847
1500	6 - 2	112.299	18866.171	1.152 - 0.847
1500	8 - 2	137.328	23071.061	1.212 - 0.848

1500	3 - 2	120.435	20233.125	1.148 - 0.848
1500	9 - 2	107.456	18052.684	1.137 - 0.850
1500	4 - 2	132.449	22251.431	1.210 - 0.850
1500	11 - 3	56.199	9441.436	1.132 - 0.925
1500	5 - 3	51.192	8600.283	1.070 - 0.916
1500	6 - 3	72.636	12202.920	1.070 - 0.916
1500	8 - 3	95.062	15970.407	1.136 - 0.903
1500	9 - 3	54.872	9218.443	1.103 - 0.891
1500	4 - 3	49.959	8393.078	1.170 - 0.911
1500	2 - 3	68.808	11559.774	1.030 - 0.918
1500	3 - 3	78.152	13129.575	1.105 - 0.909
1500	7 - 3	48.361	8124.676	1.086 - 0.907
1500	13 - 3	99.863	16776.963	1.180 - 0.927
1500	10 - 3	97.344	16353.713	1.155 - 0.858